ITT INDUSTRIAL LABORATORIES
FORT WAYNE, INDIANA

[redacted]

GPO PRICE $ _____

CSFTI PRICE(S) $ _____

Hard copy (HC) 3.00

Microfiche (MF) .75

ff 653 July 65

ITT INDUSTRIAL LABORATORIES
A DIVISION OF INTERNATIONAL TELEPHONE AND TELEGRAPH CORPORATION
3700 East Pontiac Street
Fort Wayne, Indiana 46803
Area Code 219
Telephone 743-7571
TWX 241-2065

August 30, 1965

FINAL REPORT

RESEARCH IN THE DEVELOPMENT EFFORT OF AN IMPROVED MULTIPLIER PHOTOTUBE

Contract No. NASw 1038
National Aeronautics and Space Administration
Washington D.C. 20546

Prepared by

F. Barr and E. Eberhardt

Approved by

S. M. Johnson, Manager
Advanced Product Development

M. F. Toohig, Manager
Tubes and Sensors Department

Dr. C. W. Steeg Jr., Director
Product Development

TABLE OF CONTENTS

INTRODUCTION

The purpose of this program was to investigate the single electron counting characteristics of the standard line of ITTIL multiplier phototubes with the objective of improving their ability to unambiguously count single photoelectrons excited at the photocathode by the input radiation.

The following paragraph delineates the problem areas that were deemed to be most pertinent to the development effort. It should be recognized, however, that definite answers to all the problems originally posed were not finalized during the course of the present contract. It seemed wiser, for example, to concentrate our first efforts on basic tube design problems rather than on equipment or pulse circuit problems (although some work here was required) and on some less significant tube processing procedures.

Problem Areas

A discussion of the investigation of many of the following questions is presented in this report along with some indicated modifications which may hold promise of providing the NASA user with an improved single electron counting tube of known capabilities.

a. What is the source of dark pulses? How many are thermionic emission? How many come from the first dynode? Is ion feedback present? What happens in a cesium-free tube?

b. Why do the dark pulses have an exponential type pulse height distribution?

c. What causes spurious pulsing occasionally encountered, particularly in windowless multipliers?

d. What happens when the primary electron energy for electrons striking the first dynode is raised to give maximum secondary emission yields?

e. What role does aging (now used on all ITTIL multiplier phototubes) play?

f. Does space-charge saturation actually occur in the high gain multiplier for single electron inputs?

g. Is a based tube superior to an unbased tube?

h. Can higher multiplier gains be used to get improved counting efficiency?

i. Is a charge sensitive ringing circuit as used by Kerns, et al, more suitable for distinguishing signal from dark current pulses?

j. Does the output distribution of the tubes actually obey the expected Poisson characteristics?

k. Why does the signal pulse height distribution appear to have a noticeable rise for very low pulse amplitudes, even when dark current pulse rates have been subtracted?

l. Is the amplifier-counting system significant in determining the pulse height distribution?

m. What happens when the tubes are cooled?

n. Can improved pulse counting characteristics be incorporated in windowless multipliers for the extreme ultraviolet region?

1.0 DEVELOPMENT TECHNIQUE

The technique selected by ITTIL for development of an improved photon-electron counting multiplier phototube is based primarily on achieving a better understanding of the counting process occurring within the tube itself. In particular, emphasis has been placed on following a single photoelectron generated pulse as it travels through the multiplier structure to produce a single countable output pulse. While the role of cathode quantum efficiency has been universally emphasized in the design of multiplier phototubes (probably because it is so easily conceived and measured), and has been given extensive experimental and theoretical attention, our attention has been devoted more to over-all effective quantum efficiency, a much more difficult parameter to define and measure but also more significant.

The most important experimental technique used has been measurement of the output pulse amplitude distributions for various operating conditions, using a multi-channel analyzer. These include total count (with signal flux present), total dark count (no signal input), dynodes only dark count (cathode biased off) and other operating conditions selected to clarify as much as possible the conditions existing inside the tubes. Preliminary tests were made on standard ITTIL tubes constructed on other contracts or purchase orders; thus providing extensive initial and control test data at minimal cost. This was followed by the construction of custom tubes especially designed to provide key information as to the internal multiplication processes occurring.

Probably, the principal difficulty encountered with this procedure was the wide variation in test results for nominally identical tube types. Certainly it is well known that significant variations in the shape of the photoelectron counting spectrum, and of the dark count spectrum, are commonly observed experimentally. A major emphasis was therefore placed on determining the causes of these variations and methods of minimizing them in future tube design. In order to accomplish this, extensive tests were made on many different tube samples - a rather laborious and time consuming task, but indispensable for proper accomplishment of the project goals.

2.0 DISCUSSION OF PRESENT TUBE DESIGN

Since the starting point of this tube development was the present ITTIL design, a more detailed discussion of this design may be advantageous. Probably most noteworthy is the use of a true focusing electron lens between photocathode and aperture rather than the more usual electron condensing electrode configuration erroneously called "focusing" lens. The critical distinction between these two configurations is illustrated in Figures 1a and 1b. With the true focusing lens, Figure 1a, all electrons emitted from a point on the photocathode, regardless of energy and emission angle, are focused at an electron image point in the image plane of the lens. On the other hand with the condensing lens all cathode photoelectrons leaving the cathode perpendicularly at low emission energy regardless of their point of emission are concentrated into a small area or point, sometimes called the "cross over" point as shown in Figure 1b. As can be seen in Figure 1a the true focusing electron lens, if electrostatic, also involves an electron cross over point prior to the image plane so that such a lens could be either focusing or condensing depending on whether the aperture is placed at or near the image plane or at the cross over point respectively. The converse is definitely not valid, i.e., the usual condensing lenses would not also produce true electron images at some position following the cross over point if this region were unobstructed.

The reasons that true focusing offers advantages over condenser lens action are many; and not all presently understood. Certainly one reason is that the photoelectrons leaving the cathode at a finite emission angle are more closely controlled in the focusing lens, and in fact bombard the same area of D1 as the orthogonally emitted electrons, whereas in the condensing lens, these angularly emitted electrons spread out radially and may well be lost as far as the first dynode is concerned, a serious and intolerable deficiency for optimum detection.

Secondly, not only does the condensing lens bring cathode electrons into the cross over point, but it also brings other electrons from all over the front end of the tube into the same point, and thus into the multiplier structure. While this maximal collection of all electrons may be advantageous from the standpoint of increasing effective cathode quantum efficiency for large area detection problems such as scintillation counters, it does cause serious related difficulties. For example, the transit time spread may be increased due to differing path lengths for electrons from the peripheral and front end side wall areas compared to the central cathode areas. Furthermore, these peripheral areas may be more subject to excitation by spurious noise sources such as feedback, corona around the front end of the tube, field emission, etc. It must be remembered that these side wall areas are often coated with highly reactive cesium metal as well as other cathode constituent materials, and may therefore be overly sensitive to spurious excitation.

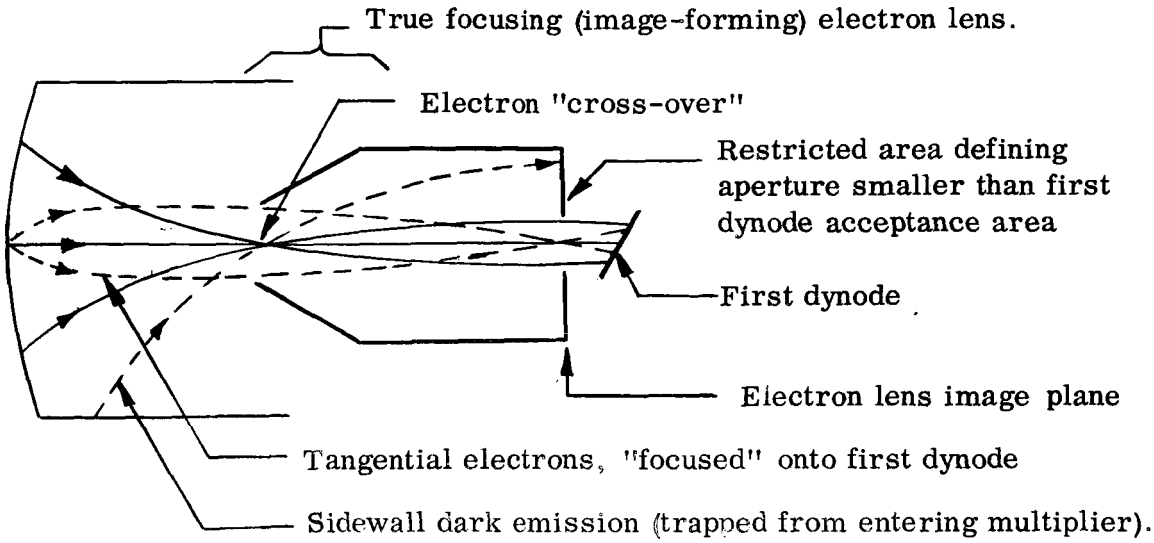

Figure 1 (a) ITTIL multiplier phototube "front-end" design with true image forming electron lens showing improved collection efficiency for selected cathode area plus sidewall dark noise suppression.

So-called "focusing" electron lens, actually a condensing or converging electron lens

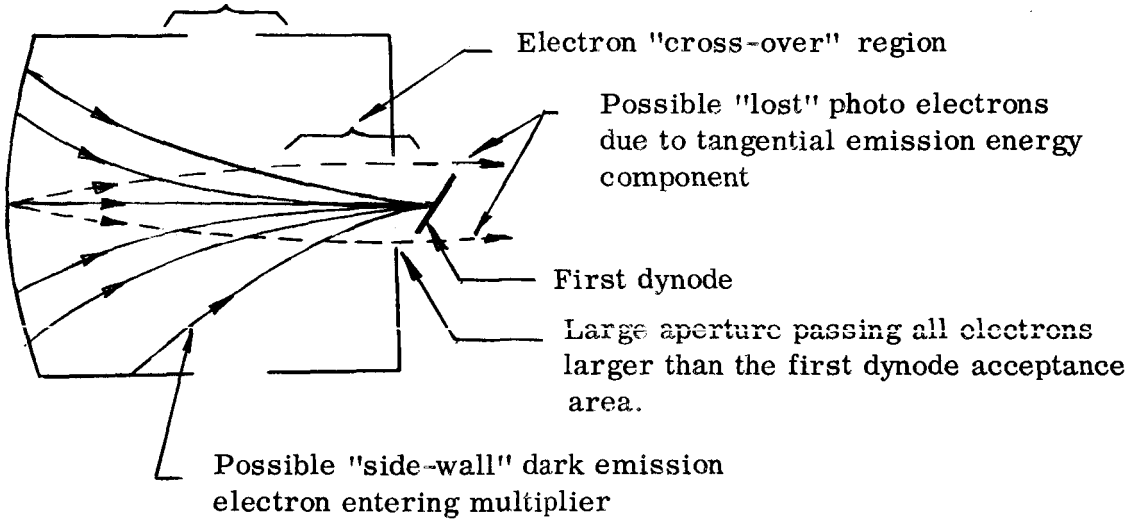

Figure 1 (b) Conventional multiplier phototube "front end" design with condensing electron lens showing possible poor collection efficiency plus excessive side-wall dark noise

ITTIL has accumulated reasonably conclusive evidence that precisely such peripheral electrons are almost automatically suppressed in the true focusing design with defining aperture. They do not fall onto the same points in the electron image plane as do photoelectrons from cathode points but are normally focused instead into other image points, much farther off-axis than the desired image points and thus outside the effective D1 area. This noise suppression is implemented in the ITTIL design by an aperture mask in front of D1 which delineates the desired photocathode area but masks off the peripheral electron emission. By shaping this aperture, any desired cathode areas up to the full faceplate area can be imaged onto D1 provided that D1 has the proper acceptance area. In present ITTIL tubes the full cathode faceplate area (approximately 3/4 inch OD) cannot be accepted by the present first dynode. This dynode can be enlarged and the magnifications of the focusing lens changed to accommodate whatever effective photocathode area is desired. If such modifications are required, a magnification change can be accomplished by an alteration of electrode dimensions and spacings, accompanied, of course, by a change in D1 to accommodate the new effective cathode, as mentioned above. Such modifications have recently been made on standard tubes which verify these expected results, though it appears that electrostatic focusing is required to partially correct for abberations that are inherent in simple electrostatic lenses.

A third advantage of the ITTIL focused front end design is the use of two apertures, one for focusing and a second for defining the desired effective cathode area. This combination of two relatively small apertures at some distance apart combined with the extension of the defining aperture plate out to the sidewalls of the tube, effectively isolates the cathode and image section of the tube from the multiplier section. Very little probability exists for any particle such as a gas ion, visible photon, or X-ray photon generated in the multiplier section of the tube to return to the sensitive photocathode region. This isolation of the two tube sections is believed to be critical in producing low dark noise as well as low spurious noise under counting conditions permitting high gain and high operating voltages.

A fourth advantage of the ITTIL design is the effective removal of photocathode suppression electric field effects at D1. When D1 is placed at the cross over point in the usual design, the secondary emitting surface of D1 is exposed directly to the suppressing electric fields from the photocathode. This may suppress some secondary electrons or cause improper trajections so that these electrons either miss D2 or strike D2 improperly. In the ITTIL design D1 "sees" the cathode only through the two small apertures, a negligible effect. This design also permits a unique experimental procedure, (used extensively in this contract), namely the effective biasing off of all photocathode electrons by operating the cathode electrode positive with respect to D1 (usually at D2 potential). This condition, called "dynodes only" in the experimental data, permits a clear

separation of output pulses originating in the dynodes from those originating from the photocathode.

3.0 PULSE COUNTING CIRCUITS

A critical problem in single electron pulse counting is the selection of proper counting circuitry. Such circuits must introduce minimum noise or false electron counts while at the same time deriving maximum results from the multiplier phototube under investigation. Contrary to expectations, it has been found during earlier work at ITTIL that the selection of proper circuits is quite difficult. In fact, there is considerable evidence that improper choices have been made in previously reported attempts at single electron counting which have masked the true characteristics of the multiplier phototubes proper, and led to erroneous conclusions regarding their capabilities.

The multiplier phototube is enclosed in a dark netic-conetic shielded holder, suitably blackened inside, and fitted with a point light source of variable intensity. This unit is mounted on the test fixture which consists of a metal box with tube socket and voltage divider so constructed as to allow the cathode to be biased off, and changing of certain resistors in the divider string. The high voltage R-C filter shown in Figure 2 is located in a shielded enclosure located in the high voltage lead coming from the power supply.

Considerable care must be taken to shield all portions of the multiplier phototube circuits, particularly variable voltage sources, high voltage input and signal output leads, used in the various performance tests. Without these precautions stray pickup, sometimes causing signal pulse troubles, as well as spurious dark noise, can appear.

A number of features of this present equipment, see Figure 2, need comment here.

The Tennelec TC M170 Preamplifier with a selectable gain of 5 or 50 is mounted as close to the anode of the multiplier phototube as possible, with a 10 K ohm load resistor. Repetition rates are maintained low, by adjusting the light source, so that the relatively slow R-C time constant of the anode-preamplifier circuit does not interfere with pulse amplitude distribution measurements (minimum pulse overlap). Furthermore, the dead time of the counting equipment helps avoid errors due to pile up.

Coupling from preamplifier to the TMC Model 101 pulse height analyzer must be carefully selected to give proper pulse rise and fall times, minimum over-shoot, etc. The coupling circuit (see Figure 2) appears optimal for this equipment. Mr. Edward Pairstein of Tennelec Instrument Co. was consulted on this matter.

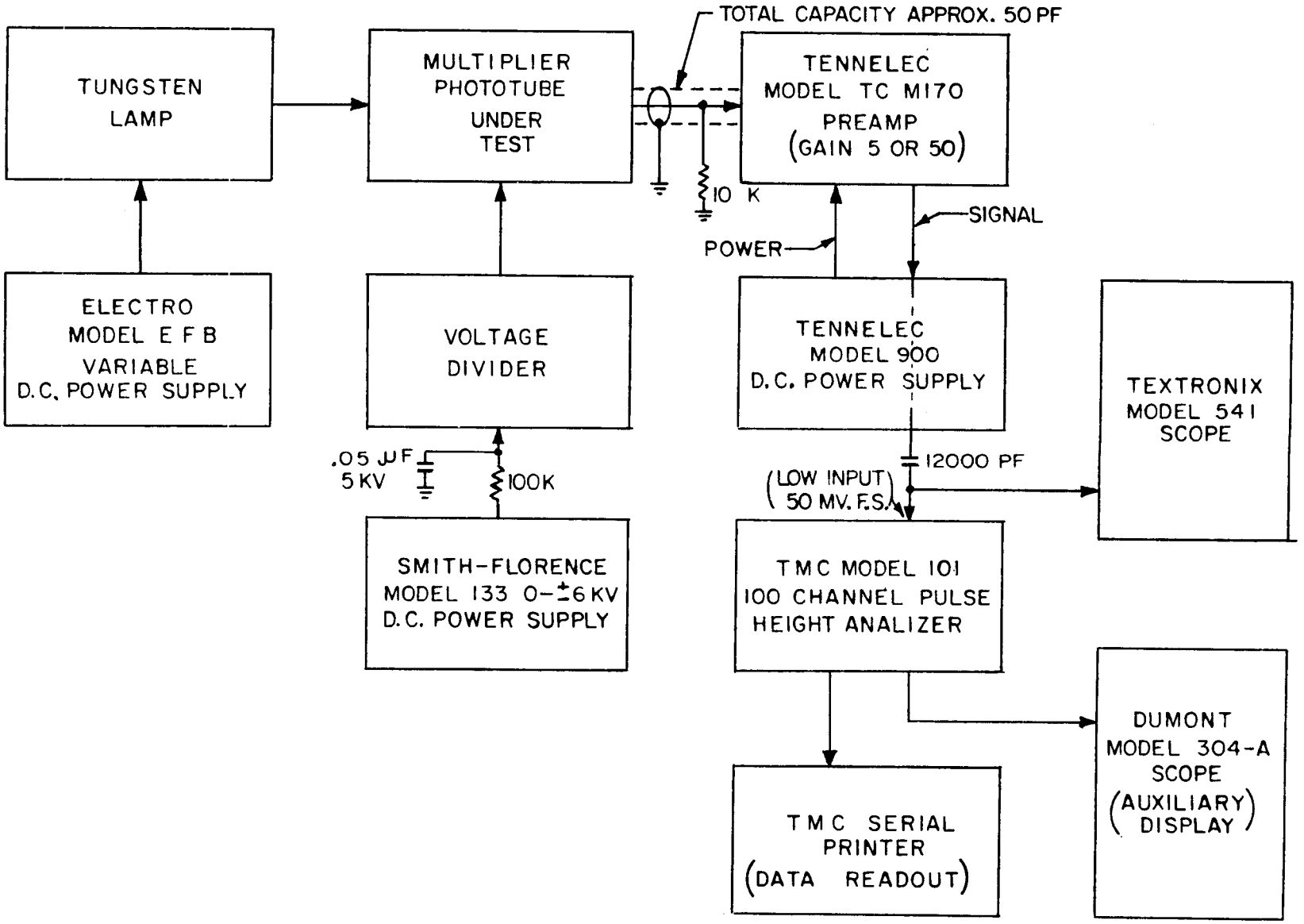

Figure 2 Block Diagram of Pulse Counting Equipment

Since the multi-channel analyzer used does not print out total counts, a Hewlett-Packard Model 523B Eput meter has been adapted to read out integrated total counts within the selected window of the analyzer. By adjusting this window, it is possible to select portions of the pulse amplitude spectra for special study. A useful technique for example, is to set this window to include all pulses between the valley or minimum normally occurring on the small amplitude side of the single electron peak (at about 0.2 to 0.5 $\bar{V}$) and some upper level usually channel 100 of the analyzer. Thus the Eput meter will read, with good selectivity most of the true single electron pulses while rejecting smaller and larger spurious pulses. Effectively this would then be the output used in a single electron counting application without the complicated multi-channel analyzer in use.

Normally, the multi-channel analyzer is used with zero offset in the gain control. An internal offset adjustment of about 70 percent of channel 1 is necessarily retained, however, to avoid the enormously large number of small amplifier dark noise pulses. All channel 1 counts must therefore be interpreted with this internal offset in mind. Multiplication of a recorded channel No. 1 count by 7/3 will give a corrected count useful in plotting analyzer spectra.

Some difficulty has been experienced in the analyzer in recording spurious pulses in certain specific lower channel numbers when ultra-large pulses (normally to be "recorded" only above channel No. 100). This highly undesirable effect was investigated using a Hewlett-Packard Model 212A pulse generator and a pulse simulating circuit as shown in Figure 3 to generate known amplitude pulses of given numbers to feed into the multi-channel analyzer. This test technique proved to be particularly useful in checking analyzer performance. With the cooperation of TMC the difficulties with large pulses was corrected by appropriate internal adjustments of the analyzer. A further assurance of elimination of this problem is achieved by adjusting tube gain and analyzer gain to set $\bar{V}$ in about Channel 15-20. This avoids appreciable numbers of large counts beyond channel 100, and speeds up the print out process (we normally print out only 40-50 channels) and conserves storage space on print out records.

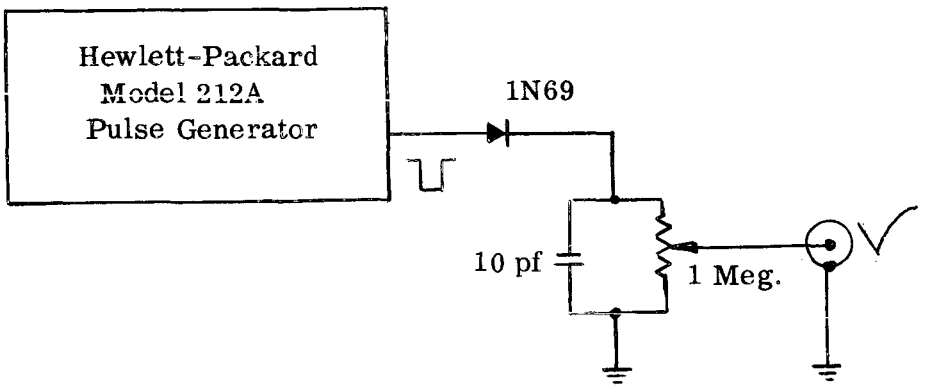

Figure 3 Pulse Simulator

3.1 Noise Source Investigation

Although the intent of this contract was to investigate the characteristics of the multiplier phototube proper, and the pulse amplifier and external counting circuits, various other circuit problems unfortunately could not be entirely neglected. It was discovered that the purchase of a good low-noise pulse amplifier, such as the Tennelec M-170, was, in itself, insufficient to assure proper counting characteristics, possibly due to the previous emphasis by circuit designers on multi-electron counting (scintillator applications) and high energy particle counting (solid state detectors) as opposed to our emphasis on the counting of low energy (0 to 1 ev) electrons and photons (1 to 2 ev).

In addition, we attempted to operate most tubes tested at as low an over-all voltage as possible to minimize high voltage troubles with corona, field emission, glass fluorescence, etc., so that we were dealing in general with charge pulses of about 10^{-12} to 10^{-14} coulombs (1.6×10^{-19} coulombs for the electron, times 10^5 to 10^7 multiplier gain). Although these, in turn, produced voltage pulses of about 0.1 to 10 millivolts in the 10 to 100 picofarad output capacitance, considerable difficulty was experienced with stray pickup of spurious pulses in our counting equipment originating from many sources, including tesla coils, 1 to 10 kw r-f generators for tube processing, and fluorescent lighting fixtures with defective lamps or starters.

As reported in the third quarterly report, there was concern expressed about the possibility of noise being generated in the carbon resistor voltage divider. An experiment was conducted in which the dark count obtained from a tube in our standard 100 K ohm-per-stage divider was compared to that obtained from the same tube in a low-noise 20 megohm resistor divider. Figure 4 shows the two spectra with a 6:1 difference in dark counts. A subsequent experiment using these same dividers and an additional divider of 100 K low-noise resistors was performed. At the time, the tube laboratory engineering staff was asked to suspend the operation of such equipment as would interfere with this work, for a time long enough to get the three spectra shown in Figure 5. As can be seen, no essential difference exists in the three dark spectra. A small gain change is apparent in the third signal spectra due to a slight difference in the voltage distribution obtained with the 20 megohm divider. Perhaps it should be noted here that steps could be taken if necessary to avoid interference from many types of equipment causing stray pulse pickup. For example r-f generator pulses have a characteristic damped sinusoidal appearance on the monitoring display oscilloscope, which cannot be mistaken visually for true dark count even though they are recorded by the multi-channel analyzer. Circuits could certainly be devised to avoid this interference should it succeed in penetrating, as it does, the tube and circuit shielding.

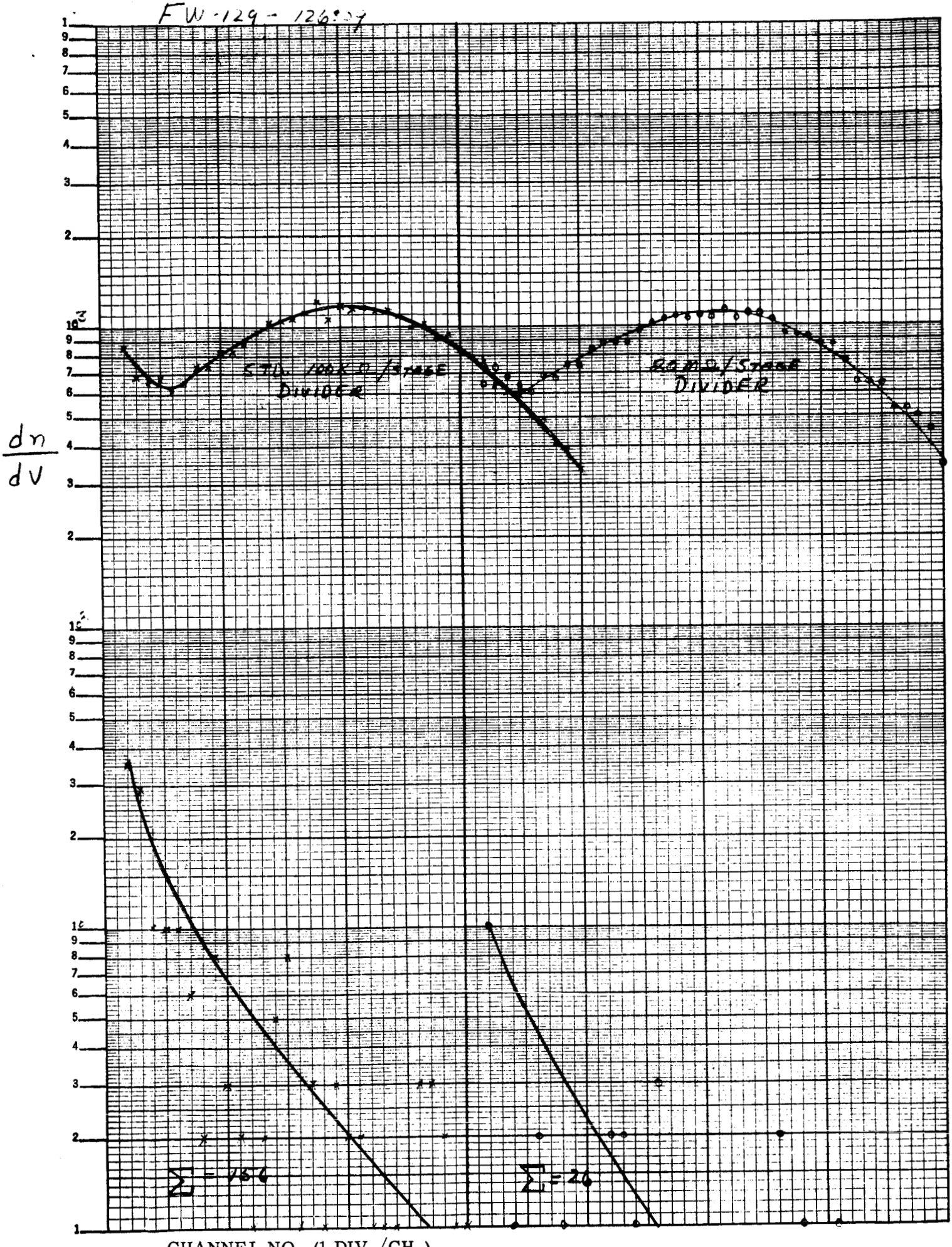

Figure 4

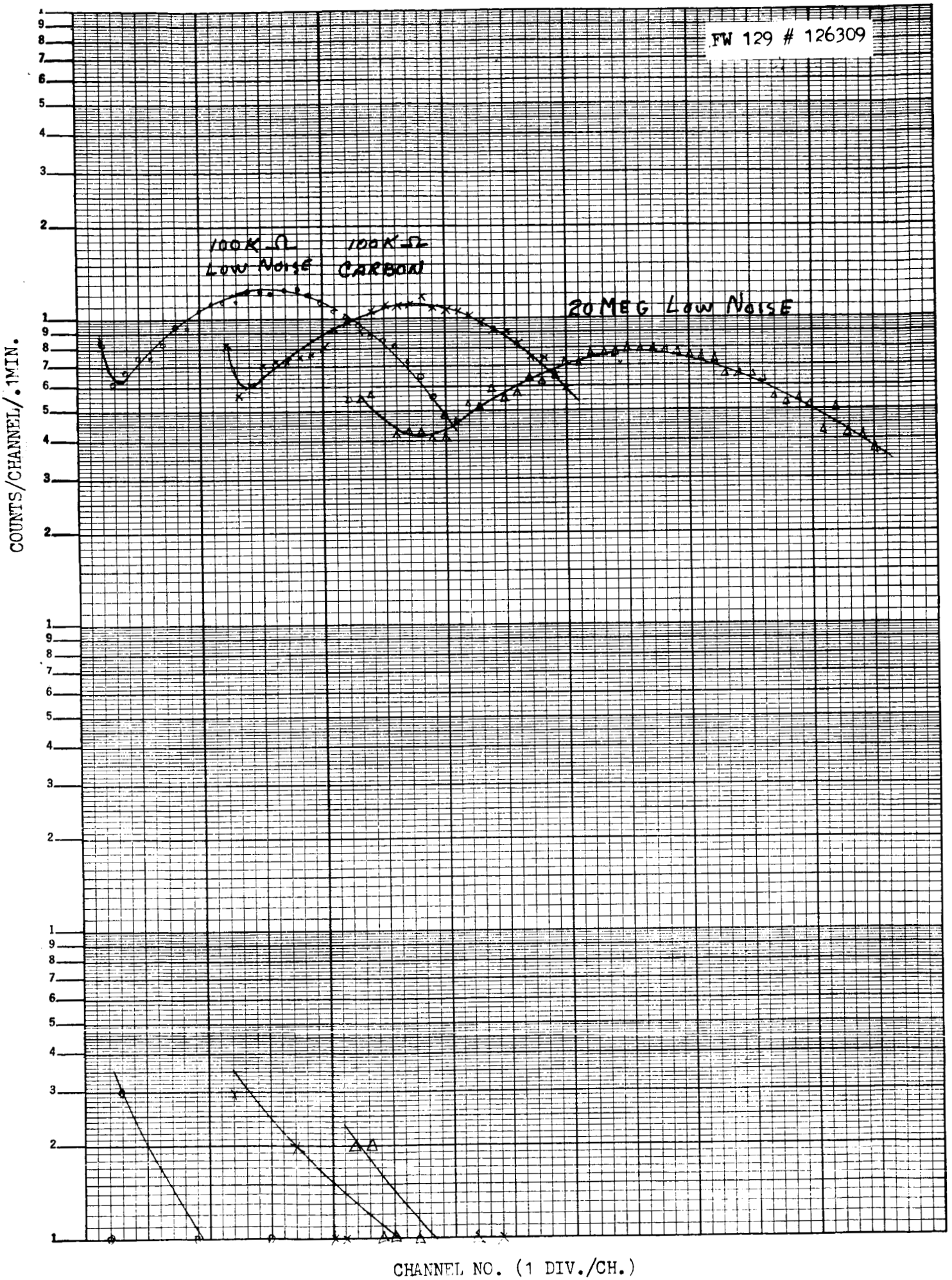
FW 129 # 126309
100K Ω
Low Noise
100K Ω
CARBON
20 MEG Low Noise
COUNTS/CHANNEL/.1MIN.
CHANNEL NO. (1 DIV./CH.)

Figure 5

Although stray pulse pickup is normally not eliminated by removing the high voltage from the multiplier phototube (except for some high frequency pulses attenuated by the R-C filter in the high voltage lead, see Figure 2) or by the installation of r-f power line filters, we did observe some stray pickup which appeared to be tube high-voltage supply sensitive, for which the generation mechanism is presently unexplained. The possibility still exists that voltage breakdown in the divider resistors, pin contacts, solder joints, etc may lead to spurious dark pulses present only when the high voltage is applied and bleeder current is present but this seems to be below the level of the other noise sources.

Another known problem area is dark current leakage in the tube, including socket and base, which can produce erratic bursts of pulses, tending to invalidate some of our test runs. Although these bursts can be readily identified upon visual observation at low counting rates, their presence in a tube is a serious fault to which considerable attention has been paid. A significant reduction in these leakage pulses has been accomplished recently on all production tubes by the inclusion of internal anode lead guard ring electrodes to prevent current bursts from the negative high voltage electrodes (cathode, etc) from reaching the anode pin.

4.0 EFFECTS OF PRIMARY ELECTRON ENERGY ON THE PULSE HEIGHT DISTRIBUTION

Figure 6 shows a family of pulse characteristic curves as a function of the voltage applied between cathode and D1. At the lower voltage, 15 volts, no peak appears in the signal spectrum and the total signal count, 9.1×10^3, indicates that approximately 90 percent of the photoelectrons have been lost, if we choose the 285 volt curve as optimal for reasons which will be discussed later. This loss is probably due to nonexcitation of secondary electrons at the first dynode. At 60 volts, a suggestion of a plateau in the distribution appears near channels 2 and 3 and the loss of primary electrons has dropped to about 60 percent. With the application of 135 volts, a definite peak is apparent in the signal spectrum with a peak-to-valley ratio of 1.5 and a loss of only 20 percent of the primaries.

Optimum results, from several viewpoints, seem to be obtained at approximately 285 volts. First of all, the peak-to-valley ratio is 2:1, with no readily observable loss of primaries. The significance of a well defined peak becomes apparent when one considers the problem which arises in counting applications, of setting the discriminator bias in the pulse amplifier in order to count signal pulses with maximum efficiency, i.e., biasing off as many dark pulses as possible, while counting a large percentage of the true signal pulses. Without this well defined peak, this decision is difficult, if not impossible to make. Secondly, it will be noted that the dark count is not appreciably higher than for lower voltage. The position of the peak is, as would be expected, shifted somewhat toward higher channel numbers, due to the higher primary electron energy.

At 595 volts, the peak-to-valley ratio has fallen to about 1.8:1 but the counting efficiency is for all practical purposes unchanged in spite of the fact that the dark count has risen suddenly 5 or 6 times. Careful inspection of the data will show that these counts are primarily in the early channels where they may be biased off, without seriously affecting the counting efficiency, as was explained earlier. There are, however, a measurable number of larger pulses in the peak region at this voltage.

With 885 volts, operation is definitely inferior. There is no peak, only a plateau, the counting efficiency has fallen, and the dark count has risen 200 or 300 times as compared to that at voltages below 300. A significant number of these dark counts now fall in the region of the peak which accounts for the reduced counting efficiency.

In these tests the multiplier potential difference was held fixed at 1300 volts, so that multiplier gain, following D1, remained approximately constant. Thus the

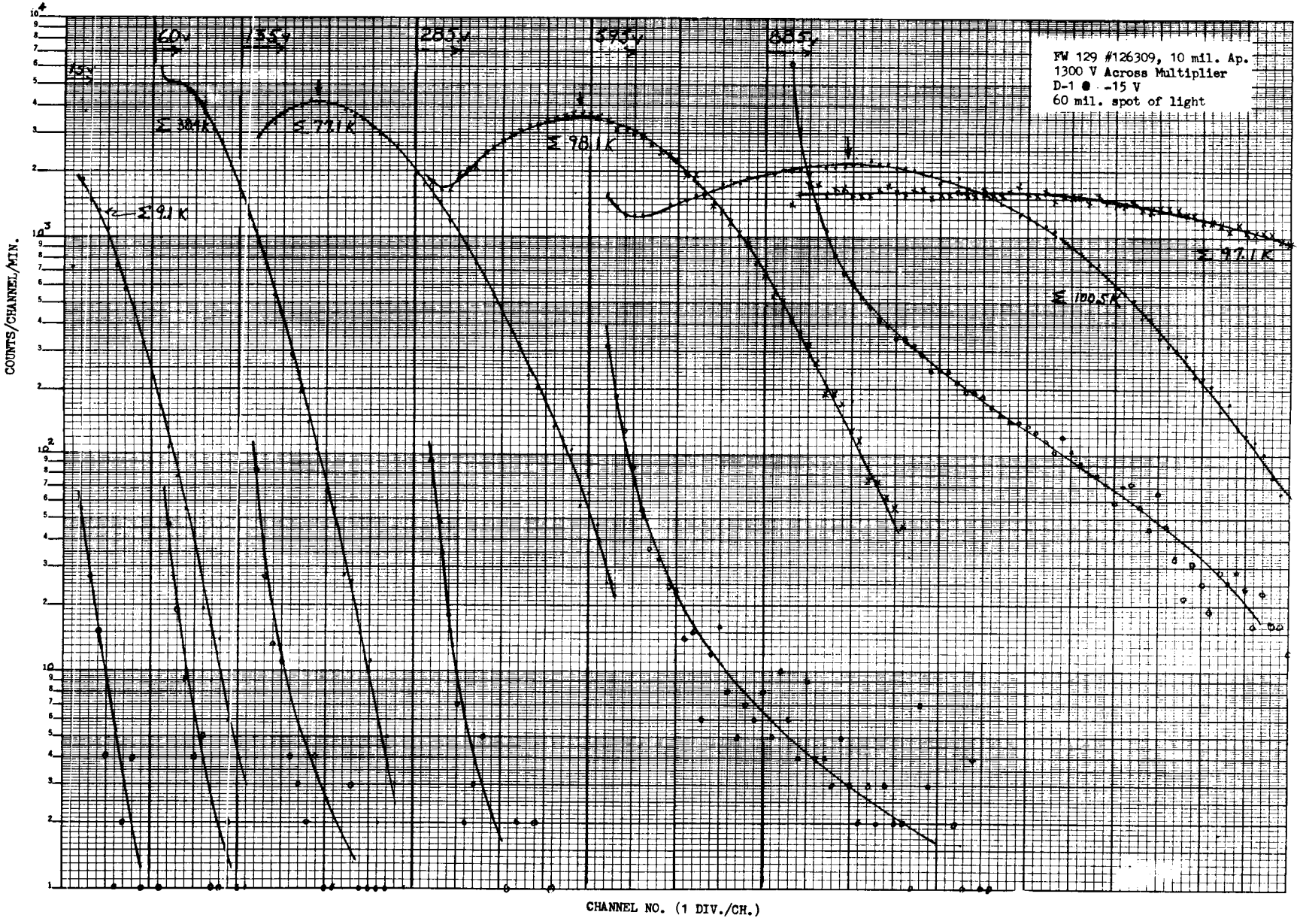
FW 129 #126309, 10 mil. Ap.
1300 V Across Multiplier
D-1 ● -15 V
60 mil. spot of light
60V
135V
285V
593V
685V
Σ 30.1K
Σ 77.1K
Σ 98.1K
Σ 91.1K
Σ 97.1K
Σ 100.5K
COUNTS/CHANNEL/MIN.
CHANNEL NO. (1 DIV./CH.)

Figure 6

channel number, at which the peak appeared, is directly proportional to the effective SE gain at D1. Figure 7 is a plot of this parameter versus primary energy for the three primary energies for which a definite peak was observed. These points do fall near a typical SE curve for MgO as indicated. The gain at 75 volts is about 1/6 of the peak, or 1/6 x 10 = 1.7, a typical MgO surface. This is somewhat lower than the average dynode gains of 2 to 2.5 determined from over-all multiplier gain measurements, and thus indicates that improvements in processing D1 surfaces are needed, as suspected earlier.

It is worth noting that reliable absolute gain measurements for D1 are not readily made using ordinary current measuring techniques in the dynode circuits. The various sources of error-producing currents, such as current from D1 to aperture electrode, or D1 direct to D3, etc., as well as the changes in gain and current levels occurring when any potentials other than true operating potentials are applied to following dynodes such as D2, D3, etc., cause serious errors. This is particularly true if the current levels during test are anywhere near as low as they are during actual multiplier operation. Consequently, no absolute gain calibration has yet been placed on the ordinate of Figure 7. A compromise technique yielding fair results is described in ITTIL Memo 326 attached, but even this refinement is not considered to be particularly accurate.

The loss of true peaks and counting efficiency in the signal electron distributions of Figure 4 checks qualitatively with the expected multiplier behavior predicted by Lombard and Martin and others. If the primary energy is too low, many electrons will be trapped completely at D1 and the distribution may have no true peak (i.e., $p(o) > p(1) > p(2)$, etc. where the $p(n)$ refers to the probability of n electrons being ejected.)

The behavior at high energies was not unexpected based on our previous experience, but is definitely anomalous, both from the standpoint of a loss of a peak in the distribution and the great increase in dark count. Further experimental work is required on this problem for it bears directly on the ability to produce improved counting capabilities by increasing the primary electron energy. It presently appears that this may be merely a field emission related problem in the image section front end of the tube. If so, improved electrode design, as used in such high voltage ITTIL image tubes as the IC6, IC16, 6032, 6914, or others, may lead to a satisfactory solution.

Figure 8 is another family of curves showing signal and dark counting characteristics, as a function of the voltage difference between the aperture electrode and D1, with approximately 300 volts between cathode and the aperture electrode. As the D1-to-aperture potential is decreased from +20 to -40 volts there is a

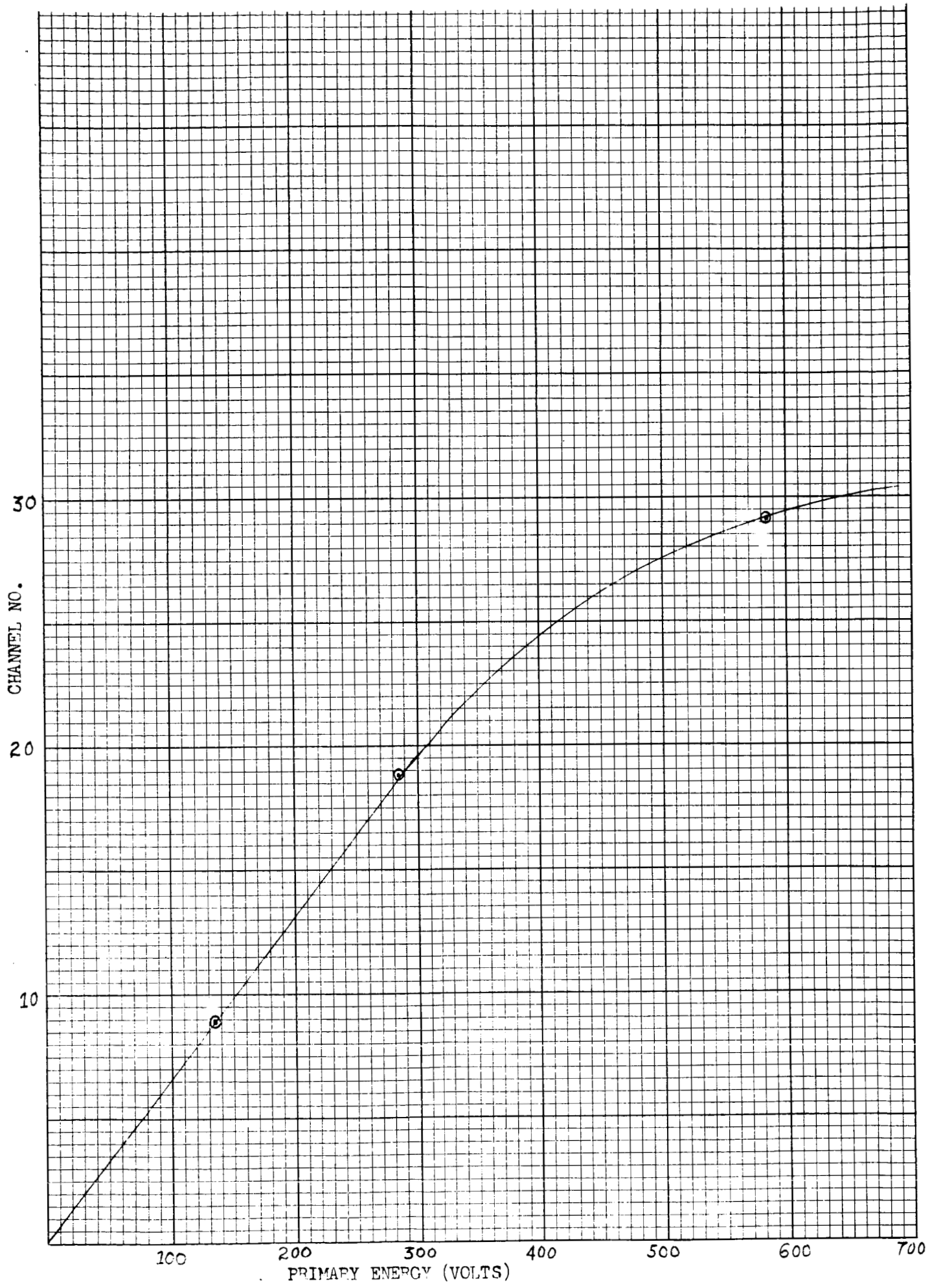
30
20
10
CHANNEL NO.
100
200
300
400
500
600
700
PRIMARY ENERGY (VOLTS)

Figure 7

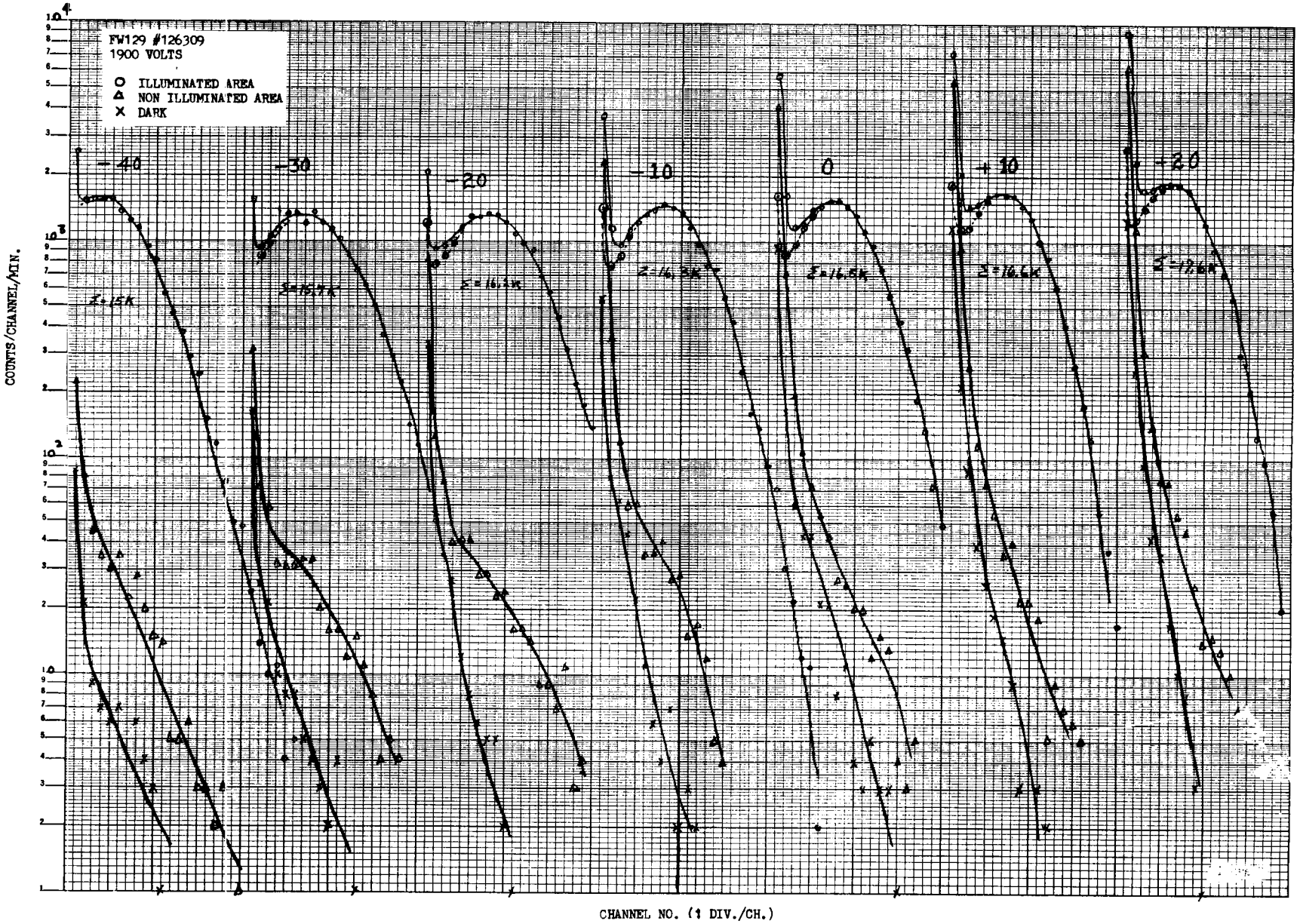
FW129 #126309
1900 VOLTS
ILLUMINATED AREA
NON ILLUMINATED AREA
DARK
-40
-30
-20
-10
0
+10
+20
COUNTS/CHANNEL/MIN.
CHANNEL NO. (1 DIV./CH.)

Figure 8

substantial reduction in total dark count notwithstanding the fact that there is an increase in the gain of D1, and therefore, an over-all increase in multiplier gain for this same change. It appears then that in this tube negative values of D1-to-aperture potential are doubly effective in that the absolute counting efficiency goes up while the dark count goes down for a given pulse amplitude discrimination level.

Tentatively, one might assume that the negative D1-to-aperture potential tends to suppress secondary electrons from the aperture electrode, produced by thermionic emission from the total cathode area, which might enter the aperture. These electrons would tend to be of low energy (elastically scattered electrons being energetic enough to travel back to other portions of aperture electrode surface) so that the -10 to -40 volts would be sufficient to produce this suppression. This hypothesis is partially supported by the pulse amplitude characteristics obtained by flooding the photocathode with light and magnetically deflecting the IEPD (instantaneous effective photocathode diameter) area under a small (approximately 0.080 inch diameter) opaque mask displaced slightly from the center of the cathode. Direct illumination of the IEPD area is then minimized, but production of secondaries internal to the aperture electrode from bombarding photoelectrons is greatly enhanced. The resulting pulse amplitude distributions shown in Figure 8 are quite similar to the dark count distributions and are similarly suppressed by negative D1-to-aperture potentials. A detectable difference can be observed for the larger pulse amplitudes, near the peak, where it would appear that a group of true electron pulses is beginning to occur. Such pulses are to be expected on the basis of light passing through the flooded areas of the photocathode and being scattered (by tube parts, etc) back onto the central (nominally masked off) area of the photocathode producing photoemission directly from the IEPD area. Under these test conditions, it can be seen that this back scattered emission ranges from about 3 to 5 percent of the directly excited magnitude. Consequently, minimum "dark" noise (no input flux directly incident on the IEPD area) will require optical masking of any stray or flooding radiation on surrounding photocathode areas.

Of particular note in this tube was the low magnitude of total dark count at comparatively high effective photoelectron counting efficiencies. By integrating both the signal distribution curves and total dark curves, the corresponding counting efficiency (relative total signal counts recorded above a given channel number) and total dark counts above the same channel were computed and shown in Figure 9. It can be seen that only one dark count/second was recorded at 85 percent counting efficiency, a remarkably low dark count at such a high counting efficiency.

If this dark count varied linearly with the IEPD area, this would imply approximately 800 dark counts/second/cm^2 of photocathode. However, since the shape of the dark count curve shows that these dark counts are not coming primarily from the photocathode, the total dark count density should be less than this magnitude.

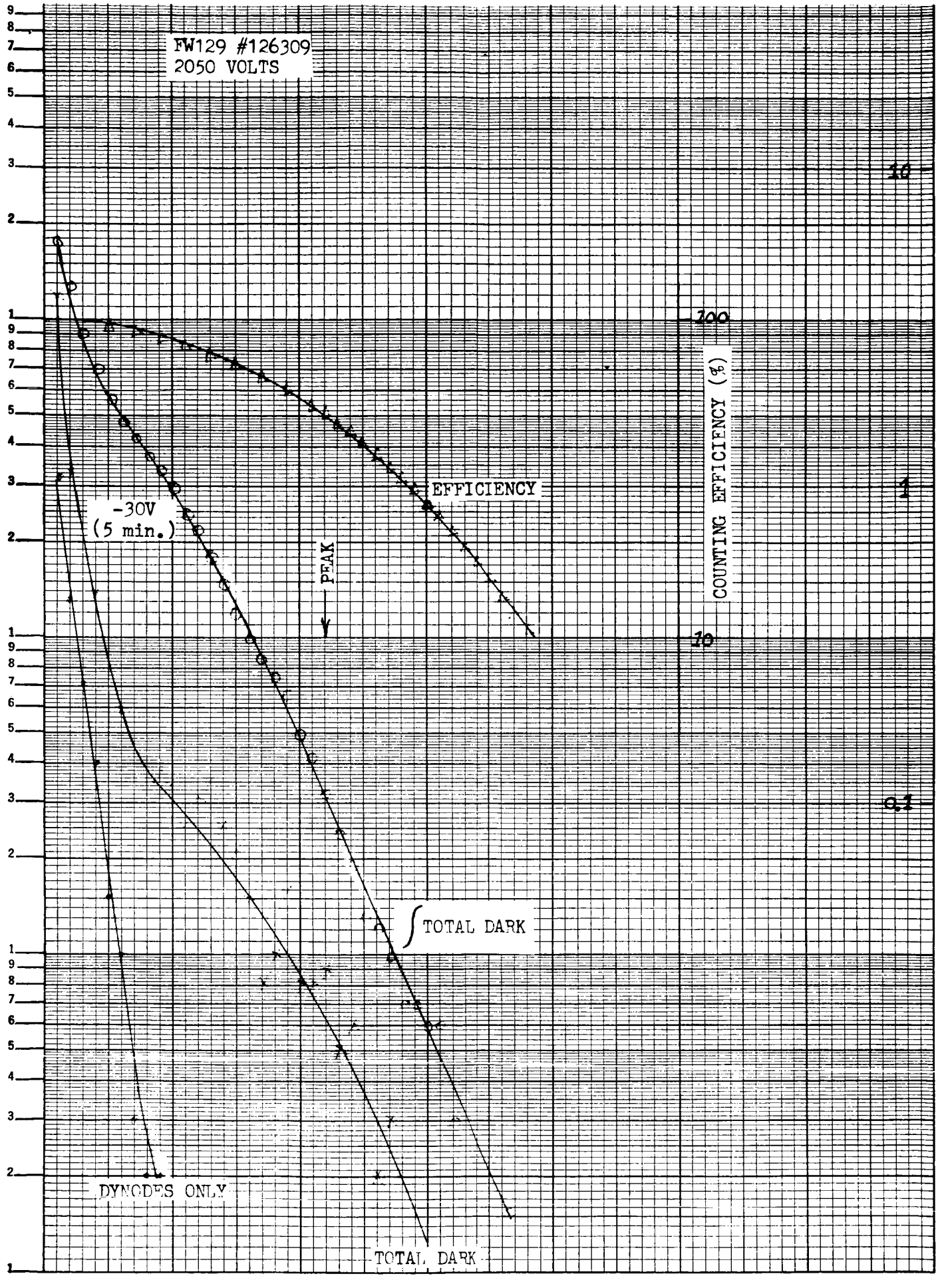
FW129 #126309
2050 VOLTS
EFFICIENCY
-30V
(5 min.)
PEAK
TOTAL DARK
DYNODES ONLY
TOTAL DARK
COUNTING EFFICIENCY (%)
COUNTS/CHANNEL/ SEC.
CHANNEL NO. (1 DIV./ CH.)

Figure 9

When this tube is operated with the cathode biased off (at D2 potential) the residual dark count ("dynodes only") still depends on the D1-to-aperture potential as shown in Figure 10. The residual dark count appears to level off below -30 volts for D1-to-aperture, and increase steadily as this potential is increased to +20 volts as shown. A possible explanation is that the more positive D1 potentials tend to collect stray electrons from various sources, such as aperture electrode, side supports, etc. generating secondaries or reflected primaries which then proceed down the multiplier chain. The inefficiency of this process and low gain characteristics at D1 are evidenced by the fact that the resultant pulse amplitudes are much smaller than $\overline{V}$ (average pulse amplitude). However, since fractions of one electron cannot be transmitted from D1 to D2, the pulse amplitudes observed appear to be anomalously low. Note that the observed effect is of incorrect polarity to be a result of variations in collection efficiency for secondaries going from D1 to D2; higher negative voltages on D1 should then increase, rather than decrease the dark count magnitude.

5.0 DYNODE SECONDARY EMISSION RATIO ENHANCEMENT

A number of experimental tubes were built with special processing of one or all of the dynodes. In general, none of the processes applied was successful in increasing the secondary electron yield of the dynodes. In fact, most of them were inoperable due to excessive multiplier noise.

Two FW-129's had antimony evaporated on the surface of all dynodes and two others had antimony on D1 only. While those with antimony on D1 only were somewhat less noisy than the others, the techniques described earlier, i.e., of operating D1 somewhat negative with respect to the aperture, did not produce the expected improvement in dark counting rate. No data is included here on the dark count distribution because the pulse rate exceeded the resolving time of the analyzer which precludes the acquisition of meaningful data. It can only be assumed that our technique for producing this type of dynode surface requires refinement since it is known that competitive tubes do, in fact, use CsSb secondary emitting dynode surfaces. However we have not confirmed that low dark counting rates and good single electron counting characteristics can be obtained with CsSb dynode surfaces.

It has been shown[1,2,3] that the SE ratio of an insulating material can be enhanced by producing an electric field internal to the material so that secondary

1 "Study of Electrical and Physical Characteristics of Secondary Emitting Surfaces", WADL Tech. Report 59-473 p-6 (1959).
2 "Study of Electrical and Physical Characteristics of Secondary Emitting Surfaces", WADC Tech. Documentary Report No. ASD-TDR-62-707 p-34 (1962).
3 "An Investigation of Secondary Emission by Pulse Techniques", L. G. Wolfgang, Doctoral Thesis, Purdue University, 1963.

COUNTS/CHANNEL/MIN.
CHANNEL NO. (1 DIV./CH.)
FW129 #126309 2050 V
LIGHT (.060 in. dia. spot)
TOTAL DARK
DYNODES ONLY

Figure 10

electrons generated by primaries penetrating the surface see an accelerating field out of the material. Because of these principles and the fact that a high gain D1 is of critical importance to good single electron counting characteristics, a tube with a single fringe (thickness 0.085 microns)[4] of MgO evaporated on D1 was built. This tube originally gave signs of erratic behavior, its operation being characterized by the ragged pulse shape shown in Figure 11. After a few weeks on the shelf, its operation appeared to have stabilized and its output pulses are now of the more normal smoothly decaying type. (See Figure 39a.)

To perform this experiment the tube was connected as shown in Figure 12.

The high voltage was applied between aperture and ground with D1 at aperture potential. The photocathodes were made 360 volts negative with respect to aperture-D1. Under these normal operating conditions a spectrum was taken and is shown in Figure 13 (a). Next, with the high voltage applied as before, the photocathode was made 90 volts negative and D2 was connected to aperture and D1 made -45 volts with respect to aperture. The light intensity was increased so that D1 was bombarded strongly to charge it to aperture-D2 potential, thus producing an accelerating field, for secondaries, out of the MgO. Following this charging procedure D2 was returned to its proper potential on the divider and the light intensity reduced to its previous level, the photocathode was returned to -360 volts but D1 remained at -45 volts. A spectrum was taken which is shown in Figure 13 (b).

The charging procedure described above was repeated except that D1 was operated at +45 volts with respect to aperture, thus producing a retarding field. A spectrum thus obtained is shown in Figure 13 (c). The net result of these tests indicate that the accelerating field does improve the distribution but unfortunately the time actually spent in counting (0.1 min.) was short enough so that statistical variations make it difficult to detect any shift in the peak location of the distribution.

At first thought it was felt that longer counting times were impractical because of the possibility of changing the electric field across the MgO layer. It appears now from the following calculation, that much longer counting times could be used without the possibility of this trouble. The capacity of the MgO layer on D1 can be calculated as follows:

4 ITTIL Research Communication No. 23 Control of Layer Thickness of Vacuum Deposition During Evaporation by G. Papp.

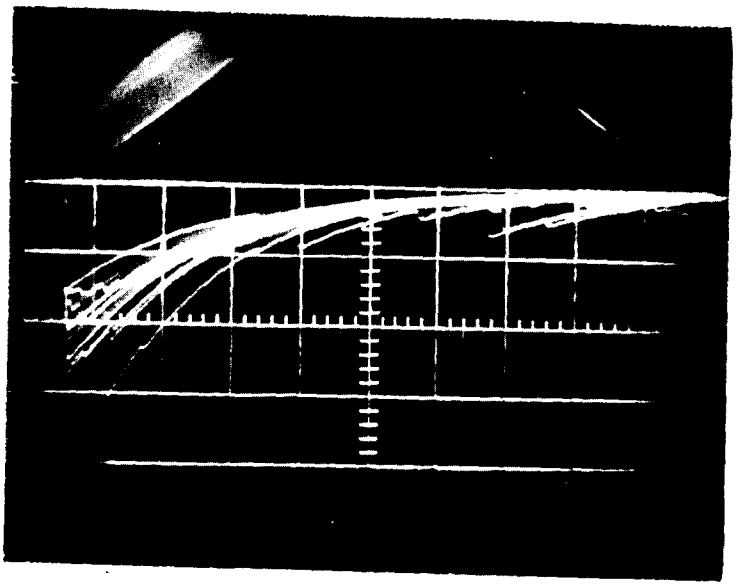

Figure 11

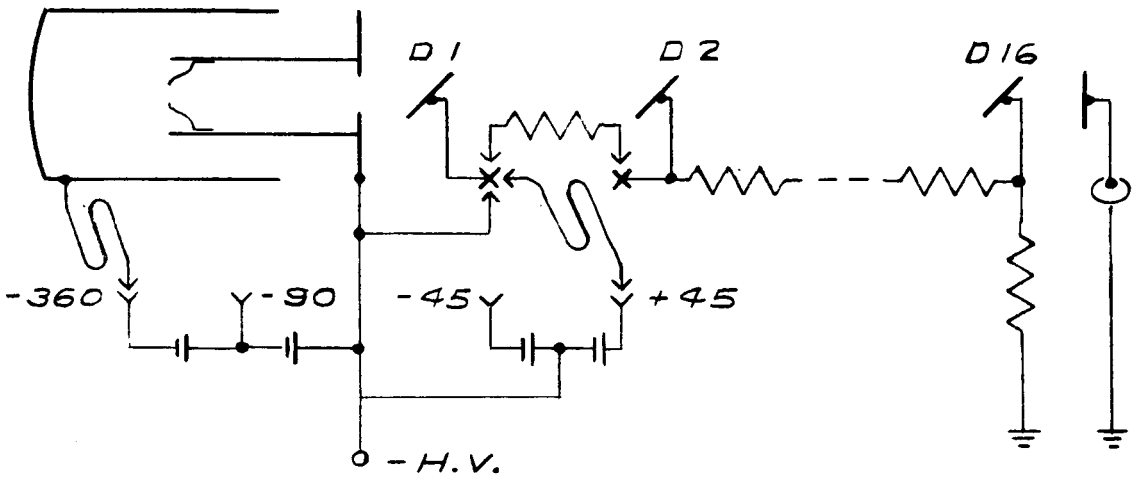

Figure 12

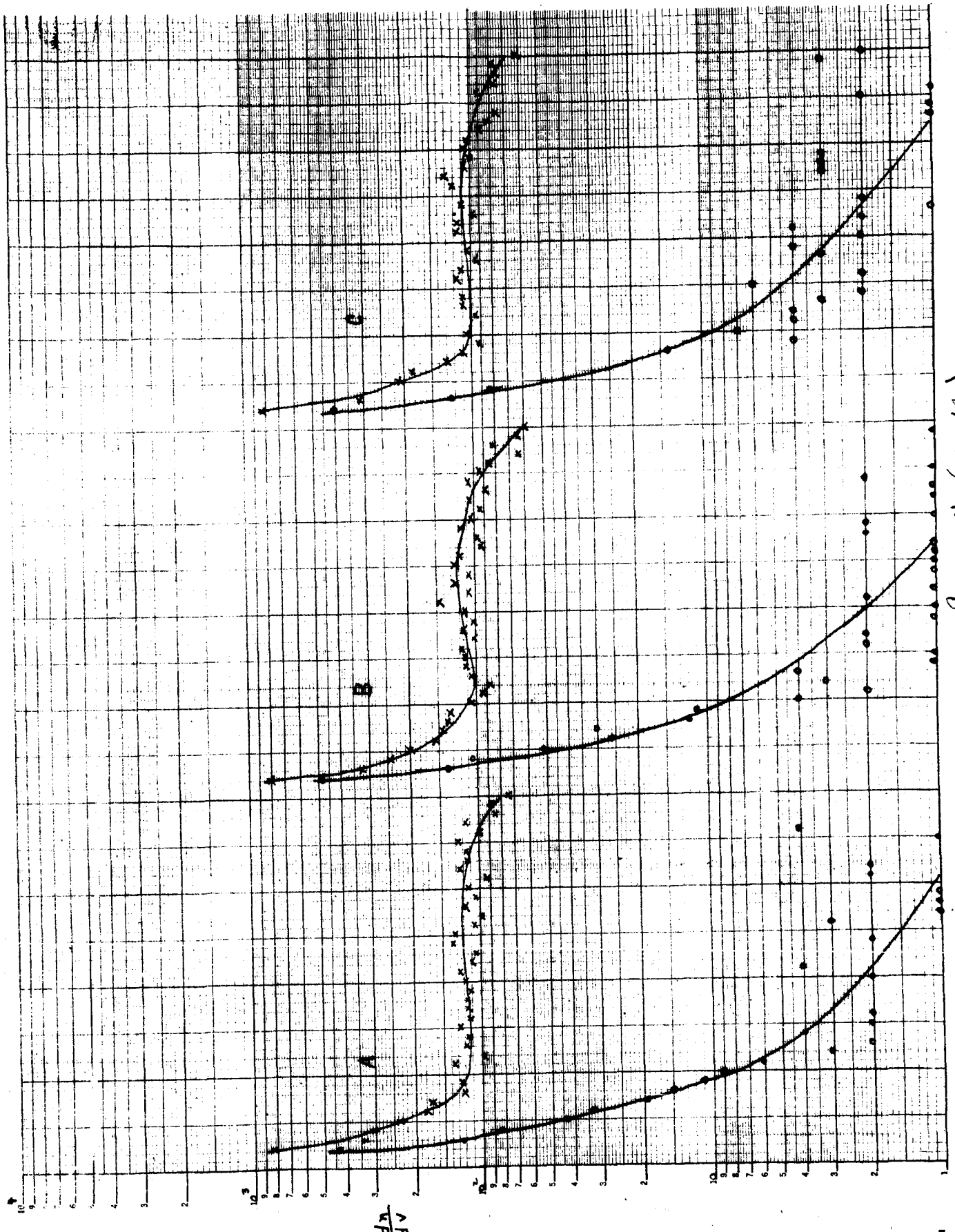

Figure 13

$$C = K \epsilon_o \frac{A}{d}$$

where

K = dielectric constant of 10 for MgO

$\epsilon_o = 8.85 \times 10^{-12}$ farads/m (in vacuo)

A = effective dynodes area of 4×10^{-6} m^2

d is MgO thickness $\approx 0.1\ \mu = 10^{-7}$ meters

$$C = \frac{10 \times 8.85 \times 10^{-12} \times 4 \times 10^{-6}}{10^{-7}} = 3.54 \times 10^{-9} \text{ farad}$$

since Q = it = cv we can write

$$t = \frac{cv}{i} \qquad (1)$$

If we assume a counting rate equal to the limit of the analyzer's capability, namely 10^5 counts, then

$$i = \frac{10^5\ e}{\text{sec}} \cdot \frac{1.6 \times 10^{-19} \text{ coul.}}{e} = 1.6 \times 10^{-14} \text{ amperes}$$

Substituting in (1), and assuming a 1 volt change in the electric field:

$$t = \frac{3.54 \times 10^{-9} \times 1}{1.6 \times 10^{-14}} = 2.2 \times 10^5 \text{ sec.}$$

$$2.2 \times 10^5 \text{ sec.} \times \frac{1 \text{ hr.}}{3.6 \times 10^3 \text{ sec}} = 61 \text{ hr}$$

If we assume a secondary emission ratio as high as 10 the time required to change the field is still 6 hours. In view of this favorable situation it would probably be well to return to this experiment for further investigation, in an attempt

to make use of the expected high secondary emission properties of MgO surfaces.

6.0 LOW ENERGY ELECTRON CONTROL

As a means of controlling low energy electron penetration of the defining aperture two tube types were constructed as shown in Figures 14 (a) and 14 (b). The configuration shown in 14 (a) was almost completely ineffectual in controlling these electrons. However the design shown in 14 (b) was found to be capable of the control required while, at the same time, independently controlling the electric field in the region between D1 and defining aperture. In a special cascade aperture tube, (No. 016539) a standard 0.070 inch diameter aperture, A1, was followed by a second slightly larger aperture, A2, (0.100 inch diameter) shielding the bombarded area of D1 from the defining aperture. Figures 15 to 17 describe the resulting interesting behavior of this tube as a function of the various selected operating potentials.

6.1 Mode 1: A2 at D1 Potential, A1 Variable

For Figure 15, A2 was operated at D1 potential, interposing minimum field gradients between D1 and aperture, thus simulating the most commonly selected operating condition for standard ITTIL tubes (aperture "tied" to D1). The first aperture, A1, however was operated at various potentials between +40 and -40 volts with respect to A2 and D1, with the measured results for the single electron pulse height spectrum shown in Figure 15. The most striking result obtained was the critical difference in tube behavior between negative and positive operation. With A1 negative with respect to A2 (and D1), the tube was a very poor single electron counter. The pulse height spectrum was nearly exponential, with no well defined most probable pulse amplitude (no peak in curve) and a large increase in smaller-than-expected (<20 percent $\overline{V}$) pulses even after the dark count was subtracted.

Possibly of equal significance was the large increase in the absolute dark counting rate and the "poor" shape of the dark pulse height spectrum.

For A1 positive with respect to A2 and D1, the same tube becomes an excellent single electron counter, one of the best we have monitored to date. The single electron pulse height spectrum has a well defined most probable pulse height with peak-to-valley ratios exceeding 2:1. Thus there is now a minimum of difficulty in assigning significance to near-average-height pulses, (whether or not they should be counted as independent events), and in selecting a suitable bias discriminator level for a counting circuit. In fact, from Figure 15 for positive A1 values, it can be seen that the amplitude of channel 2 or channel 3 near the least probable pulse amplitude would probably represent a satisfactory choice, (counting to all pulses

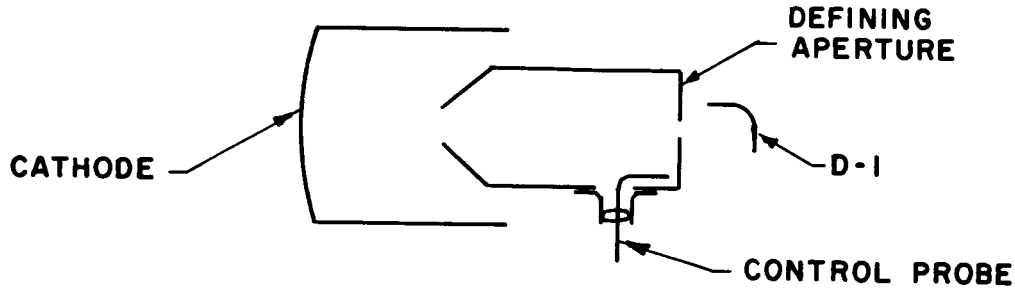
DEFINING
APERTURE
CATHODE
D-1
CONTROL PROBE

(a)

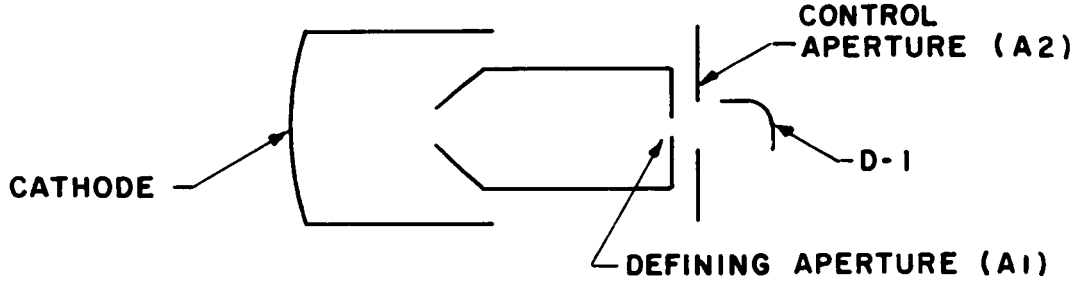
CONTROL
APERTURE (A2)
CATHODE
D-1
DEFINING APERTURE (A1)

(b)

Figure 14

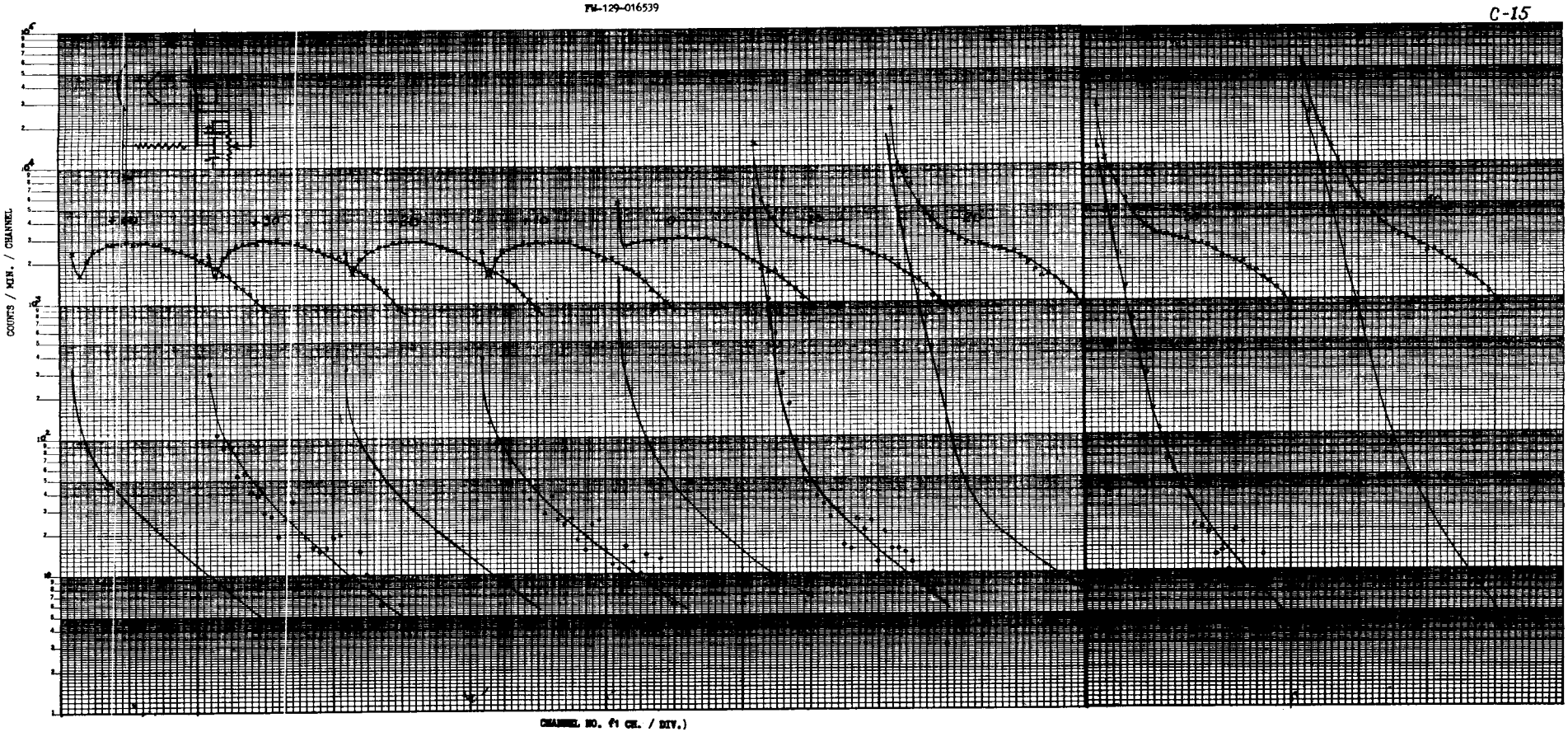

Figure 15

C-14

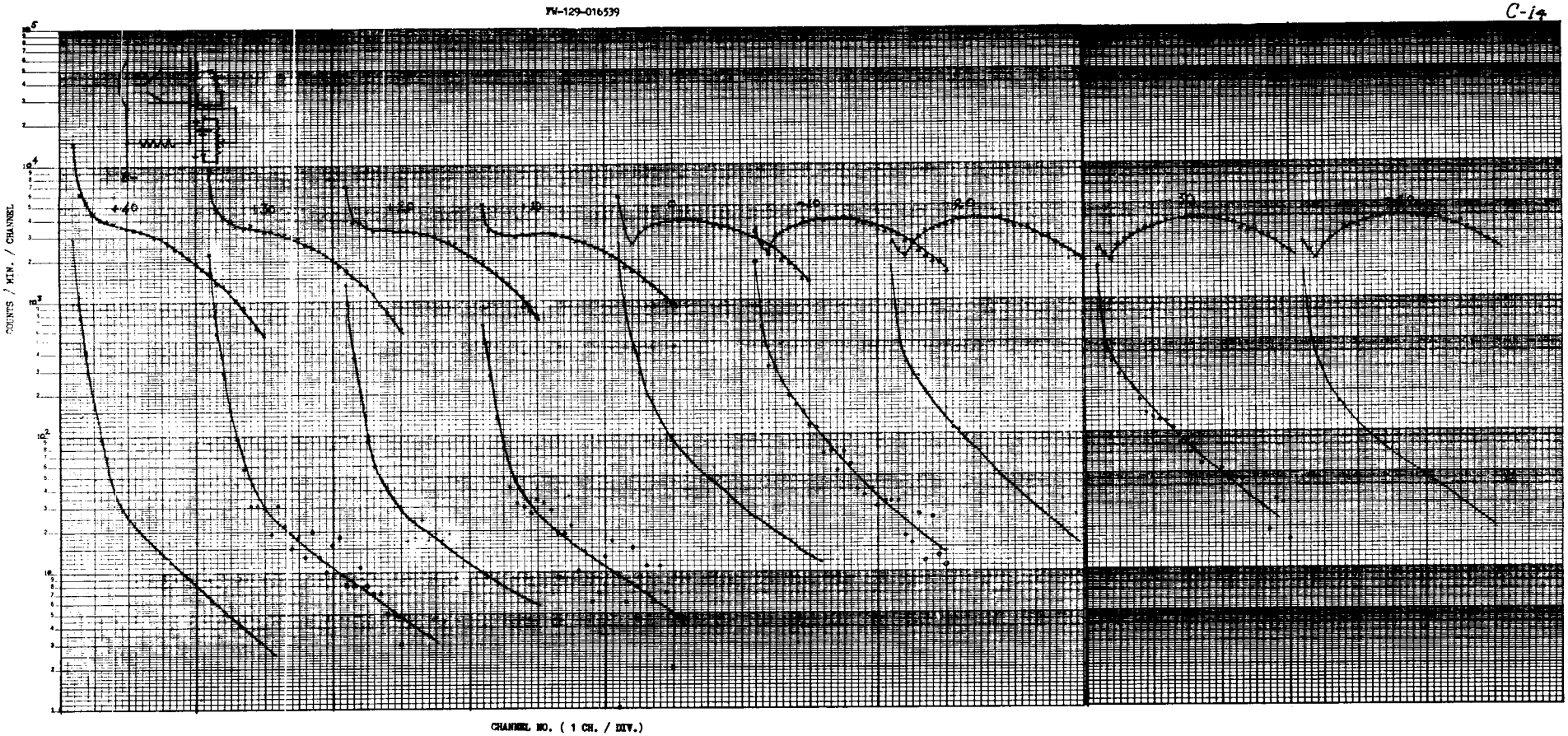

Figure 16

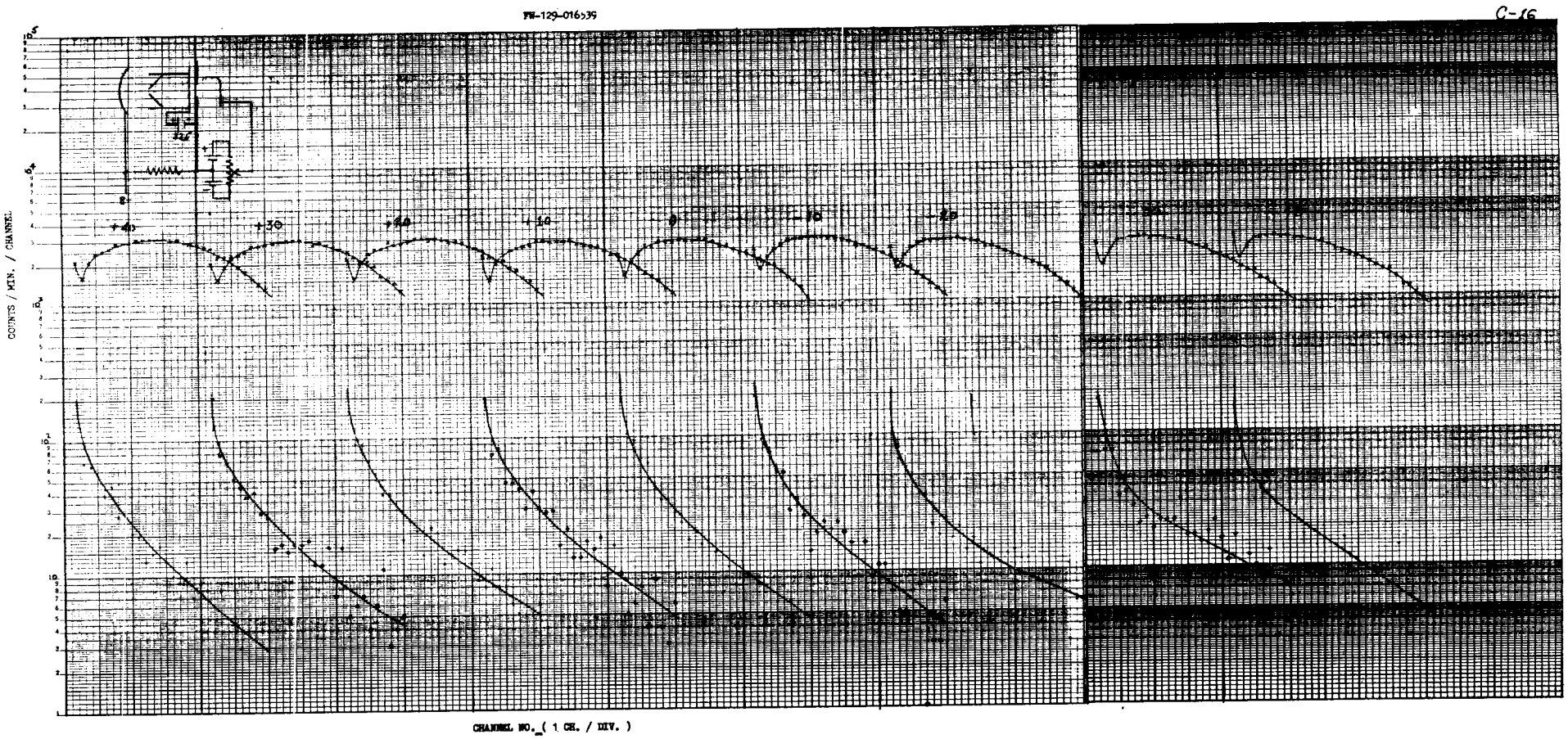
FS-129-016539
C-16
COUNTS / MIN. / CHANNEL
+40
+30
+20
+10
0
-10
-20
CHANNEL NO. (1 CH. / DIV.)

Figure 17

above this amplitude as corresponding to individual input photons). Such a choice is ambiguous for negative A1 values since no tendency toward a least probable pulse amplitude (curve minimum) is then observable.

Also quite striking from Figure 15 is the marked reduction in dark counting rate with positive A1 values, and the improved shape (with a marked break in the curve indicating a separation of dynode pulse from photocathode thermionic emission pulses). The sharp drop in absolute numbers of dark pulses was not fully anticipated before building this tube, but may be interpreted logically (see below).

6.2 Mode 2: A1 at D1 potential, A2 Variable

In an attempt to clarify the electron optical conditions existing in the neighborhood of D1 in this tube, a second set of pulse height spectra was taken with A1 tied to D1 and A2 variable. The results are shown in Figure 16. The poor pulse counting behavior now corresponds to A2 positive while good behavior occurs with A2 negative. The changes are, perhaps, not so evident as with A2 tied to D1, but the trend is the same, even though, in changing A2 as is being done here, the electric field configuration between A2 and D1 is being seriously disturbed. Thus A2 may now be collecting secondaries from D1 when positive and suppressing them when negative, which should markedly alter the pulse amplification properties. The fact that this occurs only to a minimum extent indicates that the major factor is the electric field between A1 and A2 rather than between A2 and D1. Note that the result for the magnitude of the electric field between A1 and A2 is consistent with Figure 15, with optimum counting achieved when the field between A1 and A2 opposes the flow of electrons to D1.

The changes in the dark noise spectrum is not as marked as in Figure 15, a result needing further interpretation.

6.3 Mode 3: A1 positive 22-1/2 volts with respect to A2, D1 Variable

Figure 17 shows the test results when A1 is operated at a fixed 22-1/2 volts positive with respect to A2, a reasonable choice for good counting behavior based on Figures 15 and 16, and D1 potential variable. Under these conditions good counting characteristics are achieved throughout the range of ±40 volts for D1, although some minor variations can be seen. Clearly, the electric field existing between D1 and A2 is not as critical as was indicated by experiments performed on single aperture tube earlier on this contract. It would appear that the collecting field of D2 does reach into the D1 surface adequately, and that the higher energy (about 600 volts) photocathode primary electrons reach the D1 surface satisfactorily regardless of small voltage differentials on A1, A2, and D1.

6.4 Mode 4: Same as Mode 2, except cathode masked to small area

In all test conditions in Modes 1 - 3 for this tube, the photocathode was approximately uniformly illuminated within about a 0.5 inch diameter area.

This would simulate tube behavior when looking at a scene of illumination, or with background lighting present while tracking a star, etc. On the other hand, it was established earlier that photoemission from nominally apertured cathode areas did produce anomalous output pulses. Therefore, tube FW-129 - 016539 was now operated with a small (0.012 inch diameter) spot of light (optical mask on the photocathode) approximately centered on the effective 0.1 inch IEPD area of the tube. Figure 18 shows the measured test results otherwise under the electrical test conditions of Mode 2. The tube, as before, shows a better pulse height spectrum with A2 negative, but even with A2 positive it shows a peak, unlike Mode 2 operation.

On the other hand, the difference in the dark pulse height spectra remain identical to those of Figure 16, (as they should since only the light on test condition has been changed) with a decided operational advantage for A2 negative.

Following the experiments described above two additional tubes of this design were constructed except for the fact that the second aperture was made mechanically and electrically, an integral part of D1. This has the slight disadvantage of making the tube somewhat more difficult to assemble due to alignment requirements between the image section and the multiplier section of the tube. This requirement, however, is far outweighed by the fact that no additional contact need be brought out through the glass envelope of the tube and the control voltage may be applied to the aperture electrode which has a base pin connection. The pulse height spectra obtained with these tubes were quite comparable to those of the earlier tubes.

6.5 Interpretation of Cascade Tube Test Results

At the risk of premature conclusions, the test results on tube FW-129 - 016539 indicate that a source of low energy electrons exists somewhere between the cathode and the defining aperture of ITTIL tubes. These low energy electrons contribute smaller-than-average output pulses when allowed to bombard D1 (or later dynodes), as would be expected based on their low energy. Their absolute numbers depend on the magnitude of the flooding light on the photocathode outside the nominally active IEPD area, but cannot be entirely removed by optical masking, presumably because of thermionic electrons emitted from the photocathode in these same peripheral areas. They can be prevented (to a large degree) from reaching the multiplier by a comparatively small decelerating field produced between the two apertures, A1 and A2. No

C-18

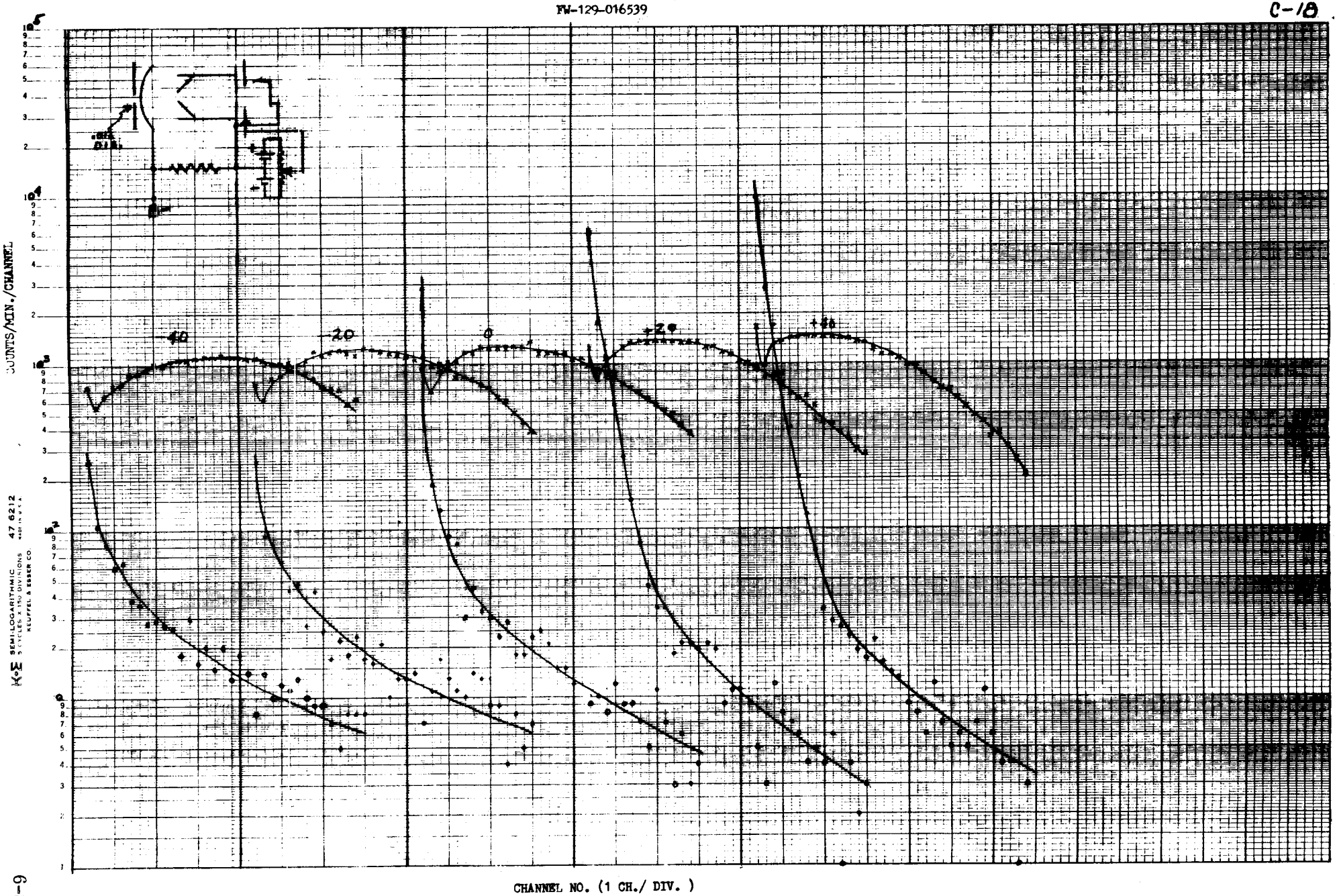

Figure 18

sharp minimum required potential is observable for this suppressing voltage, but the minimum test value of 10 volts appears adequate.

The electric field between A2 and D1 is not particularly critical in determining pulse amplification properties, but further analysis of the test results and further experimentation is desirable.

The weak immersion lens action of A1 and A2 at 10 volts differential and 600 volts primary electron energy does not seem to be likely to play a role, especially when the insensitivity to A2 - D1 potential is considered, but may play a limited role in determining the bombarded area on D1.

Several possible sources of the disturbing low energy electrons can be postulated. Possibly the most obvious of these would be secondary electrons produced by primary photocathode electrons (both photo and thermal) striking the defining aperture or internal "anode" surfaces. These secondaries "see" an essentially field free region within the anode cylinder and may find their way out through the defining aperture to the multiplier. However, their directional properties with respect to the aperture plate (their prime originating source area) is such that they seem unlikely to do this without positive accelerating fields to the aperture, contrary to the evidence of Figures 15 through 17. An alternate, and possibly more likely source of low energy electrons, would be photoelectrons produced on the inner surfaces of the anode cylinder by soft X-ray excitation, the soft X-rays in turn being generated by the primary photocathode electrons striking the aperture plate. Since the primary electrons have sufficient energy (600 volts) to excite soft X-rays efficiently, this could be a source of the low energy "tertiary" electrons, and the resultant tertiary electrons would have directional emission properties appropriate to going through the A1 aperture even at zero A1-A2 potential difference.

Regardless of the explanation of the small output pulses for certain operating conditions, it is clear that a means (cascade apertures) has been found to control the output pulse height spectrum and create a more satisfactory pulse counting tube. Although cascade aperturing may not be the most practical way of achieving this performance, it has permitted us an insight into tube behavior which should enable us to develop more suitable pulse counting tubes, the basic objective of this contract. Certainly the possible presence of anomalous low energy electrons and X-ray effects in the "front end" section of multiplier phototubes must be carefully considered in all pulse counting tube designs. For example, in "ordinary" scintillation type multiplier phototubes in which the bombarded surface of D1 is exposed by rather large solid viewing angles to the photocathode, X-rays generated at D1 may return to the photocathode producing added electrons and consequent spurious after-pulsing. This might be a possible explanation of the experimental results of Tusting, Kerns, and Knudsen in which they observed few smaller-than-expected output pulses when the

multiplier phototube was gated on for observation only when a light pulse occurred.

7.0 COOLING TESTS

Although it is recognized that NASA has minimal interest in detectors requiring cooling for long term operation in space, yet the interpretation of cooling characteristics on multiplier phototubes is nevertheless desirable because of the insight it provides into tube operating principles. Furthermore, tubes with low thermionic dark current at ambient temperature, or even at elevated temperatures are needed for space applications. Also, since moderate cooling by radiometric methods is quite feasible in space, the improvement expected in multiplier phototubes should be established. For this reason, ITTIL has performed a few cooled tests on pulse counting tubes, primarily of the S-1 photocathode variety. Although, such S-1 tubes are high in thermionic dark current, they offer probably the best means of detection between 0.8 and 1.2 microns, a spectral region covering many important radiation sources, including several practical laser wavelengths.

Figure 19 shows a thermionic pulse count curve as a function of cathode temperature for FW-118 - 016506. Note that the curve saturates near room temperature at a maximum counting rate of about 5.5×10^6 cpm. Suspecting that this was due to pulse overlap and the finite resolving time of our pulse circuits, we measured the d-c output current at room temperature, using our standard test procedures to measure multiplier gain, and converted to the total number of expected input electrons per minute (counts per minute with 100 percent counting efficiency). The resulting point fell closely upon the nonsaturated rising portion of the cooling curve, confirming our prediction of circuit resolving time problems. Note that, with this correction this tube did follow an approximate Richardson law, i.e., falling exponentially with temperature over small temperature changes. ITTIL Applications Note E4 describing these cooled characteristics is attached to this report.

Other tubes do not cool as well as FW-118 - 016506 above. Figure 20 shows a test run on another FW-118 - 036402 in which the counting rate as well as the d-c dark current reached a sudden saturation at about -20 to -30 degrees C. This residual current is at least partially originating from the photocathode, since both dark current and dark count fall further if the cathode is biased off by changing it to D2 potential. An explanation of this behavior has not been found, but it may be due to stray light leakage in our rather crude cooling apparatus. Figures 21, 22, and 23 give the test results on three additional experiments made to clarify the role of photocathode thermionic emission on dark noise. In all three cases, standard ITTIL FW-118 tubes, constructed on other funds, were used. The total dark noise spectrum

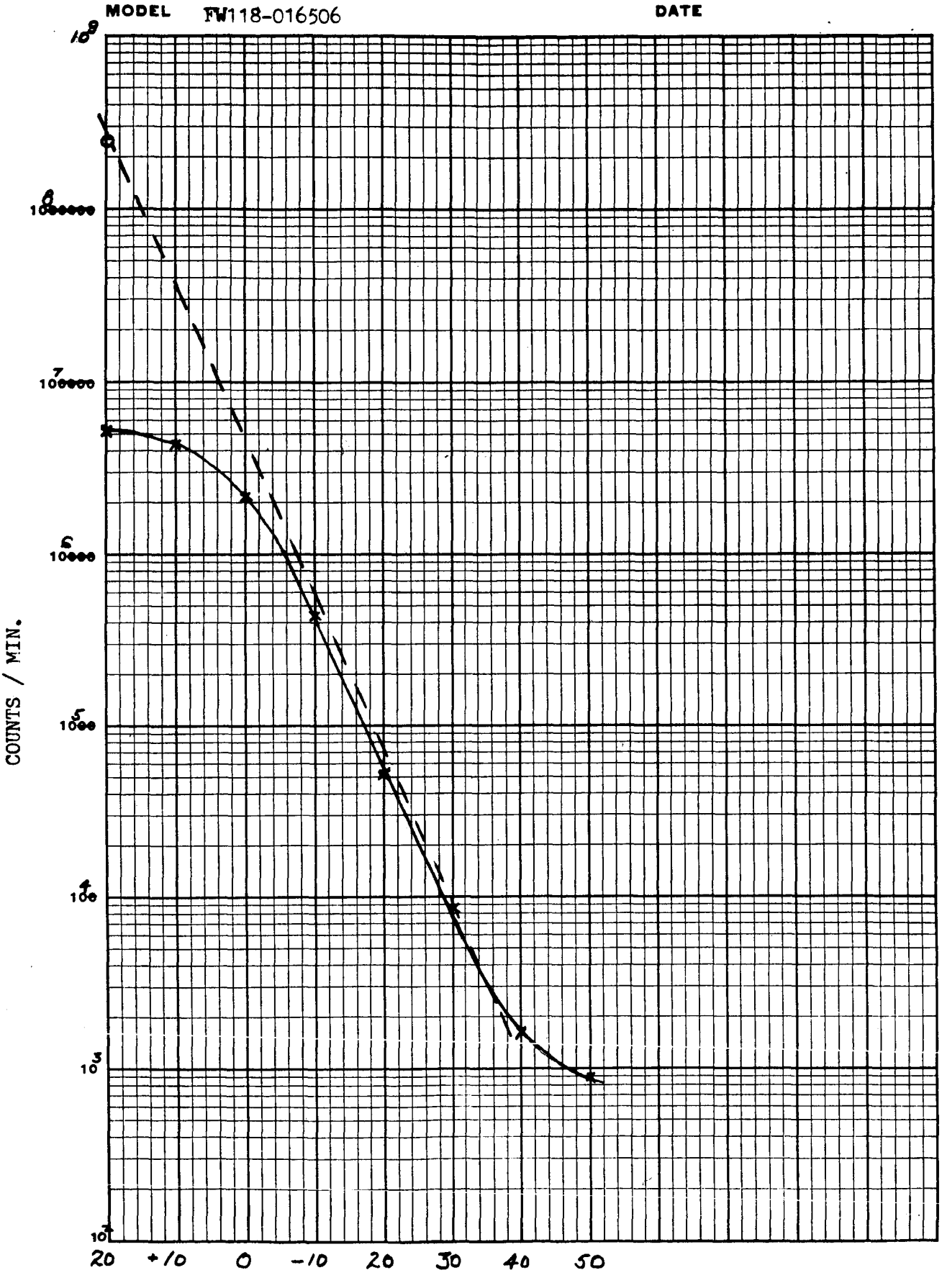
MODEL FW118-016506
DATE
COUNTS / MIN.
10^9
10^8
10^7
10^6
10^5
10^4
10^3
10^2
20 +10 0 -10 20 30 40 50
DEGREES CENTIGRADE

Figure 19

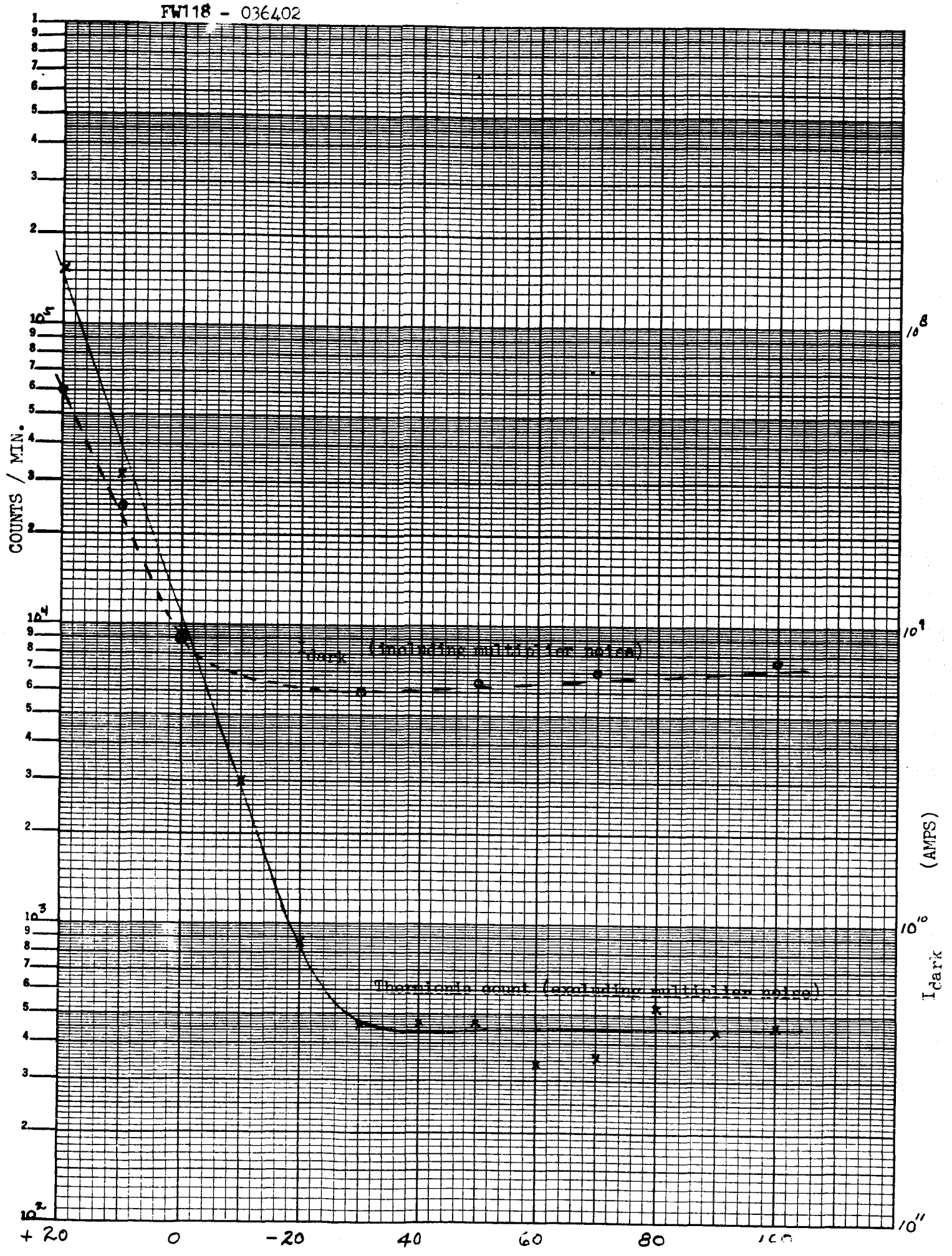
FW118 - 036402
COUNTS / MIN.
10^5
10^4
10^3
10^2
10^8
10^9
10^{10}
10^{11}
I_{dark} (AMPS)
+ 20
0
-20
40
60
80
DEGREES CENTIGRADE

Figure 20

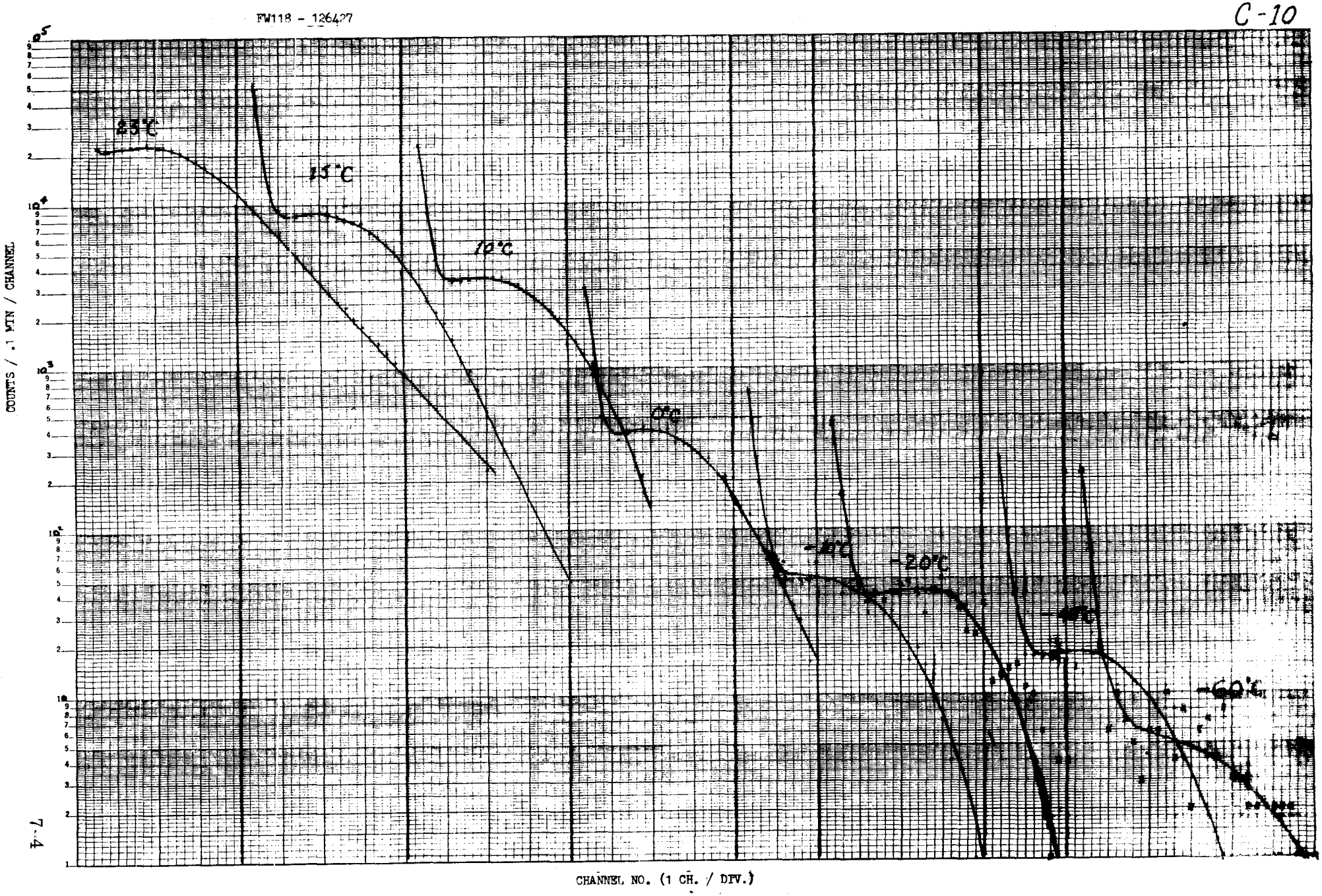
FW118 - 126427
C-10
25°C
15°C
10°C
0°C
-10°C
-20°C
-60°C
COUNTS / .1 MIN / CHANNEL
CHANNEL NO. (1 CH. / DIV.)
7-4

Figure 21

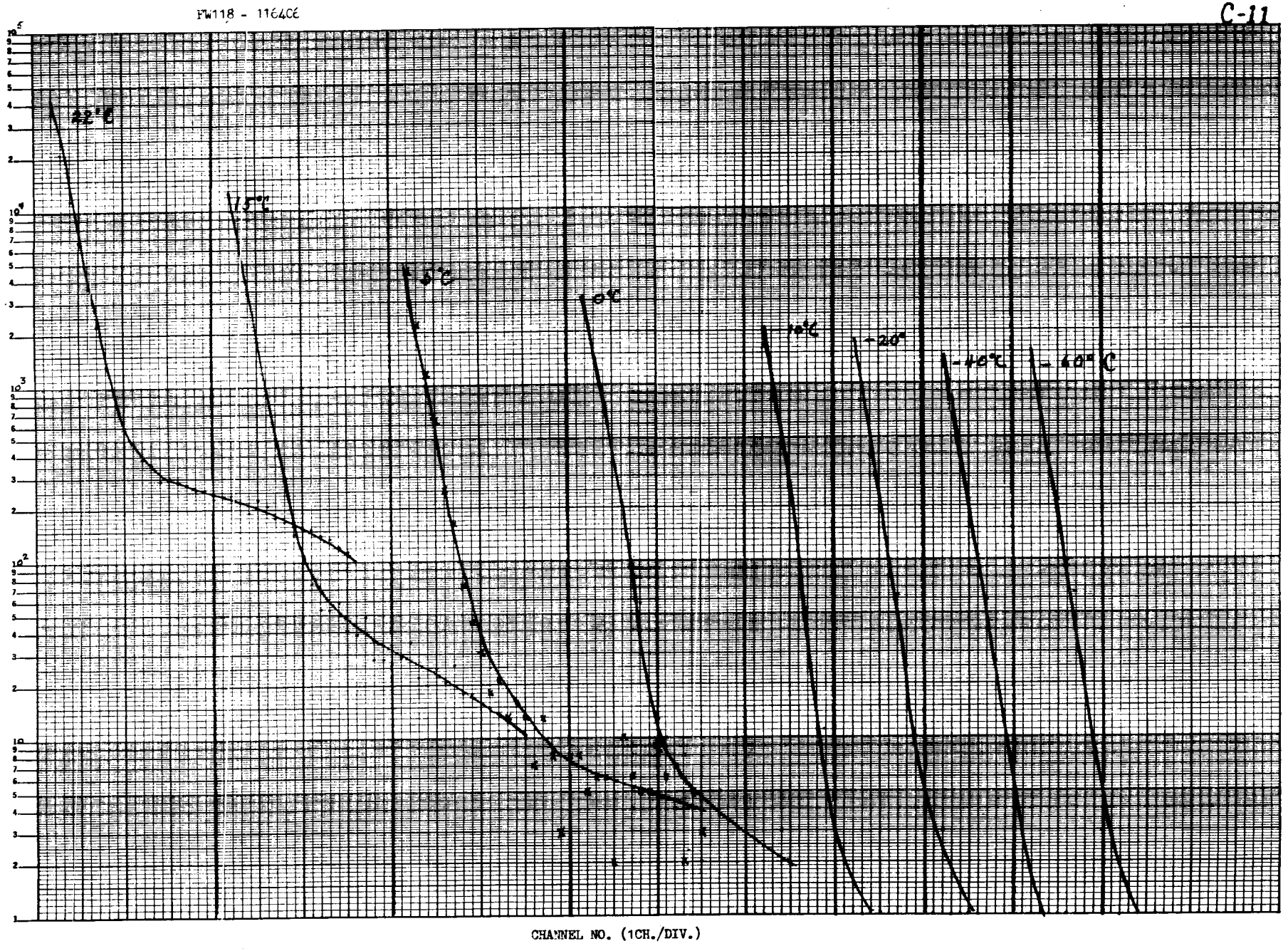
FW118 - 1164CE
C-11
22°C
15°C
5°C
0°C
-20°
-40°C
-60°C
COUNTS / .1 MIN. / CHANNEL
CHANNEL NO. (1CH./DIV.)
K&E SEMI-LOGARITHMIC 359-91
KEUFFEL & ESSER CO. MADE IN U.S.A.
5 CYCLES X 70 DIVISIONS

Figure 22

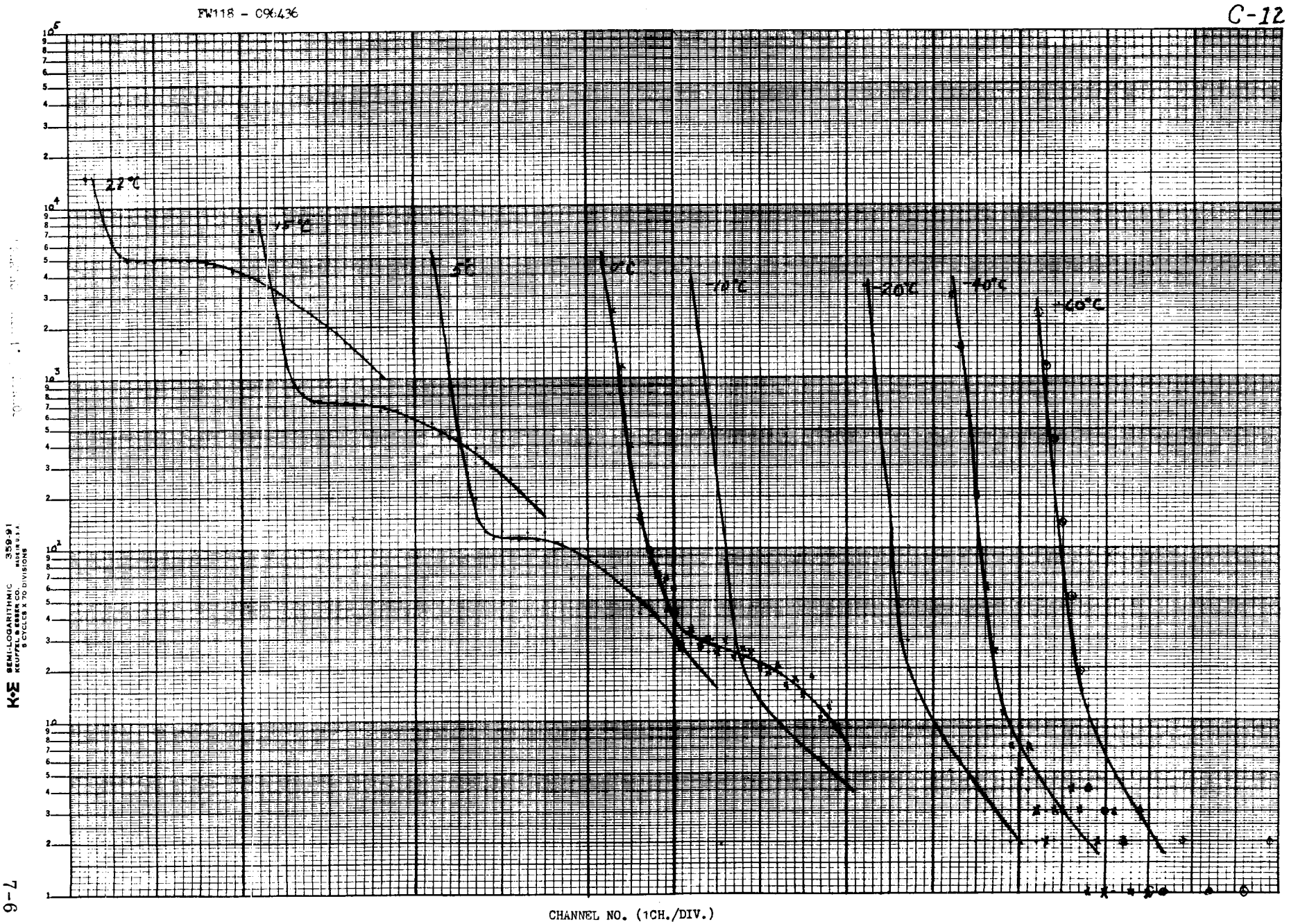

Figure 23

of these tubes was then measured as a function of the faceplate temperature (no intentional multiplier cooling). As can be seen, the portion of curves corresponding to larger pulses, above approximately channel 5 to 10 in amplitude, drops rapidly with cooling, approximately an order of magnitude for each 10 to 15 degrees C.

In Figures 22 and 23, this drop in large pulse numbers becomes ambiguous below about 0 to -10 degrees C, with the effects of further cooling becoming indeterminant, because of the very low pulse rates observed (below 1 to 10/.1 min./channel) and the obscuring effect of smaller dark pulses presumed to be dynode noise pulses. In Figure 21, however, it can be seen that further cooling into the -60 degree C region produced a further drop in the larger output pulses, as expected. The inconsistency in the curves of Figure 21, with the curve for -5 degrees C showing more pulses than the curve for 0 degree C, is believed to be due to gross uncertainties in the calibration of our cooling apparatus, presently a makeshift affair, with only the cathode cooled and a thermocouple not integrally attached to the faceplate of the tube. Nevertheless, the general trend downward with cooling is clear.

The change in slope of the curve for 23 degrees C for increasingly larger pulses is believed to be related to the finite resolving time of the pulse circuits and subsequent overloading as confirmed for tube FW-118 - 016506. If this tentative explanation is correct, a slope measurement of this type may be useful in checking for overload experimentally.

8.0 FIRST DYNODE GAIN MAPPING

The importance of well designed electron optics preceding D1, in a multiplier phototube, to its ability to efficiently count single events at the photocathode has been reported earlier. A second critical parameter is the gain uniformity of D1. To investigate this characteristic some special tubes were built which would allow as large an area of D1, as possible, to be "contour mapped". These special tubes had image sections with reduced magnification, nominally 0.35 instead of the usual 0.7, a larger D1, and larger defining aperture preceding D1 (275 x 300 mils). The net result of this design is a nominal effective cathode area of 750 by 800 mils. The image sections of these tubes were also made focusable by separating the photocathode from its cylindrical electrode and operating it a few volts negative with respect to the cylindrical electrode so that the image of a point source of electrons from the cathode could be focused on D1. Figure 21 is a schematic representation of this system.

In the performance of the experiment to be described, the tubes were operated under normal conditions of voltage, light intensity, and counting rate and in the usual test fixture. The light source, however, was modified by the

addition of a microscope objective lens so that the small aperture which normally floods the cathode was, instead, focused onto the cathode in a spot a few mils in diameter. This light source was mounted on a microscope stage compound, removed from a Bausch & Lomb metalographic camera. This complete assembly was then supported, above the photocathode of the tube under test, by the mu-metal shield that enclosed the entire tube. The calibrated two directional motion provided by this compound allowed the small spot of light to be accurately positioned at any desired point on the cathode.

The method used, in obtaining the data to be discussed, was to mechanically center the compound with its light source over the center of the multiplier phototube cathode. From this position two mutually orthogonal diameters were scanned across the cathodes with points located 80 mils apart. To the right and left and above and below these diameters at 80 mil intervals other lines were scanned with the same point spacings. This method produced an array of approximately 100 equidistant points from which to plot the contour lines.

Figure 25 is a plot of the first dynode response of tube No. 016513 to the input radiation. The numbers indicate the relative anode current as read with an electrometer. The back side of D1 is to the right of the drawing with its open side and D2 at the right. The vertical line to the right of center represents the location of a wire across the top of the dynode (see Figure 24) whose function is to extend the field of D1 into a region where primary electrons might tend to bypass into D2. This wire would normally be covered by the aperture plate in smaller aperture tubes. Figures 26a and b are photographs of a raster scan of D1 in this tube. These pictures were produced by projecting a small spot of light onto the cathode and applying deflection to the tube with a special yoke designed for these tubes when used as star trackers. The output of the tube was fed into the vertical input of a Tektronix 545 scope and the amplified vertical signal from the 545 was applied to the Z-axis input of a DuMont 304A scope, with X and Y inputs driven in sync with the multiplier tube scan, to produce intensity modulation of the beam. Unfortunately, this scope operates with the cathode of the CRT at high negative voltage so that d-c coupling to the Z input was not feasible, hence the video signal is differentiated which makes the pictures somewhat difficult to interpret. However with careful attention to the direction of the scanning signals applied to the multiplier tube and taking into account the image inversion produced by the electron optics of the image section of the multiplier, these photographs provide useful information for determining the orientation of D1 and D2 when making the contour plots. Another interesting feature of these two photographs is that the effect of clipping by the conical aperture is shown. The spot of light projected on the cathode was moved off center in opposite directions so that in Figure 26a the back edge of dynode is rounded off while the wire across the forward edge and the area in front of D2 is plainly defined, in Figure 26b the forward edge of D1 is severely

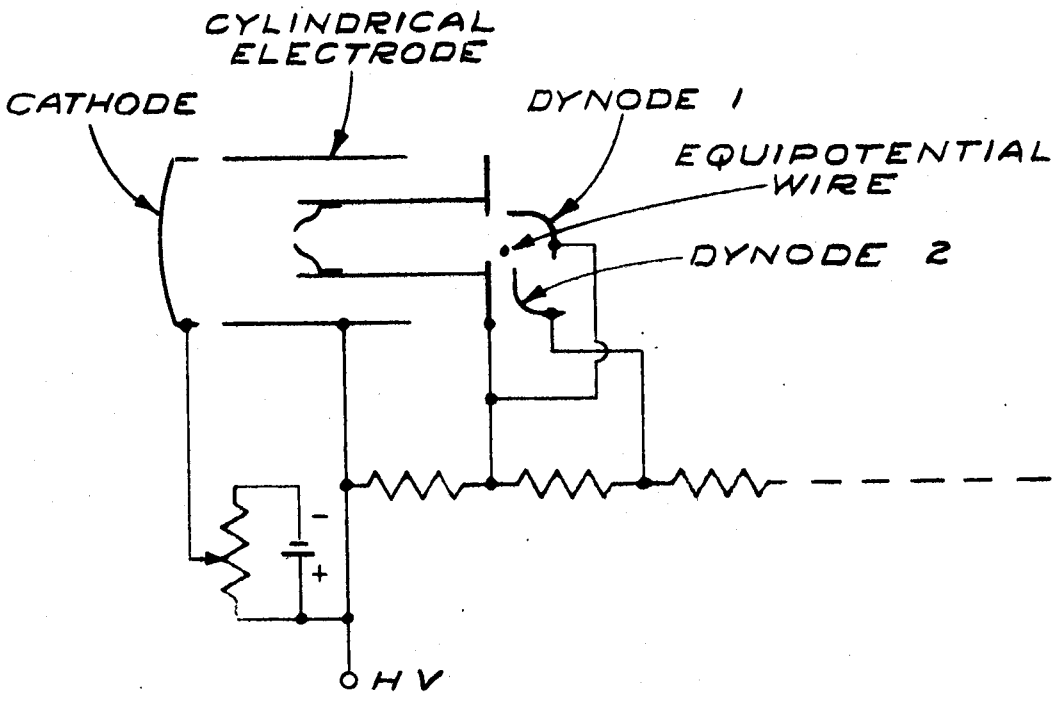
CYLINDRICAL
ELECTRODE
CATHODE
DYNODE 1
EQUIPOTENTIAL
WIRE
DYNODE 2
-
+
HV

Figure 24

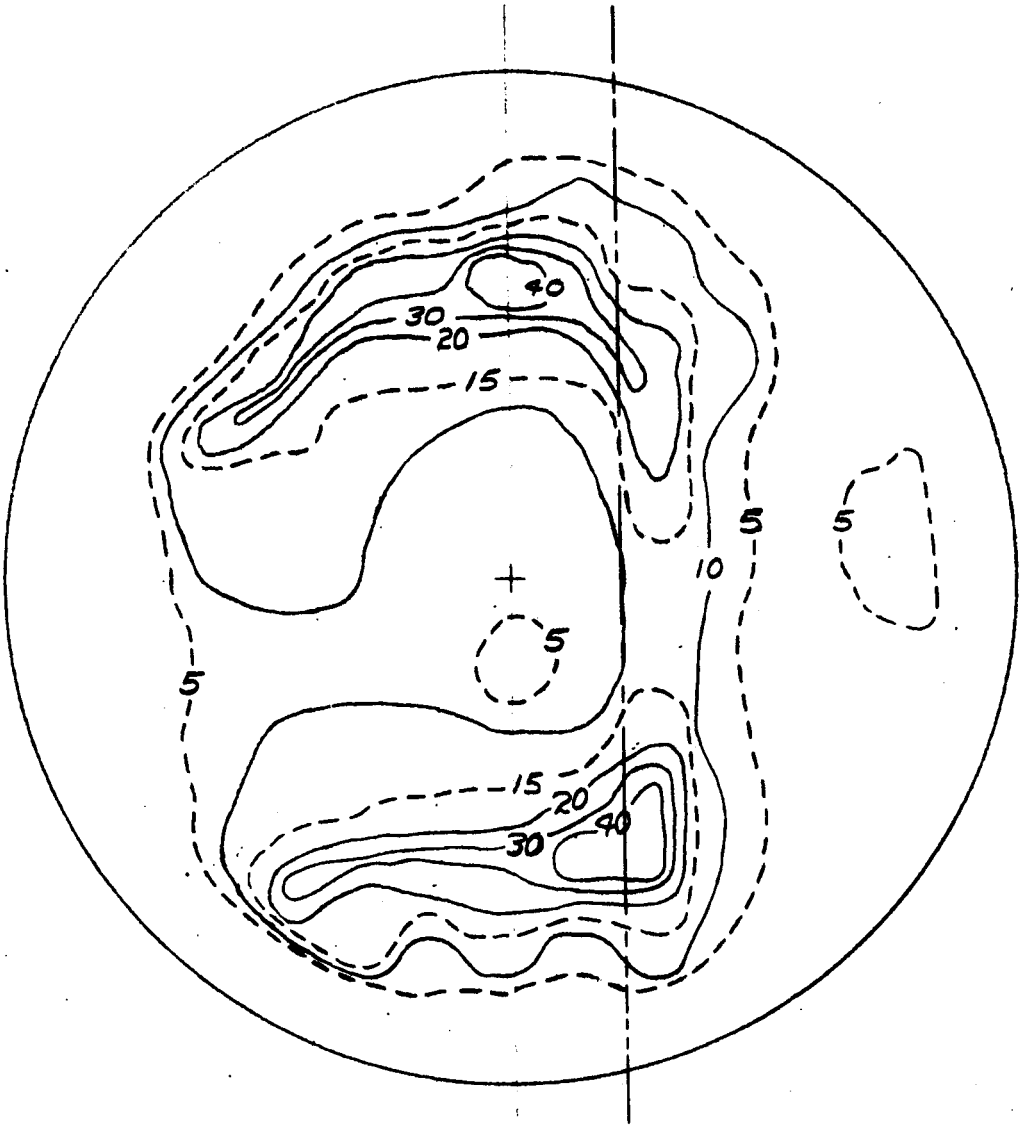

Figure 25

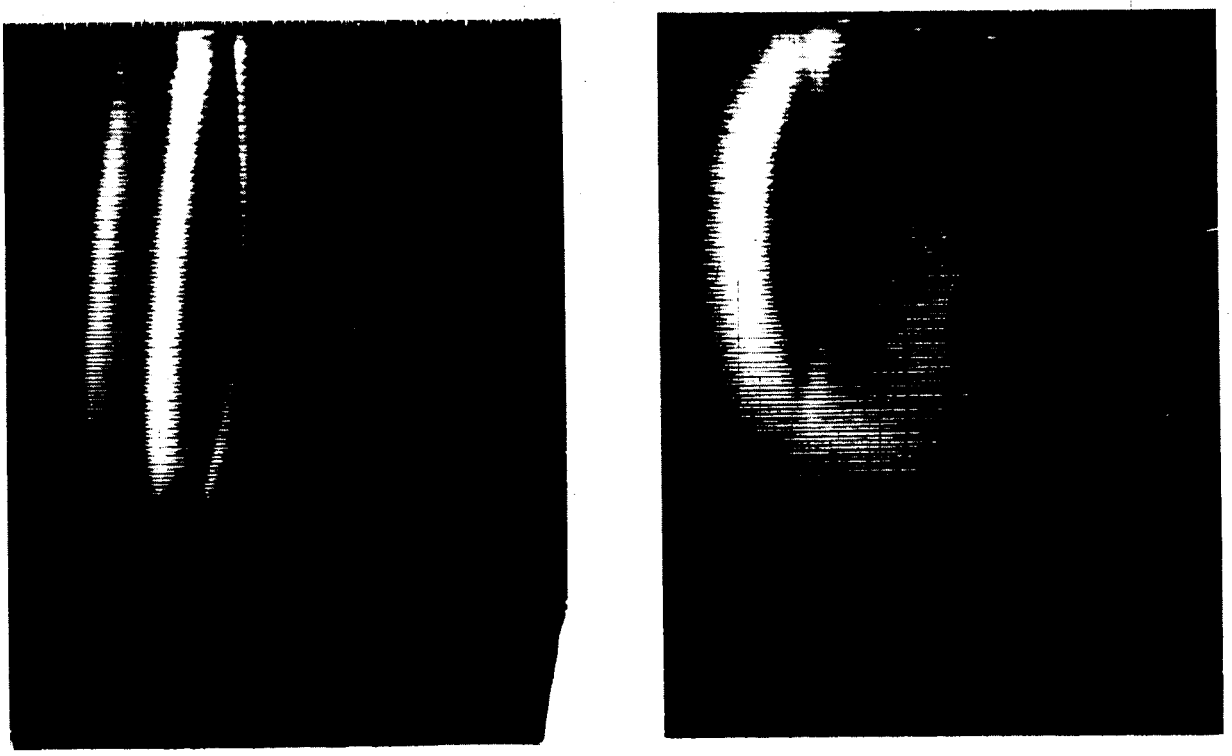

(a) (b)

Figure 26

rounded while the square corners at the back of D1 are easily identified. This effect is a clear demonstration of one of the advantages of this tube design which was described earlier, namely that electrons, thermal or photo, which originate outside the effective cathode area are excluded from regions of the tube immediately adjacent to D1. A comparison of Figure 25 and Figures 26a and b shows good correlation between high and low secondary emission ratio areas. While it is difficult to determine from the photographs which is high and which is low it does show nonuniformities which the plot in Figure 25 quantitatively identifies. While the peak dynode SE ratio areas are mainly restricted to the ends of the dynode significant portions of these peaks do extend well toward the front edge of D1 where collection efficiency is good.

Figure 27 is a plot of the total signal count, in thousands of counts, for pulse amplitude distributions taken over the surface of D1. Note that the high total count areas are located at the edge of D1 toward D2 with the low total count area at the back of the dynode where the field penetration of D2 is small. The low total count area just in front of D2 is probably due to electrons that bypassed D1 and perhaps even D2 so that the output pulse amplitude due to these electrons were below the threshold of the analyzer and therefore not counted. It was necessary to raise the threshold of the instrument to cut off channels 1, 2, and 3 so that the unusually large number of low amplitude noise pulses did not seriously reduce the live time of the analyzer and increase the time required to collect the data.

A plot of the channel number in which the peak of the single electron spectrum fell for each point on the cathode is shown in Figure 28. Two areas are shown, one in which the peak occurred in channel 10 or lower the other in which the peaks fell in channel 20 or higher. The overlap in these two areas resulted from the fact that the pulse height distributions in these areas had two peaks, which seemed to be too real to be ignored. It was suspected that under the special conditions of these experiments, it was possible to resolve the peak in the early channels (low gain) due to D2 as well as the higher gain peak in the later channels due to D1. Linear plots of these spectra were required, however, to show this detail which would not be apparent in the more usual log plots. It is interesting to note that, in general, the distributions which peak in the later channels are located in the same place on D1 as the high gain areas shown in Figure 24. Figure 29 shows several representative spectra (on a linear scale) taken with this tube and the points where the primary electrons struck D1 are shown on Figure 28.

Figure 30 is a plot of the relative cathode sensitivity. This plot indicates 3 to 1 variation in sensitivity which is significant but not sufficient to explain the large variation seen in Figures 25 and 27.

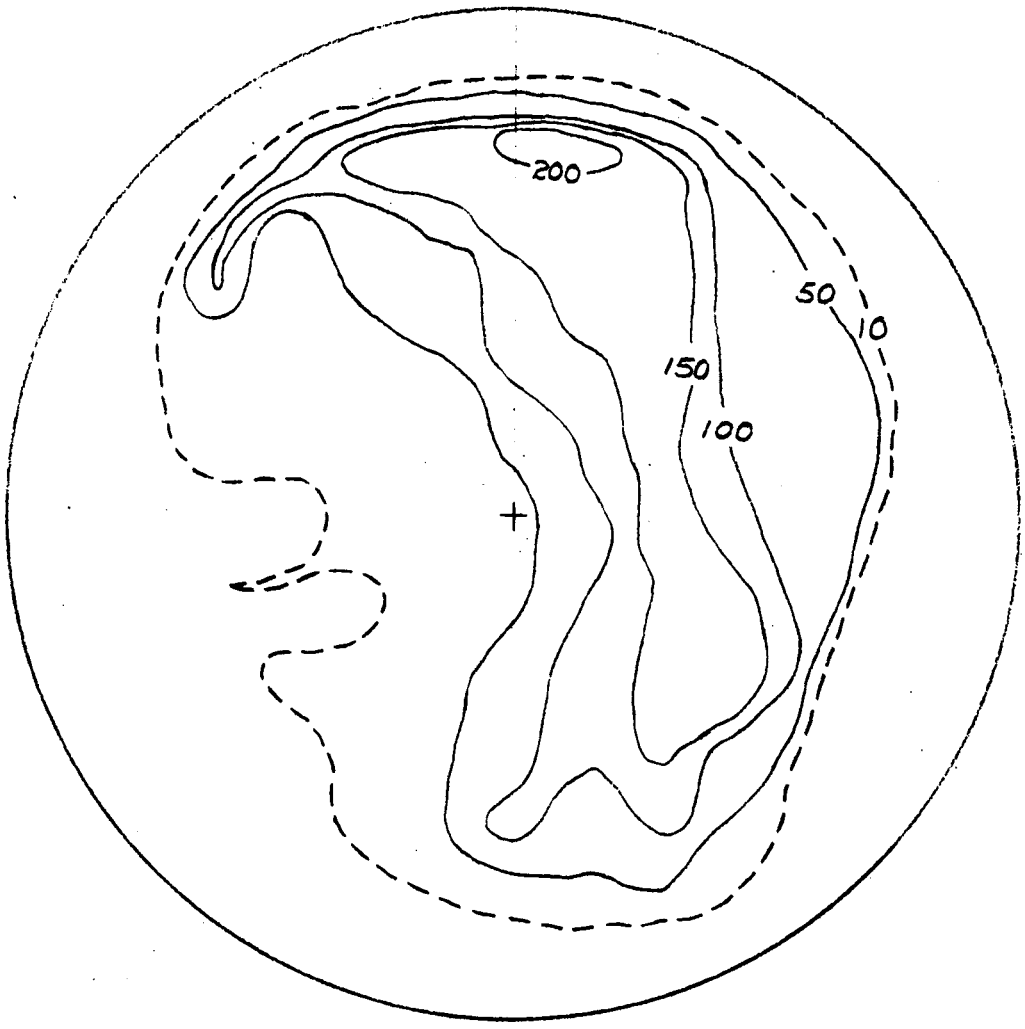

Figure 27

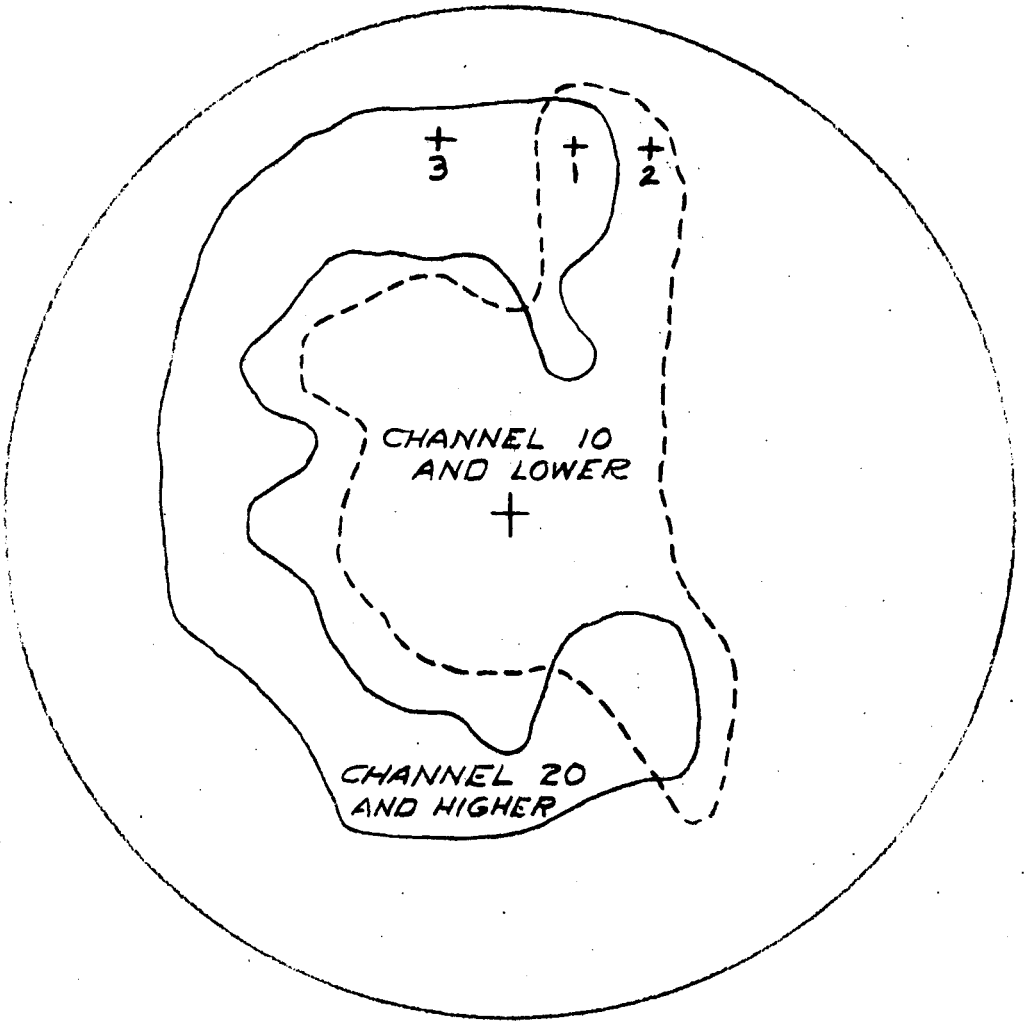

Figure 28

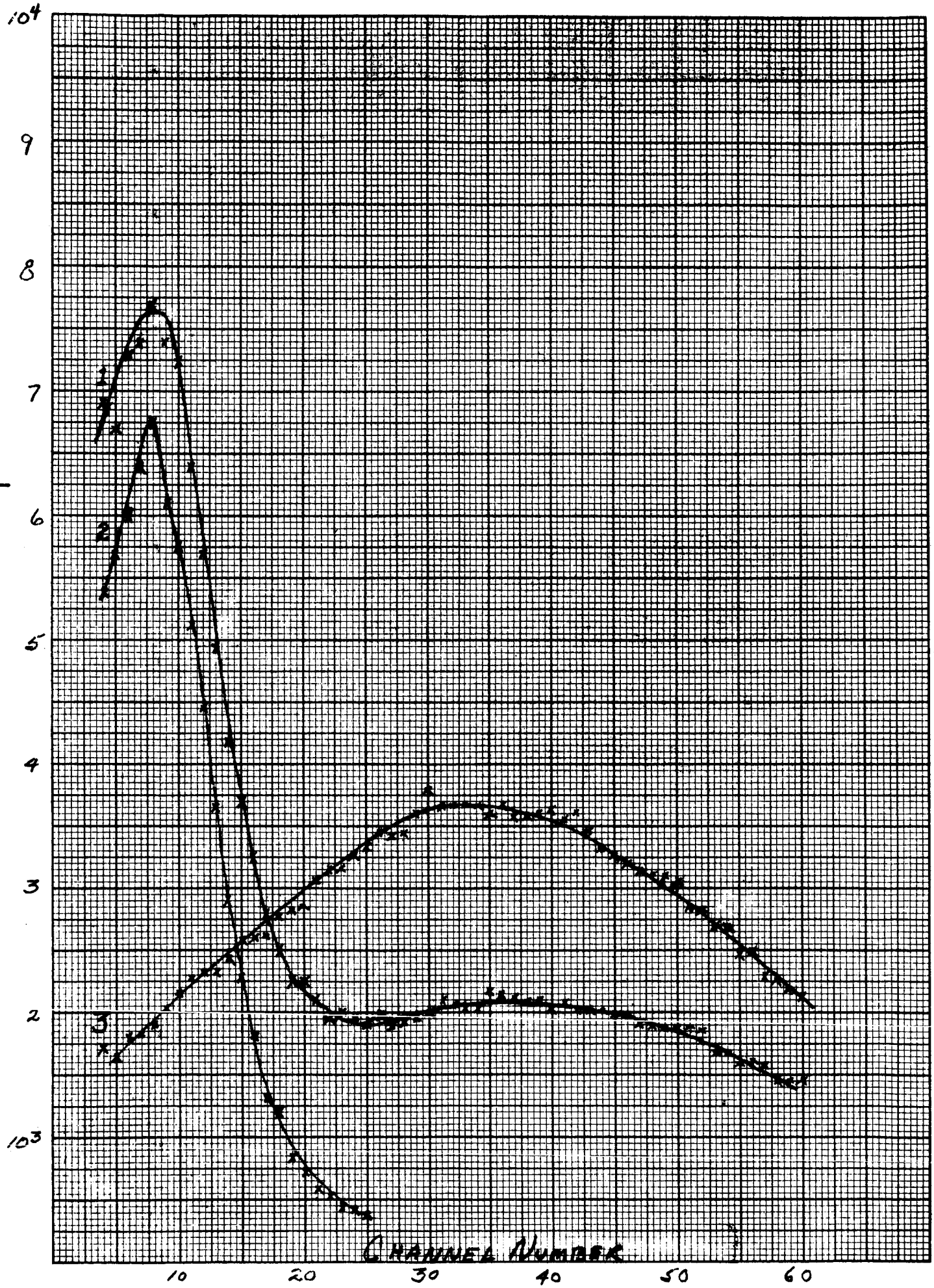

Figure 29

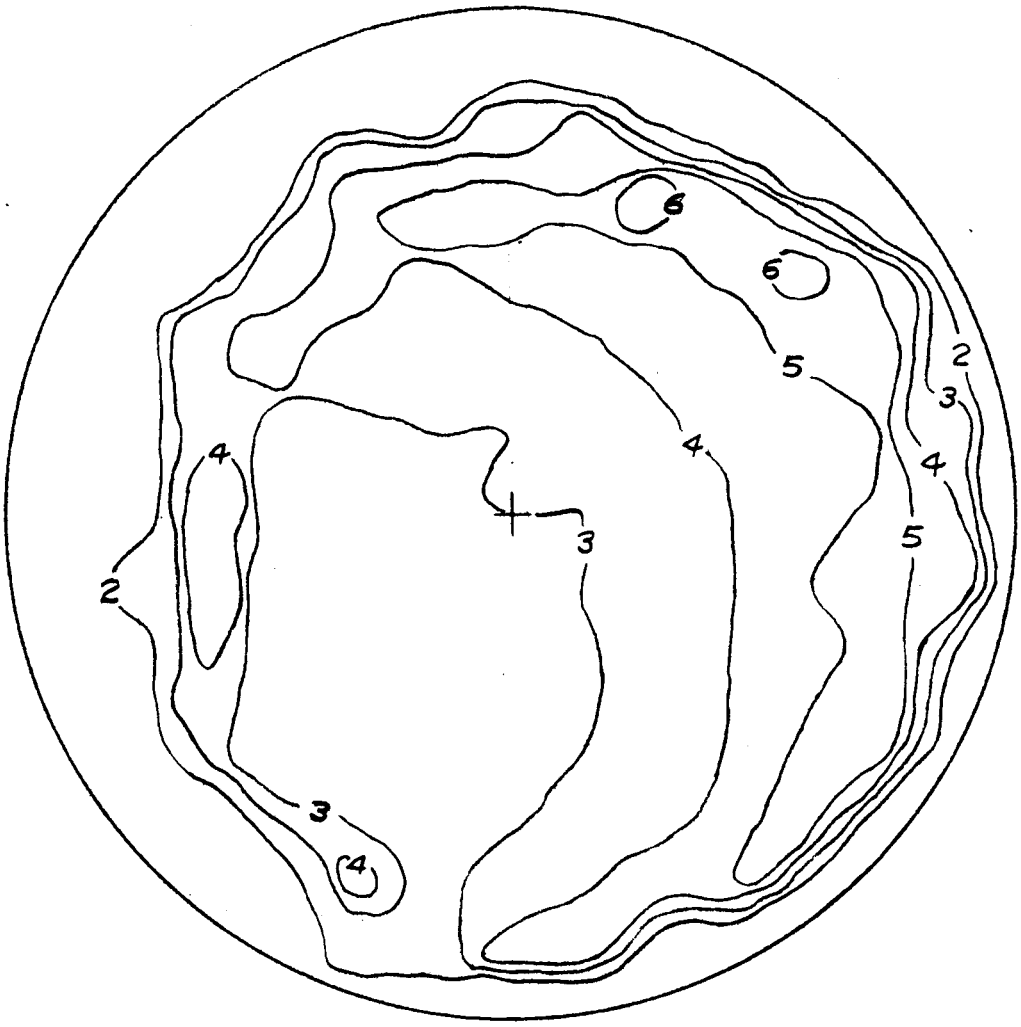

Figure 30

Similar experiments, to those just described, were performed with tube No. 016507, which was identical to No. 016513. A plot of the relative SE ratio of D1 is shown in Figure 31. A band of high SE ratio occurs down the center of the dynode with lobes extending toward the back. This characteristic is in general similar to the corresponding plot of D1 for tube No. 016513 in Figure 25 except for the low area at the center of the dynode. While careful control is exercised over the oxidation procedures in forming the dynode surface there are presently no means by which the SE ratio can be controlled point by point over the dynode surface. For this reason one might expect to see rather wide variations in this characteristic, perhaps even wider than is seen between these two tubes. The total pulse count plot of Figure 32, however, bears a marked resemblence to that of Figure 27 indicating again the higher collection efficiencies for secondaries generated near D2. Since this depends greatly on the mechanical and electrical characteristics of the multiplier one might expect this parameter to be largely invariant from tube to tube. In Figure 33 is shown the contour representing the channel number in which the peak of the single electron spectrum occurred. The resemblance between this plot and that of Figure 31 is unmistakable. An additional experiment was performed with this tube to determine that effect masking the cathode had on the ability of the tube to produce a single electron spectrum. First of all the cathode was flooded and the spectrum, so labeled, in Figure 34 was obtained. Then a mask, with a hole of the shape shown by the dotted area in Figure 33, was placed on the cathode. This mask restricted the photoelectrons to the higher and more uniform gain area of D1. As a result the other spectrum of Figure 34 was obtained.

The implication is, of course, that the gross nonuniformities of D1 have the effect of "smearing" the single electron spectrum and that high gain combined with SE ratio uniformity are critical parameters in the production of a well defined single electron spectrum by a multiplier phototube. A cathode sensitivity plot of this tube is shown in Figure 35. This variation in cathode sensitivity, of less than 1.5:1, is again insufficient to explain the larger variation indicated in Figures 31 and 33.

Following the above experiments a similar tube was built except that a 0.175 inch diameter was used in place of the large rectangular and a second 0.175 inch diameter aperture was placed on D1. Between these two apertures was located a 0.5 inch diameter tube 0.5 inch long with about 100 mils clearance between the ends of the tube and the aperture. This structure forms a converging lens more commonly known in the cathode-ray tube industry as an Einzel lens. The two apertures are operated at D1 potential with the intermediate cylinder at some other potential usually near cathode potential. Figure 36 is a schematic representative of this arrangement with the appropriate circuit values shown as used in the experiment to be described. As can be seen from Figure 36, there are two means of optimizing focus in this tube.

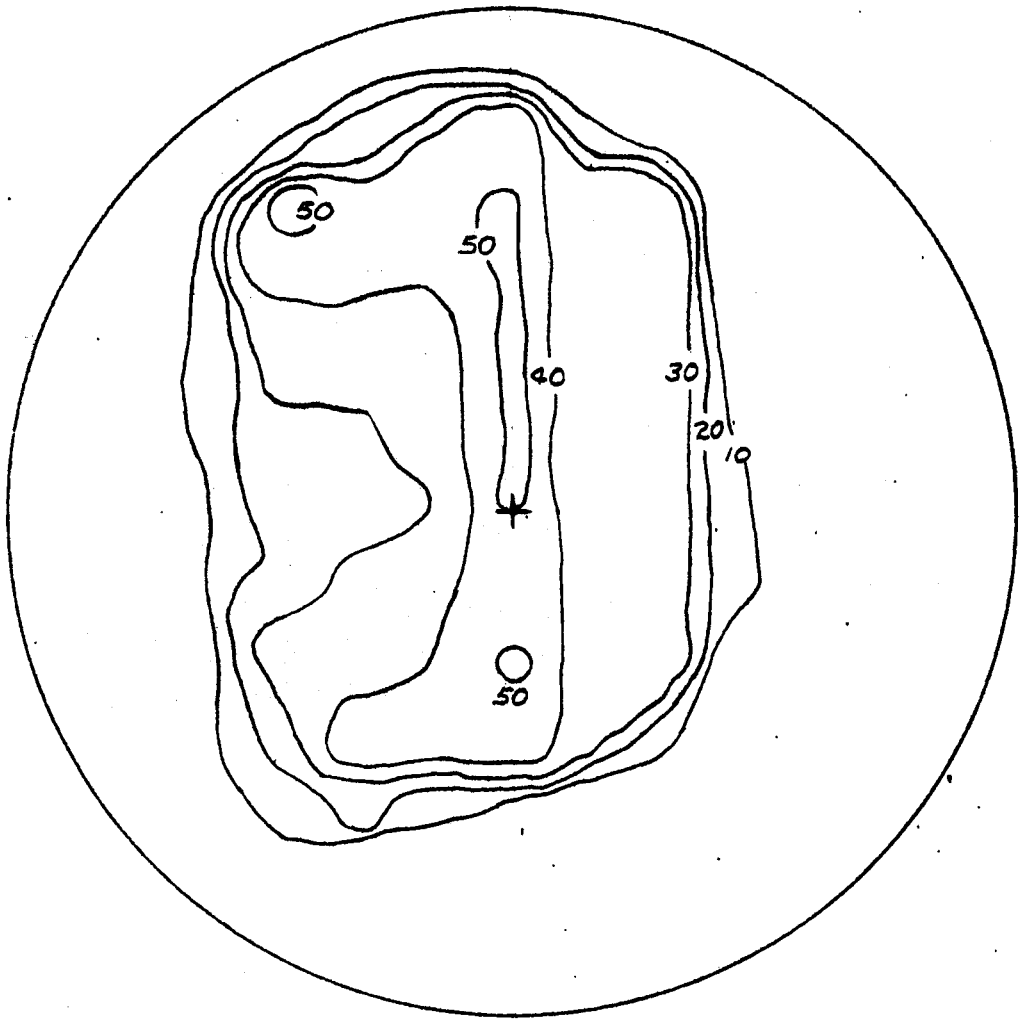

Figure 31

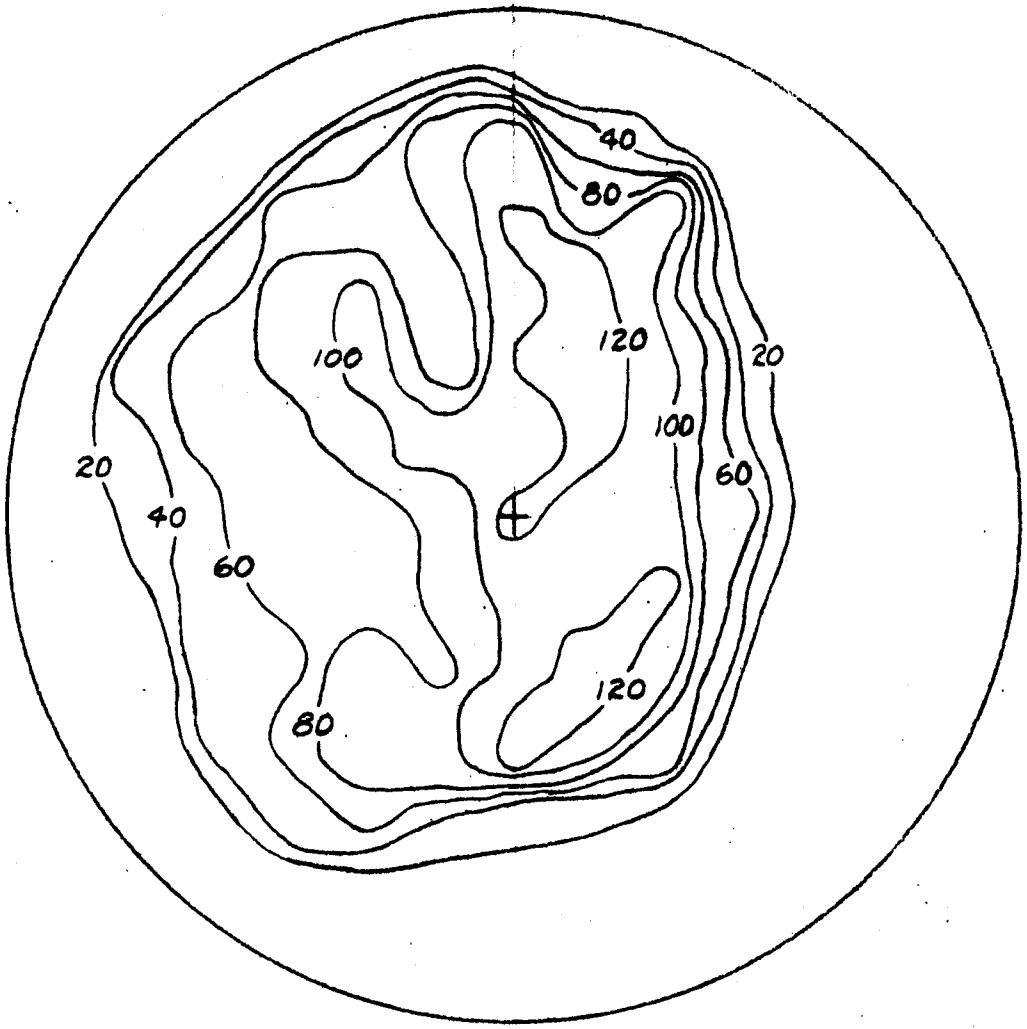

Figure 32

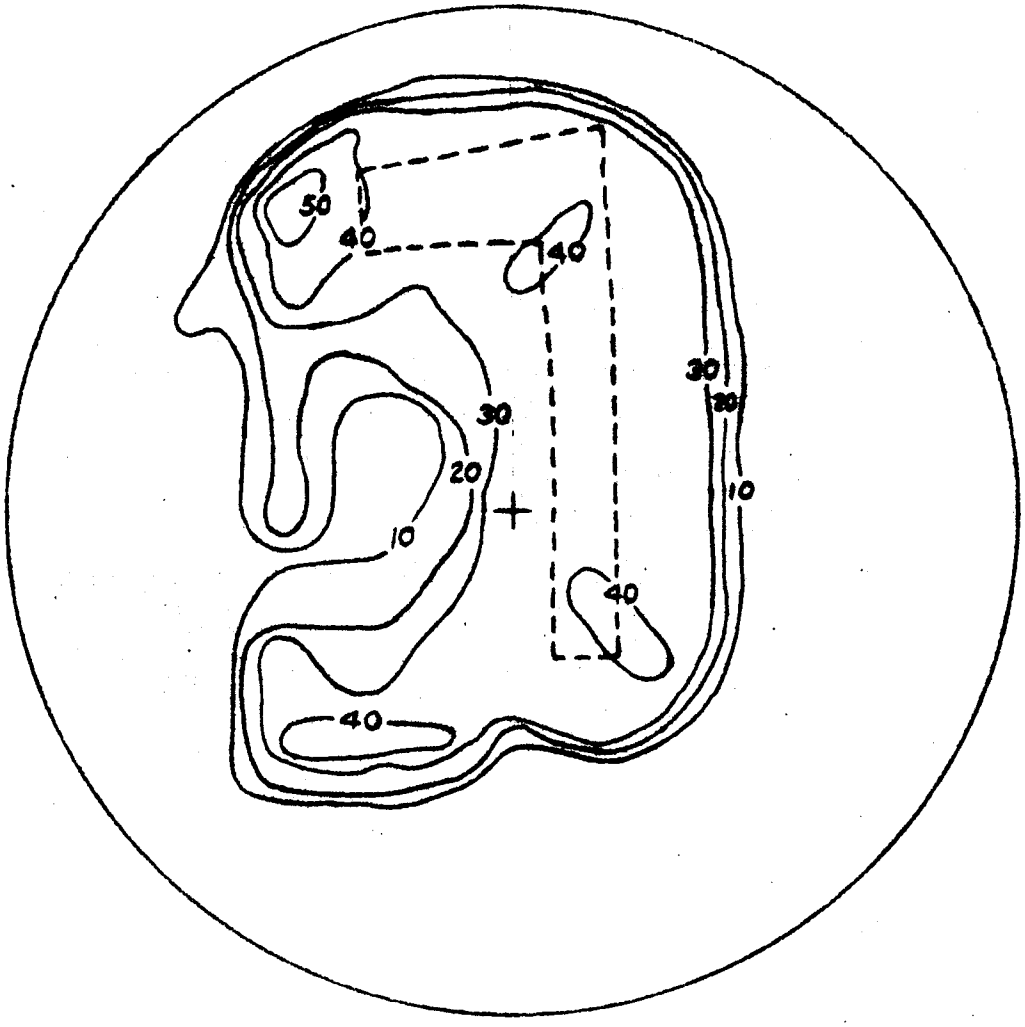

Figure 33

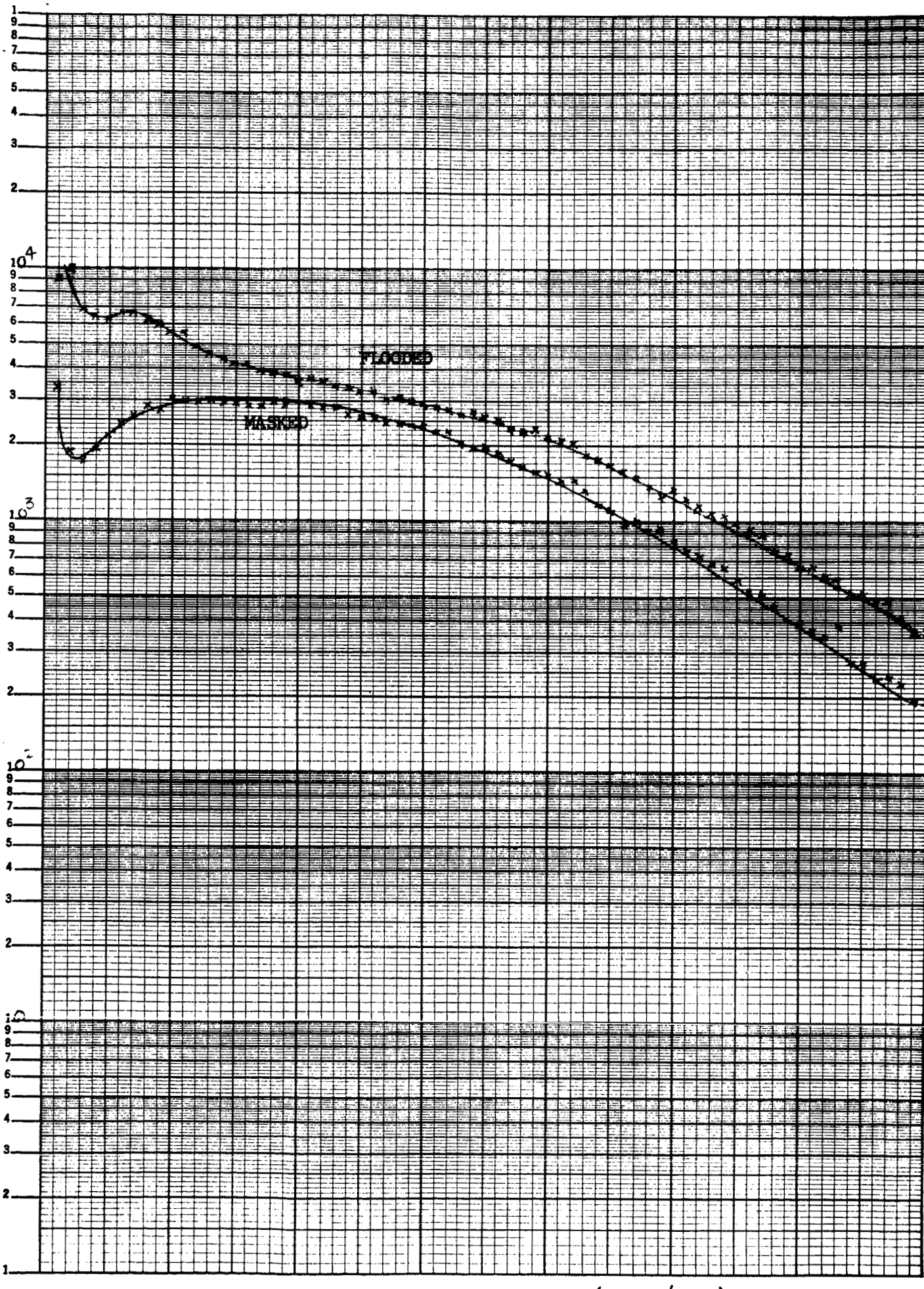

Figure 34

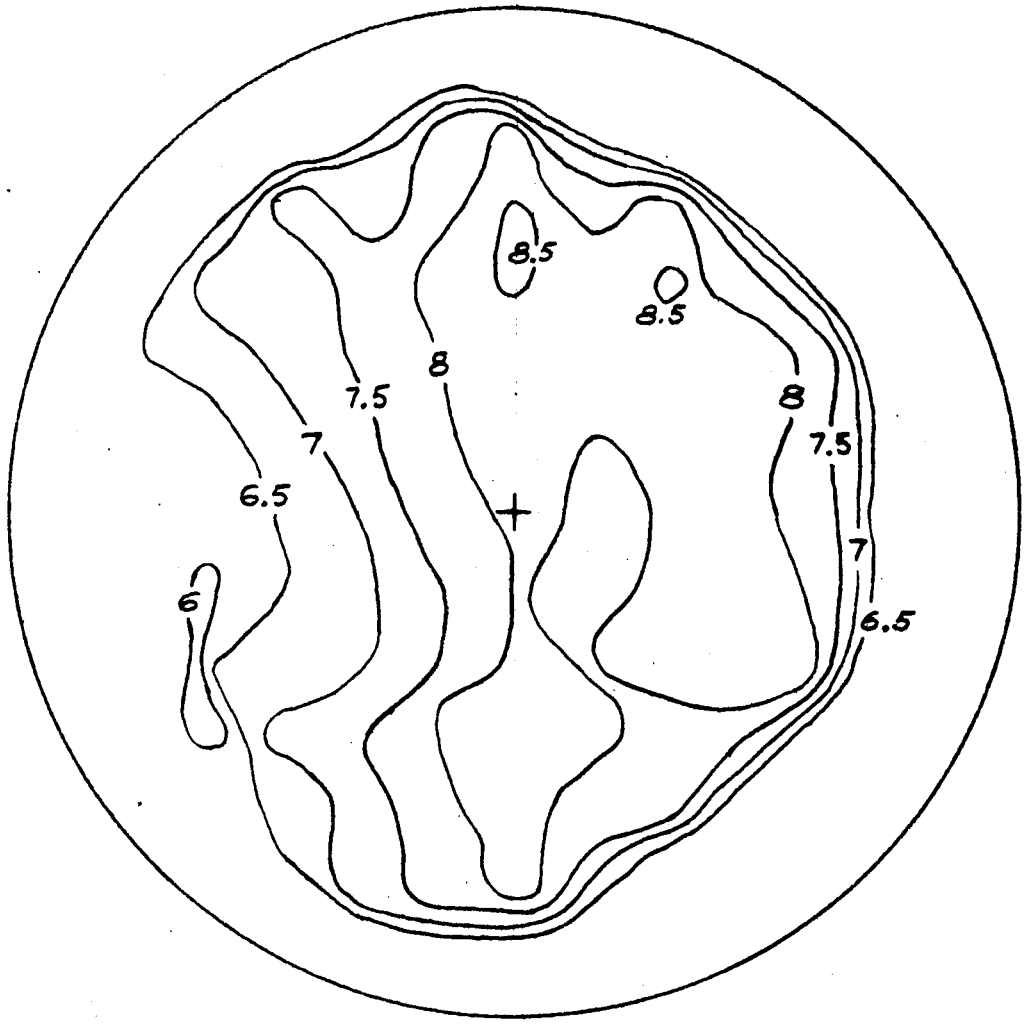

Figure 35

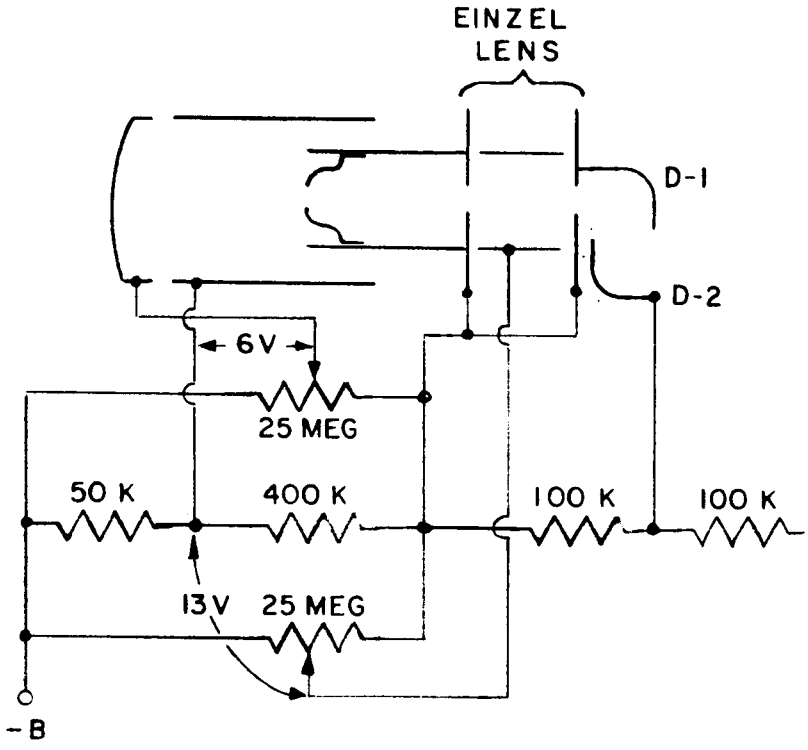

Figure 36

The potential on the cathode may be adjusted so as to produce the sharpest possible electron image of the cathode in the plane of the aperture electrode and then the Einzel lens can be adjusted to converge the divergent electron image onto as small an area of D1 as possible.

The image section has a nominal magnifucation of 0.37 so that the approximate effective cathode diameter is 0.475 inch, (aperture dia./mag). The method of mapping is the same as that described above except that a smaller spot of light was used which accounts for the fact that a cathode sensitivity plot was not taken. When the tube front end was operated as a diode there was not sufficient current generated by such a weak light source, to be measured with available instruments. However, the cathode was searched with an 0.01 lumen source and found to vary not more than 20 percent.

Figure 37 is a plot of relative d-c output of the multiplier as a function of position on the cathode while Figure 38 is a similar plot of total signal count. The similarity is as before, with the highest collection efficiency at a location close to one end of the front edge of D1. Inspection of Figure 39, a plot of peak channel numbers, shows that this area is also an area of high secondary emission as is indicated by the fact that the peak of the distribution falls in channels 15 to 20. It is also interesting to note that there is only a 2:1 variation in the gain of D1 as compared to a variation of 5:1 in one of the previous tubes. It is, however, not obvious whether this is a function of the dynode surface formation or the ability to focus the beam on a smaller area of D1 thus avoiding the possibility of smearing out the peaks due to beam overlap of high and low gain areas. A further point of interest is shown in Figure 40 which demonstrates how the peak in the distribution is lost as the potential on the Einzel lens is changed. This would seem to indicate that divergence of the beam does effect the gain either by the means just stated above or by some other more subtle mechanism not yet fully understood. The unusually high dark counting rate is unchanged.

9.0 WINDOWLESS MULTIPLIER PULSE HEIGHT DISTRIBUTION

A windowless multiplier is simply an electron multiplier for detecting externally generated electrons or similar charged particles, or for detecting input photons of sufficient energy (usually ultraviolet) for exciting D1 as a photocathode. The ITT FW-141 is a 16-stage Be-Cu multiplier with a divider string of 1 megohm Pyrofilm resistors welded directly to the dynode tabs. In practice the input particles impinge on D1 producing electron emission, but to facilitate testing they are sealed into glass blanks with 9741 windows so that the gain may be measured by exciting D1 with a germicidal lamp (2537 Å).

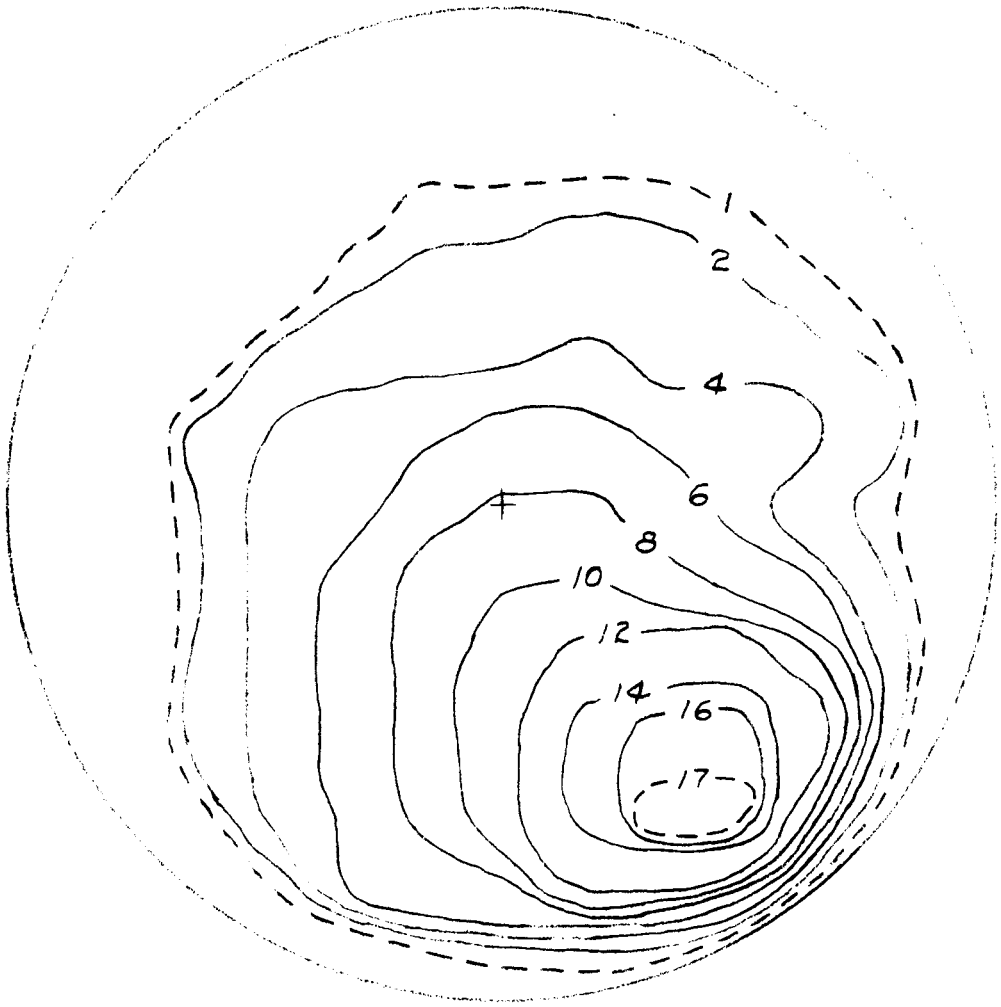

Figure 37

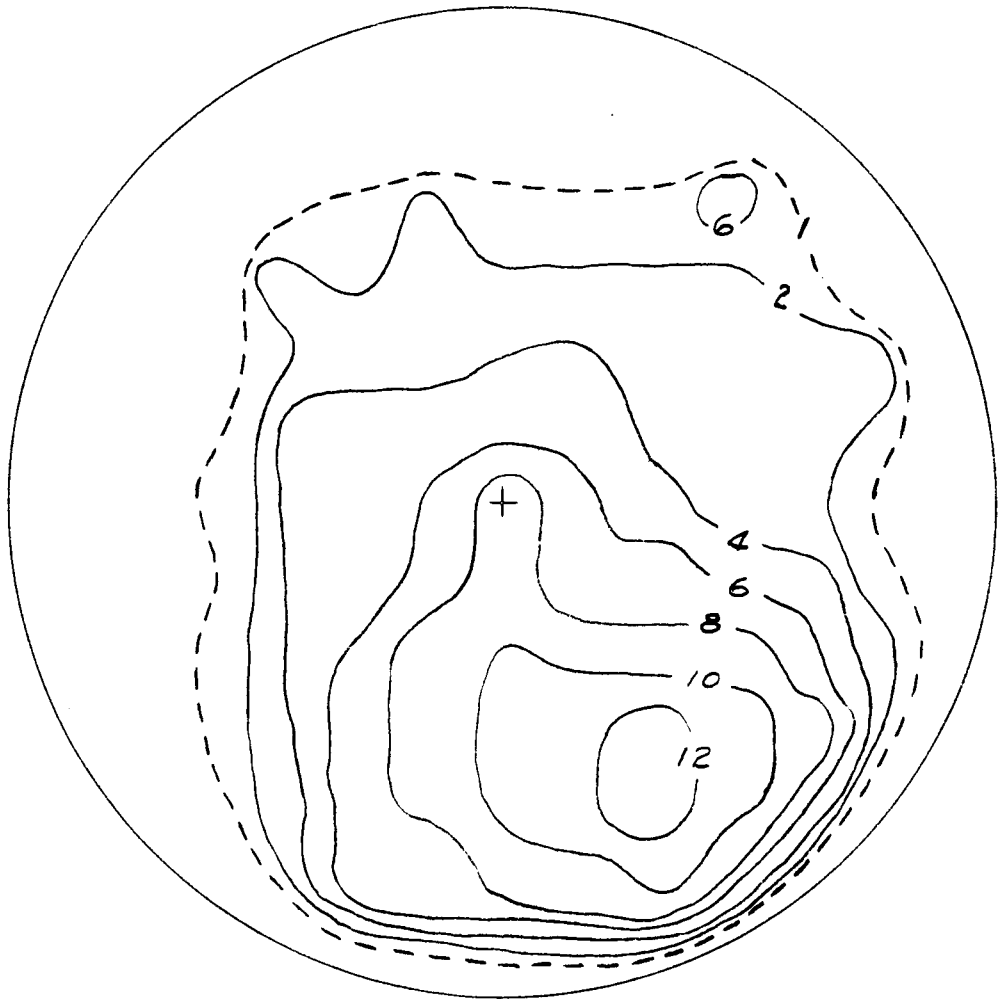

Figure 38

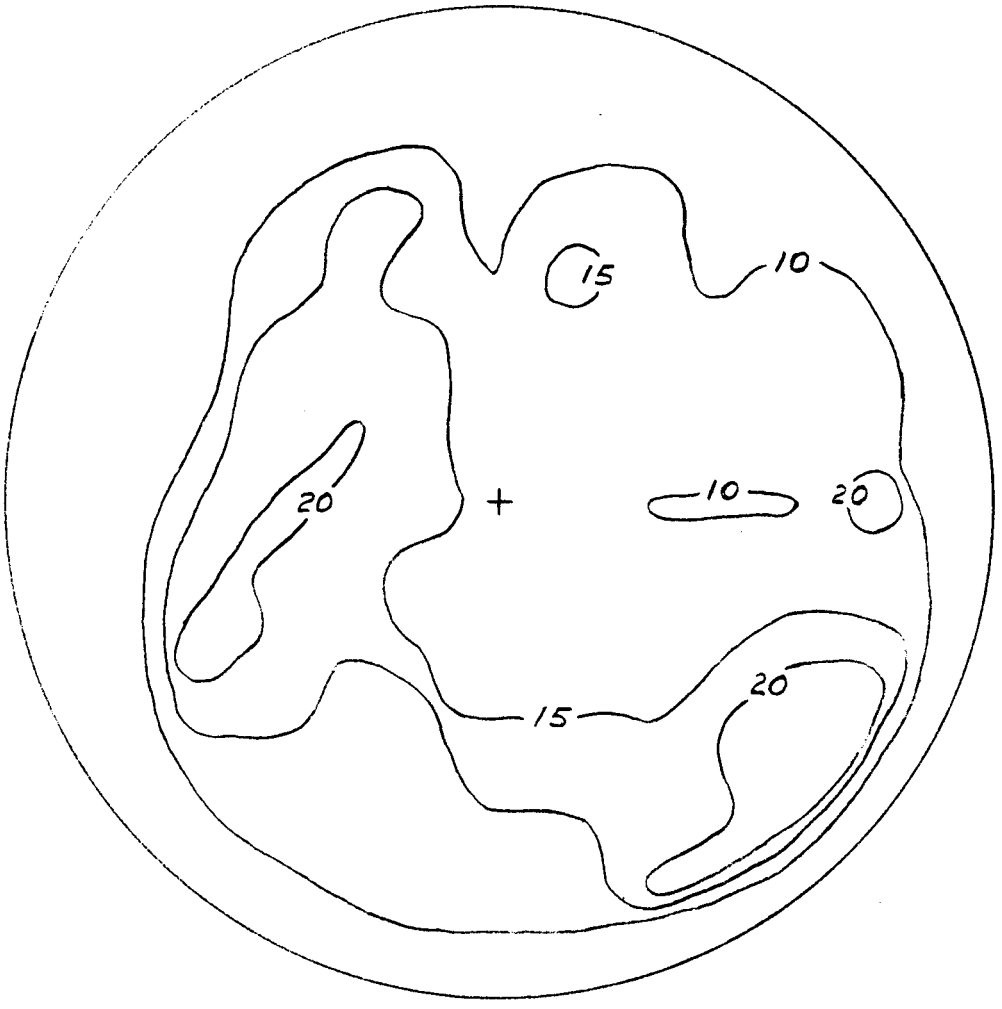

Figure 39

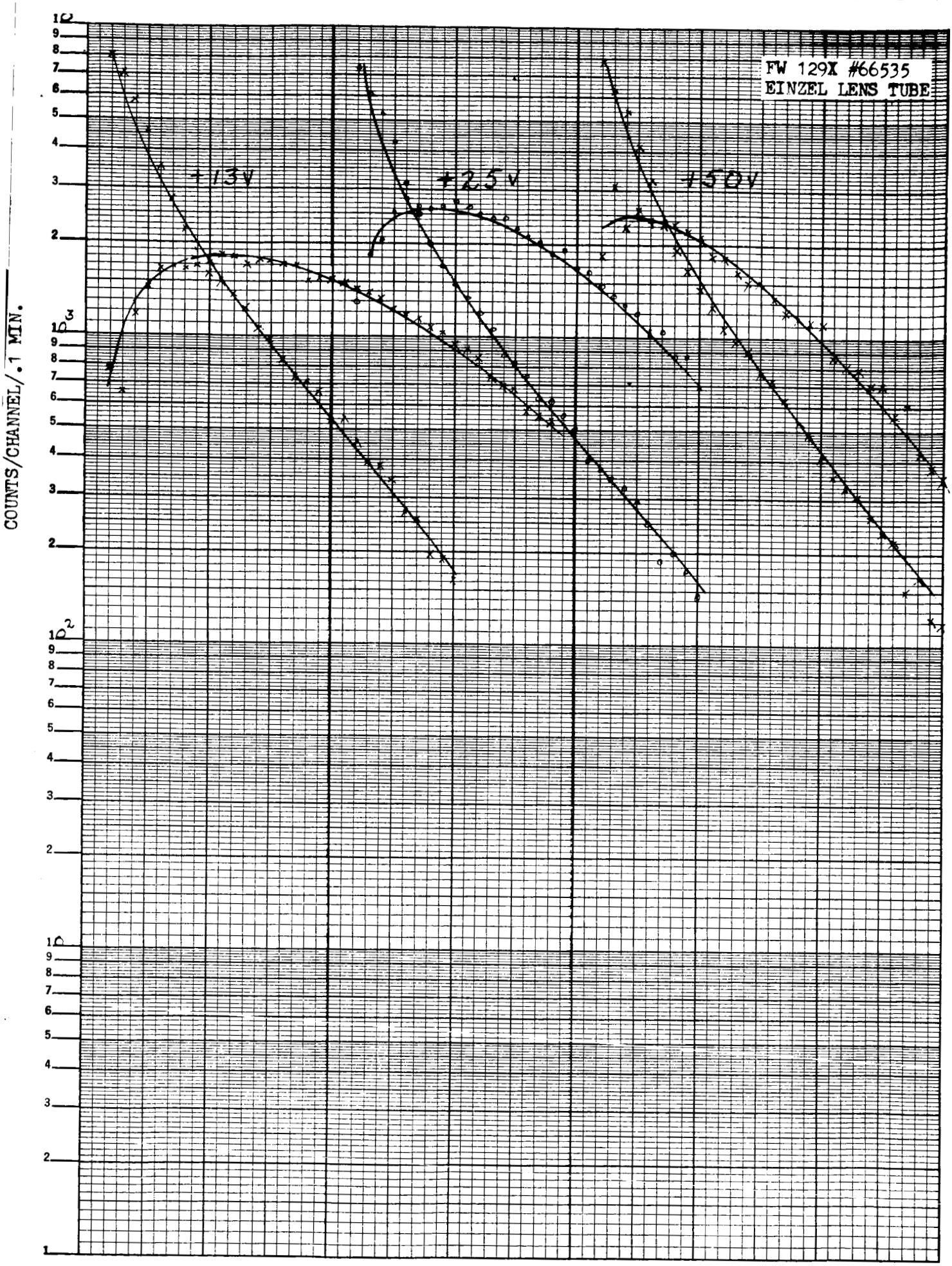
FW 129X #66535
EINZEL LENS TUBE
+13V
+25V
+50V
COUNTS/CHANNEL/.1 MIN.
CHANNEL NO. (1 DIV./CH.)

Figure 40

Experience in this laboratory has been that this type of multiplier, when excited by ultraviolet, produces a very ragged output pulse with an exponential distribution. Recently there has been an effort made to produce a superior multiplier of this type for use in a mass spectrometer. The processing of these tubes has been characterized by careful guarding of D1 and anode leads both through the glass envelope as well as the dynode support plate and attainment of a very high vacuum. Pressures of as low as 10^{-11} Torr. have been reached before tipoff with pressures of not more than 10^{-8} Torr. after the ion pump is removed prior to shipment. Figures 41a and 41b are photographs of a triggered scope display of pulses as they appear at the input to the analyzer, and the pulse height distribution as seen on the analyzer scope, respectively. The pulse height distribution is shown without subtraction of dark count since the dark count rate was only about 1 per second. This low dark counting rate is believed to be due, at least partially, to the fact that no cesium has been introduced into these tubes as in the case with tubes having a photocathode.

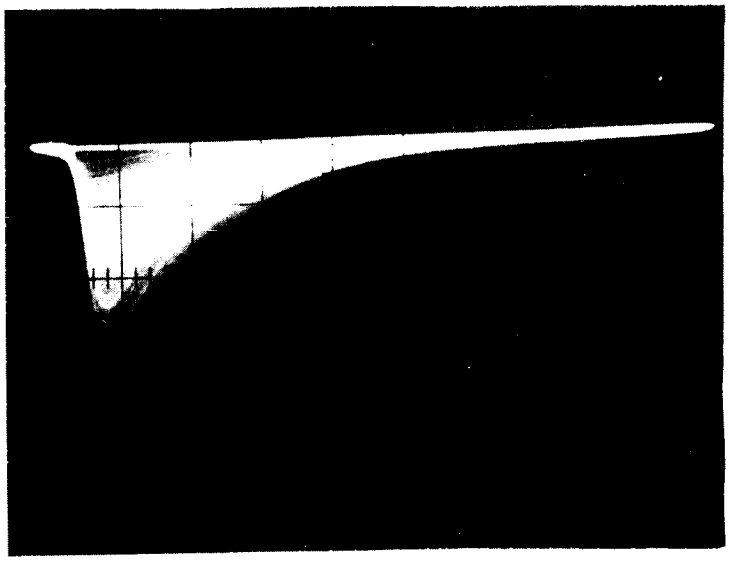

(a)

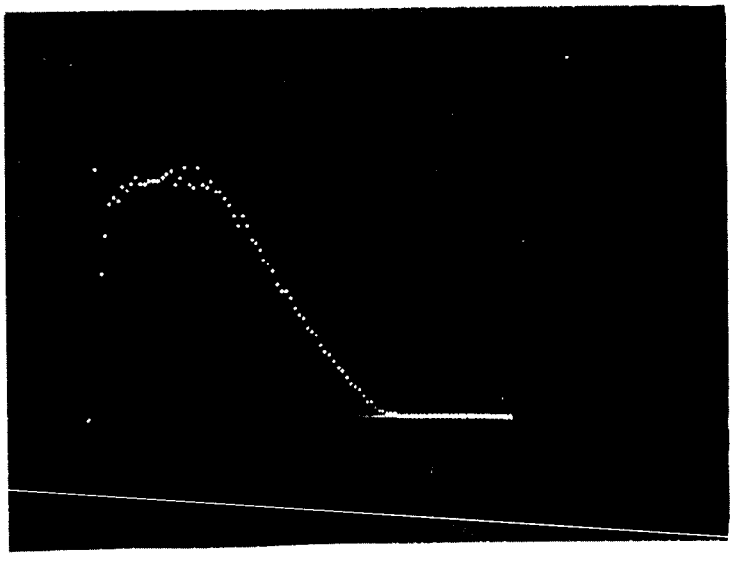

(b)

Figure 41

10.0 SUMMARY

A number of the most important factors determining the single electron counting properties of multiplier phototubes have been investigated. These include:

a. Proper low noise pulse analysis equipment and proper coupling to the multiplier phototube,

b. Sources of noise which tend to obscure the low energy side of the pulse height distribution,

c. Primary energy of electrons impinging on D1,

d. Dynode secondary emission ratio enhancement,

e. Electron optical properties between cathode and D1,

f. Control of low energy tertiary electrons produced in the region of the defining aperture and,

g. Spacial response uniformity over the D1 surfaces.

In view of the observed critical dependence of the counting properties on these as well as other parameters investigated, it is perhaps not surprising that satisfactory counting capabilities have not been widely claimed for multiplier phototubes.

Several promising specific design procedures for improving the counting properties have been either uncovered under this contract or emphasized anew, including:

a. Careful control of the bombarded area on the D1, to assure that maximal numbers of emitted photoelectrons strike uniformly effective secondary emitting areas, i.e., no "dead" spots;

b. The use of a decelerating electric field between the beam defining aperture and the D1, e.g., a cascade aperture, to suppress spurious low energy "secondary signal" electrons as well as dark electrons and,

c. The increase in the average secondary emission yield of D1, by increasing the bombarding primary electron energy (within limits),

by improving the secondary emitting surface and, by improving the collection efficiency between D1 and D2, etc.

Perhaps the most significant result of this contract was our confirmation that achievement of improved single electron counting properties (i.e., Poisson or an quasi-Poissonian pulse height distributions) can be expected in multiplier phototubes if close attention is paid to known basic principles of electron behavior.

Although the bulk of the engineering effort on this contract was expended on detailed tests of various tube varieties, including standard ITTIL types such as the FW-118, FW-129, FW-130, F4003, etc. and on careful interpretation of the results, a substantial number of special tubes were constructed (approximately 20), all involving unique design features aimed at clarifying some tentative analytical conclusion.

In addition to the issued quarterly project reports, the knowledge gained on this contract, in terms of improved multiplier phototubes, will be made fully available, not only to NASA detector users, but also to the general public.

RESEARCH MEMO NO. 326

Procedure for Measuring the Gain per Stage of Secondary Emission Multipliers

by
E. H. Eberhardt
December 5, 1960

Many different experimental techniques are available for measuring the gain per stage of secondary emission multipliers. Without describing any of these techniques in detail (with one exception, to follow), suffice it to say that the primary problem is one of evaluating the true "input" and "output" currents for each stage such that the product of all measured individual stage gains equals the measured over-all current amplification of the multiplier structure. This problem, in turn, reduces to one of inserting current meters at the proper locations and simultaneously maintaining proper operating electric fields in the vicinity of each dynode under test.

After considerable experimentation with various possible techniques, some of which appeared promising but proved to be surprisingly inaccurate, the following specific test procedure, involving "floating" batteries beyond each test dynode, proved to be the most satisfactory:

STEP 1: Input Current to the Multiplier Structure *

In the circuit of Figure 1 record the meter reading, I_1, as a function of the number of dynodes beyond D_1 to which proper operating potentials have been applied. The case for three dynodes beyond D_1 is illustrated.

Note that the meter will read negatively in this circuit whereas the current, i_1, is, by definition, the magnitude of the input electron current and is therefore a positive quantity. Thus $i_1 = -I_1$ = -(meter reading) = -(-number) = + number.

Plot i_1 ($= -I_1$) vs the number of these dynodes as shown in Figure 2.

If a plateau region exists for this curve, then the value of i_1 for this region corresponds to a satisfactory test input current for measuring the gain/stage and over-all gain.

* In applying this technique the nominal input dynode, D_1, need not actually be the first dynode, but could be any desired dynode in the multiplier structure.

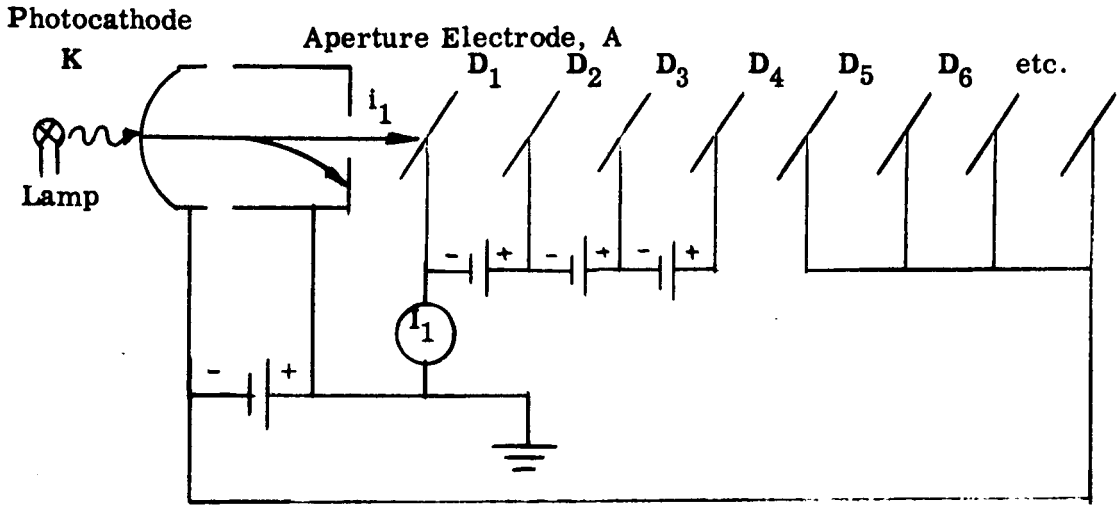

Figure 1

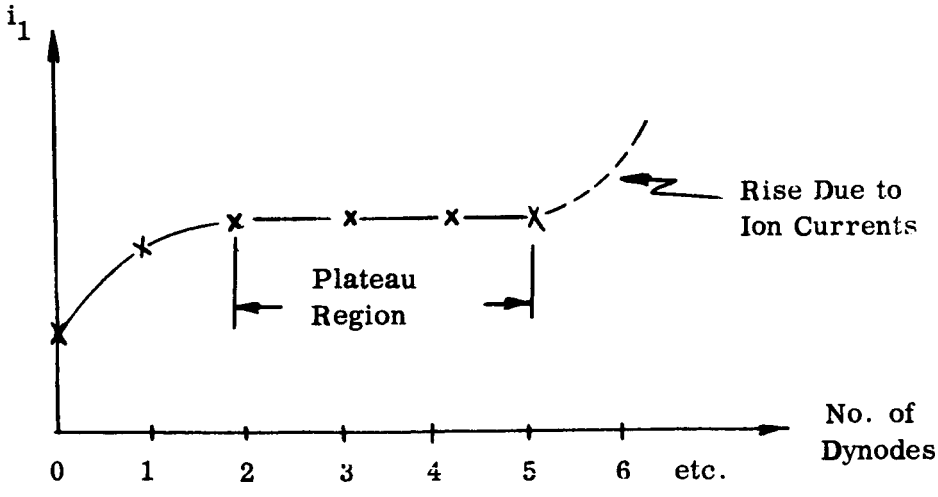

Figure 2

If not, the multiplier is not designed properly, or is not operating properly, i.e., there is excessive ion current or excessive bypassing of input electrons to later dynodes, etc. (Bypassing of electrons to the dynodes tied to D_1 is permitted).

The minimum number of floating batteries which gives saturation in the plateau region should be selected as standard operating procedure for the particular type of multiplier being tested. One floating battery stage is normally sufficient for venetian blind type multipliers, two for the standard 16 PMI, three for the new FW118, FW129, and FW130, and four or more for the standard RCA focused multiplier.

STEP 2: Current Gain of the First Dynode

Knowing, from Step 1 above, the input current, i_1, to the multiplier structure and consequently the nominal input current i_1, to the first dynode, D_1, the current gain, G_1, of D_1 is determined as follows:

Transfer the current meter to the position shown in Figure 3, keeping all other conditions constant.

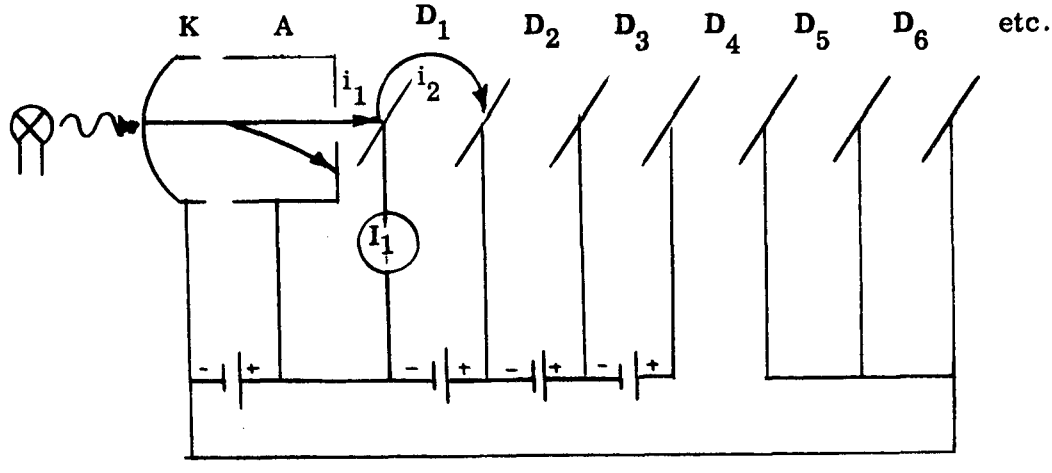

Figure 3

The currents shown in Figure 3 obey the current conservation law:

$$i_1 + I_1' = i_2$$

where I_1' is the new value of meter reading for this circuit as shown. Note that I_1' is normally a positive quantity for SE ratios exceeding unity.

The current gain, G_1, of D_1, defined by:

$$G_1 \equiv \frac{i_2}{i_1}$$

is then calculated directly from:

$$G_1 = \frac{i_1 + I_1'}{i_1} = \frac{-I_1 + I_1'}{-I_1}$$

This is the desired gain of D_1 in terms of measured quantities.

STEP 3: Current Gains of Subsequent Dynodes

The current, i_2, obtained in Step 2 above is now directly available as the magnitude of the input current to the second dynode, D_2. The current gain, G_2, of D_2 can be determined as follows:

a. Keep the light level constant,

b. Transfer the current meter to the D_2 circuit as shown in Figure 4,

c. Add a new battery to the chain of active dynodes following D_2,

d. Bias* all remaining dynodes to the D_1 position,

e. Record the new meter reading, I_2'.

* The term "bias" is used here as meaning a negative voltage with respect to the voltage applied to the test dynode (D_2 in the case illustrated), which is usually the ground point. The magnitude of this bias voltage will normally be irrelevant to the experiment as long as it is sufficiently negative to suppress all electrons from the test dynode (D_2) and the "floating" dynodes (D_3 - D_5). This normally implies a tiepoint one or two steps below the test dynode (D_2) in the dynode chain. This tiepoint should be moved corresponding with each shift to a new dynode in order to minimize electrical leakage and voltage breakdown.

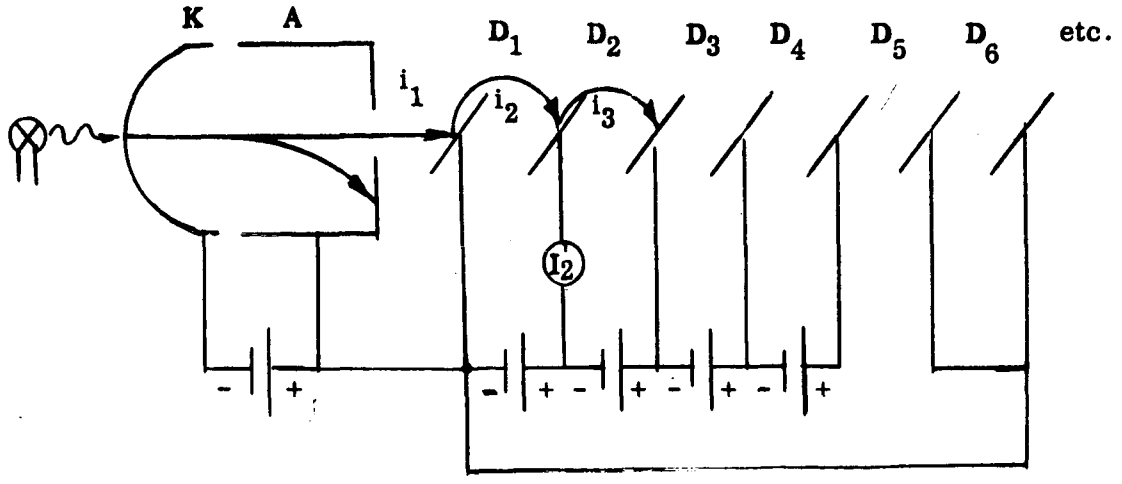

Figure 4

The new meter reading now satisfies the current conservation law:

$$i_2 + I_2' = i_3$$

so that

$$G_2 \equiv \frac{i_3}{i_2} = \frac{i_2 + I_2'}{i_2}$$

With i_2 available from Step 2 and I_2' measured here, G_2 is therefore a determined quantity.

This same process is now continued for succeeding dynodes, each step yielding a direct measurement of the current gain of the particular dynode involved.

STEP 4: Change of Current Level

As the above step-by-step process is continued from one dynode to the next with a fixed input light level, a point will ultimately be reached (usually prior to the final anode) where the current levels become excessively high. In the present setup, 10 μa is about the maximum possible dynode current.

It is necessary therefore to specify a technique for reducing the current level in this procedure, while maintaining known current magnitudes. The actual reduction can be obtained either by reducing the input light level, or, sometimes more conveniently by changing the operating conditions of early dynodes.

The proper numerical correction in the dynode gain procedure is made as follows:

Suppose that the maximum permissible current level occurs in the n^{th} dynode, and that the measured current, I_n', is then reduced to a new value, $(I_n')_{new}$. The original output current, i_{n+1}, from this dynode to the next, which was obtained from:

$$i_n + I_n' = i_{n+1}$$

will then be reduced by the ratio $(I_n')_{new} / I_n'$. In other words

$$(i_{n+1})_{new} = i_{n+1} \left(\frac{(I_n')_{new}}{I_n'} \right)$$

This new value of i_{n+1} is now used in calculating the gain, G_{n+1}, of D_{n+1} and beyond.

STEP 5: Over-all Current Gain

According to the definitions of the current gains, G_1, G_2, G_3, etc., (which incidentally, include the effects of bypass electrons and are not the SE ratios) the over-all current gain, μ, of the multiplier can be computed by multiplying all individual stage gains together. An examination of the various current ratios used in calculating G_1, G_2, etc., will reveal, however, that there is a considerable cross cancellation of terms in this common multiplication process. A more convenient computation of the over-all current gain is obtained from the relationship:

$$\mu = \frac{I_a}{I_1} \quad \frac{I_n'}{(I_n')_{new}} = \frac{I_a}{I_1} \times \text{reduction ratio}$$

where the cancellations have been carried out and I_a is the measured value of final anode current. If more than one current level reduction step is required, additional reduction ratios must appear in the above equation.

NOTES:

a. The battery test box and patch panel now in use makes each of the above circuits easy to establish at the fixed battery voltages available (225 v, 75 v, 75 v, 75 v ..... 112-1/2 v, 225 v, cathode to anode).

b. The actual meter measurements should be zero corrected in every case for leakage and thermionic currents by shuttering the light off. It is also best to keep the light shuttered off as much as possible to minimize fatigue effects.

c. To maximize the total number of dynode test steps possible at each light level, the initial test current level for each run should be kept as low as possible.

d. On measuring the current gain of the penultimate dynode, a calculated value of final output current is obtained. This calculated current can be compared to the measured final anode current as a convenient cross check.

e. The principal disadvantage of this test procedure is that it is not readily adaptable to variable dynode supply voltages.

APPLICATIONS NOTE E4

COOLING CHARACTERISTICS OF ITTIL MULTIPLIER PHOTOTUBES

The appreciable contribution of thermionic emission from the photocathode to the anode dark current observed in some multiplier phototubes makes possible a reduction in this current and consequently in the dark noise of these tubes by cooling. Figure 1 Curve (a) shows the measured decrease in anode DC dark current, I_{DC}, in an ITTIL FW-118 multiplier phototube (S-1 type) down to photocathode temperatures of about -20 degrees C. The sharply falling dark current, approximately following a Richardson type law, substantiates the predominance of thermionic emission from the photocathode in this tube at these temperatures. A decrease of about an order of magnitude for each 10 degrees C of cooling is observed.

Figure 1 Curve (b) shows the corresponding decrease in the equivalent noise input (ENI)[1] as a function of temperature, compared to the published[2] ENI characteristic Curve (c) for a competitive type tube. The FW-118 starts with a lower ENI characteristic at room temperature (at least partially because of its smaller effective photocathode area) and improves about twice as fast as the competitive detector with temperature.

At anode dark current levels below about 10^{-10} amperes, reliable and significant cooling characteristics can only be observed with difficulty in many multiplier phototubes because of the erratic and nonreproducible contribution of leakage currents (in the tube stem and base and internal parts), external pickup effects, and other low current measurement difficulties. For example, a resistance of 10^{13} ohms across the surface of nominally insulating internal anode pin support (an entirely reasonable value in view of the chemically reactive cathode materials present) can contribute 10^{-10} amperes in the typical operating range of 10^3 volts. This difficulty may be further aggravated when cooling a complete tube envelope if condensation of water vapor across various tube stem and basing lead connections occurs. Noise from this latter source can be particularly troublesome if the condensation occurs between the tube stem and base, where moisture may be trapped in the base cementing process. To avoid this, ITTIL recommends the use of unbased tubes (flying lead construction) or photocathode-only cooling.

---

1 Defined and measured according to IRE publication No. 62IRE7.S1.

2 RCA tube manual, 7102 tube type.

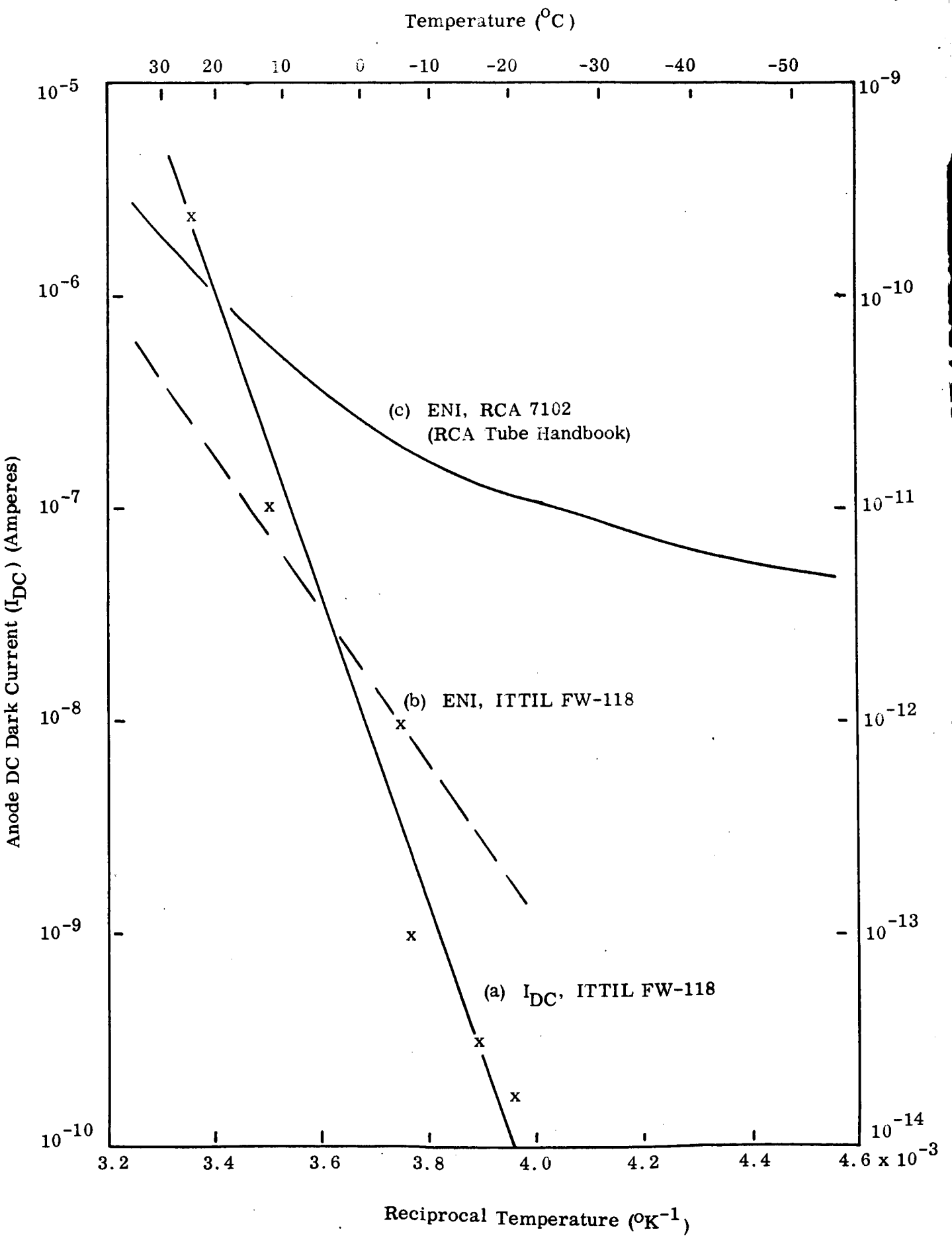

Figure 1 Anode DC Dark Current and ENI Vs Temperature for S-1 Type Multiplier Phototubes

Figure 2 shows a sketch of one type of laboratory cooling test equipment used by ITTIL. The cooled dry gas cools the tube faceplate and thus the photocathode by direct thermal contact, while the warm dry gas keeps the outer window from frosting. For field purposes, thermoelectric photocathode coolers of moderate cooling capability may be entirely adequate.

A recent and unique step taken by ITTIL to minimize internal tube leakage current and therefore improve both the room temperature and cooled dark current-dark noise characteristics, is the addition of an internal guard ring electrode surrounding the anode pin. This guard ring, when operated at quiescent DC anode potential as shown in Figure 3, bypasses surface leakage current around the anode pin and reduces the resultant minimum DC current levels to the order of 10^{-12} amperes or less. If so desired this guard ring can be voltage-driven in the more sophisticated types of feedback electrometer circuits.

For ultra-low light level detection problems, ITTIL normally recommends the use of single electron counting techniques[3,4]. By individually counting the comparatively large pulses produced in the anode circuit of multiplier phototubes resulting from single photoelectrons from the photocathode and biasing off the smaller pulses resulting from leakage current, dynode emission, etc., maximum differentiation between signal and dark noise can be achieved.

Further cooling of ITTIL tubes below the levels shown in Figure 1 is entirely feasible, the tubes being capable of operation at dry ice temperatures and probably as low as liquid N_2 temperatures. A. T. Young of Harvard Observatory has reported[5] a slight increase in over-all sensitivity for these tubes at dry ice and liquid N_2 temperatures combined with a reduction in dark current of at least 5 orders of magnitude at dry ice temperatures, indicating reasonably satisfactory performance, while W. A. Baum has reported[6] dark counting rates below 10 per minute at similar temperatures. ITTIL does not recommend cooling below dry ice temperature unless the temperature cycle is slow enough (a matter of hours) and applied uniformly to the complete tube to prevent strains from developing in the tube envelope, and unless the resultant ultra-low dark thermionic emission rates are known to be desirable (in many

3 E. H. Eberhardt, "Multiplier Phototubes for Single Electron Counting", IEEE Tr. of Nucl. Sc., Vol. NS11, No. 2, 48, 1964.
4 ITTIL Research Memos 367 and 387, and Applications Note E5.
5 A. T. Young, Applied Optics, Vol. 2, 51 (1963).
6 W. A. Baum, Vol. II, Astronomical Techniques, U. of Chicago Press, 1962, page 28.

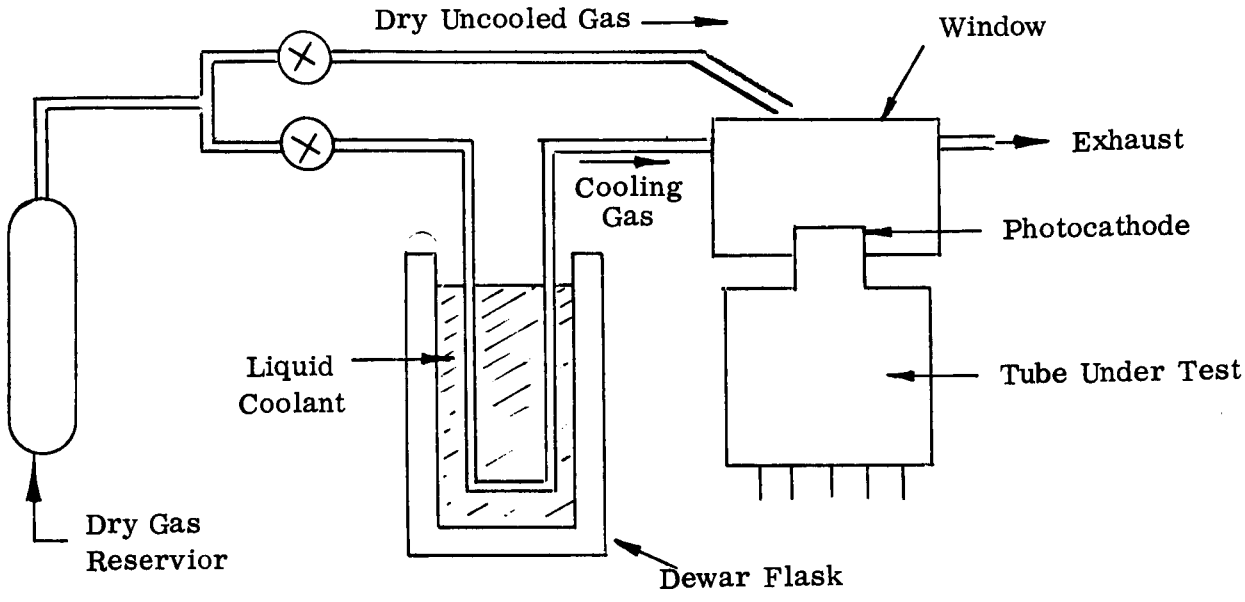

Figure 2 ITTIL Cooling Configuration

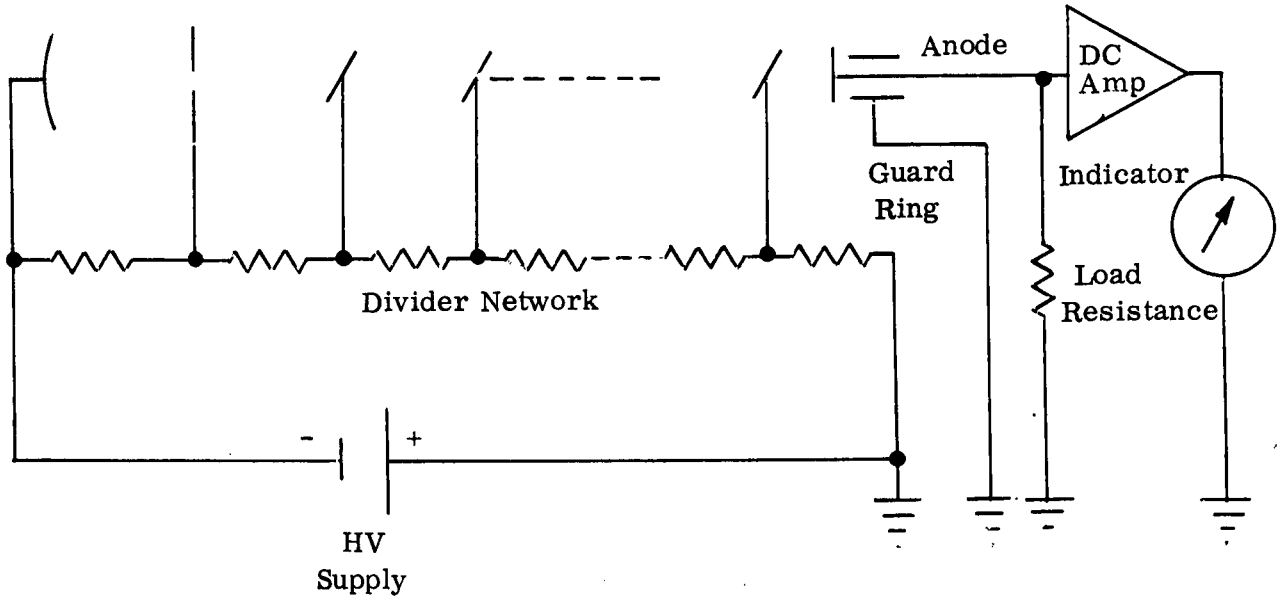

Figure 3 Typical Multiplier Phototube Circuit Using Guard Ring Electrode

applications, background light flux, present on the photocathode in the absence of the signal flux to be detected, radioactive content of the tube parts, and other dark noise sources may normally cause much more noise than photocathode thermionic emission).

The example reported by Baum in which a cooled ITTIL 16 PMI (predecessor of the present FW-118) was operated at a dark counting rate of less than 10 electrons/minute is particularly interesting. Referred to the anode circuit, under the assumption of a gain of 10^6 in the electron multiplier, this is equivalent to less than 3×10^{-14} amperes, a value well below the expected anode leakage current limits. If these 10 dark counts/minute were randomly distributed, as expected, the statistical uncertainty for a one minute observation time would have been $\sqrt{10} \cong 3$ photoelectrons, equivalent to about 13 input photons/second or a total of 750 photons in 1 minute for a peak quantum efficiency of 0.4 percent in the corresponding S-1 photocathode at 8000 Å. The ability to detect flux levels of this magnitude (approximately 3×10^{-18} watts) using single electron counting techniques with a cooled FW-118 multiplier phototube demonstrates the unique capabilities of this detector.

Cooling characteristics of S-11 and S-20 type multiplier phototubes (such as the ITTIL FW-129 and FW-130 types), are not shown in Figures 1 and 2 because of the difficulty in making reliable measurements at the dark emission rates involved. For example, a total thermionic dark count rate of only 30 electrons/second at room temperature was observed[3] in one sample ITTIL FW-129 tube. This magnitude is believed to be typical of present S-11 and S-20 tubes. Based on tentative experimental measurements it is believed that these thermionic emission dark current count rates will also fall rapidly with cooling.